Universitetet i Stavanger

DET TEKNISK-NATURVITENSKAPELIGE FAKULTET

MASTEROPPGAVE

Studieprogram/spesialisering: Environmental Technology Offshore Environmental Engineering	Vår semesteret, 2012 Åpen / Konfidensiell
Forfatter: Eirin L. Abrahamsen, 954799	…… (signatur forfatter)
Fagansvarlig: Malcolm A. Kelland Veileder(e): Anders Grinrød	
Tittel på masteroppgaven: Engelsk tittel: Organic flow assurance: Asphaltene dispersant/inhibitor formulation development through experimental design.	
Studiepoeng: 30	
Emneord: Asphaltene Design of Experiments	Sidetall: 126 Stavanger, 29.06.2012 dato/år

Organic flow assurance: Asphaltene dispersant/inhibitor formulation development through experimental design

Eirin L. Abrahamsen

Spring 2012

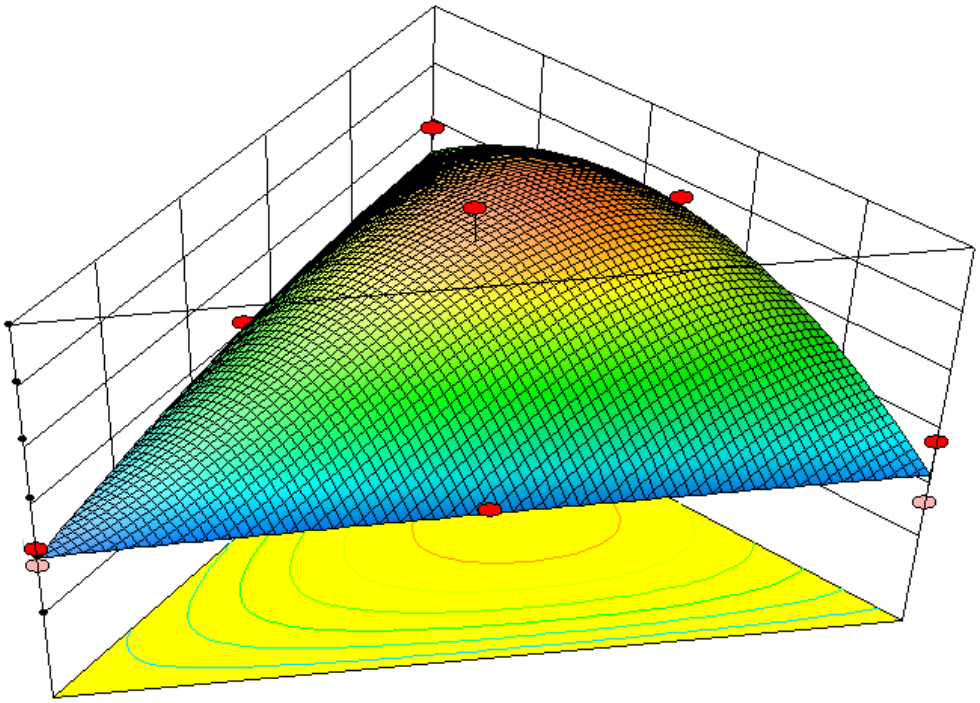

MI SWACO
A Schlumberger Company

Abstract

The exploitation of hydrocarbon has forced the petroleum production to move closer to extreme climate areas and deep waters such as the Barents Sea. These challenges require effective and safe production, transport and processing of the petroleum sources.
Chemical and physical changes in the reservoir may cause different types of unpredicted problems such as organic deposits which are mainly asphaltene and wax precipitation. Wax precipitation is very common in subsea pipelines. Asphaltenes are more affected by for example pressure drops and high shear, which may cause formation damage as well as plug-up the well-bores and tubing.
In the petroleum industry, flow assurance has become a key concern where the cold sea bottom temperatures and extreme water depths give rise to enormous technical challenges which includes the management of solids such as asphaltenes and wax. Flow assurance is defined as “safe, uninterrupted and simultaneous transport of gas, oil and water from reservoirs to processing facilities”. The term refers to the need to guarantee flow of oil and gas from the reservoirs to the processing facilities.

In this thesis the focus will be on chemical control of asphaltene and the formulation of an optimal asphaltene dispersant mixture.
An experimental method needed to be established for the screening tests of the dispersant mixtures. When performing a screening test, the experimental method is desired to be simple and quick. This will save time and money as the screening test will only give an idea of how the system works and interacts. Different methods were tested such as measurement of the asphaltene deposit level, spot test, UV-Vis spectroscopy and turbidity measurements. Turbidity measurement was decided to be used in the formulation of an optimal asphaltene dispersant mixture.
Design of experiments (DoE) and mixture design are well known methods which are often used when mixing together multiple components. DoE techniques provide an idea of how the mixtures work together and can then optimize the formulation at a minimum effort and cost. The computer software, Design Expert was used for the experimental design in this thesis. The program was used to set up an experimental plan which showed the mixture components and the mixture proportions to be tested. When the results were ready, they were inserted in Design Expert and a model was suggested. The analysis of the model was also done by Design Expert which made it possible to easily detect certain trends in the model such as identifying results that deviated from the model in form of failed experiments.
Three different crude oils were tested, Crudo-Metapetroleum a viscous and heavy crude oil with an asphaltene content of 12,1535g/100ml, Hier D02A crude oil which is a more common crude oil with an asphaltene content of 2,2380g/100ml and Jordbær crude oil with an asphaltene content of 0,2210g/100ml. Three commercial asphaltene dispersant were tested in order to find an optimal mixture formulation. The dispersants used for these tests, dodecyl benzene sulfonic acid (DDBSA), Hybase M-401 and Flowsolve 113, did not show any usable synergistic effects. The results showed that the best dispersant was Flowsolve 113.

Acknowledgements

I would like to thank Anders Grinrød for providing and outlining this thesis. His guidance and advice throughout this semester has been fantastic.
Many thanks to everyone at Mi-Swaco for taking me in and letting me experience this interesting field of research. Thank you Astrid Lone, for all the help and assistance throughout the semester in particular in the laboratory.

I would also like to thank Professor Malcolm Kelland for being my faculty supervisor. His help and advice in the process of putting together the thesis has been excellent.

Finally, I wish to thank my family and especially my fiancé Cato for their patients and support through my years as a student. I could not have done this without you.

Table of Contents

Chapter 1 Asphaltene control

Petroleum is defined as a hydrocarbon mixture which occurs naturally in either a gaseous, liquid or solid state. The mixture may also contain hydrogen, sulphide, nitrogen, oxides and traces of metallic constituents [7]. Chemical and physical changes in the reservoir and in the well stream during transportation and processing may cause different types of unpredicted problems. Production chemistry problems are in general classified as one of the four following types [6]:

- Fouling: Scales (ex. $BaSO_4$), corrosion products, wax (paraffin), asphaltenes, biofouling and gas hydrate. They all cause unwanted deposition problems in the system.
- Physical properties of the fluid: For example foams, emulsions and viscous flow.
- Corrosion related (mostly): Affects the structural integrity of the facilities.
- Environmental and economic consequences: Unwanted emissions (for example H_2S) and discharges (for example oil in water).

1.1 Flow assurance

Flow assurance can be defined as “safe, uninterrupted and simultaneous transport of gas, oil and water from reservoirs to processing facilities” [15], or simply “keep the flow-path open” [16]. Flow assurance in the oil industry is often used to describe issues such as extreme pressure drop in the pipelines which restrict the fluid flow from the reservoir to the point of sale. It is important to perform a thorough reservoir fluid characterization in order to ensure a continuous and optimal well productivity. Deposits such as waxes, asphaltenes and gas hydrates are well known causes of flow problems [15, 17].
In the petroleum industry, flow assurance has become a key concern which includes a development of strategies for controlling fouling. These strategies involve the use of chemical as well as nonchemical solutions to prevent the reduction or complete interruption of the flow of hydrocarbons, the overall objective is simply to keep an open flow-path [6, 16, 18].

1.2 Organic deposits

Wax (paraffin) and asphaltenes are the main components in the organic deposits which are found in wellbores, production systems, export lines and downstream processing equipment [19-21]. Wax (paraffin) deposition in the pipelines can inhibit flow by the increase of viscosity mainly when the temperature drops [22]. Asphaltene deposits occur mainly due to destabilization factors, for example pH, CO_2 and aliphatic solvents [20, 23]. Stable asphaltene colloids will not cause any problems. However, if they are destabilized, the problems may appear [20].

Organic deposits cause severe problems in the petroleum industry. Due to the very high reservoir temperature and the very low subsea temperatures, problems caused by complex crystallization of waxes are very common. Even so, asphaltenes are more discussed since they are considered to be the most complex molecules in nature present in petroleum and is thus also less understood than other types of fouling [6, 11, 24].

Asphaltenes are one of the more researched materials in the petroleum industry [25, 26] because it is known to cause many problems in production, transportation and processing [26]. Downhole there may be asphaltene deposits which cause wellbore plugging and even restrict flow within the formation itself. Asphaltenes can also restrict or plug the fluid flow completely in the pipelines, see figure 1.01. The deposits may also collect in surface equipment such as heater treaters and stock tanks [27].

Figure 1.01 *Asphaltene depositions in a pipe (http://www.bakerhughes.com 25.04.12)*

Crudes may contain as much as 20% asphaltenes, without necessarily causing a deposition problem. The presence of both wax and asphaltene may have major effects on the rheology of crude oils [28].

1.2.1 Wax control

Wax occurs naturally in crude oils and some condensates [29]. They consist of long chain alkanes with little branching and contain more than 15 carbon atoms [30]. Cyclic alkanes and aromatic hydrocarbons may also be present, however normal n-paraffins are the main cause of wax deposition in pipelines [6]. The wax forms a complex 3D network when it crystallizes out of solution [31]. Hard crystalline wax often form from 25 – 50 or more carbon atoms and are mostly present in crude oils, these are harder to control compared to waxes formed in condensate. Soft, slushy waxes are often formed in condensates and they contain 16 – 25 carbon atoms in alkane chains. As the size of the molecule increase, the melting temperature increases and then it becomes more difficult to prevent wax deposition [6]. Under most reservoir conditions, at high pressure and temperature, the wax is dissolved in the crude oil [20]. The temperature at which the first wax crystal is formed is called the wax appearance temperature (WAT) or cloud point. Often the pipeline holds a temperature below the WAT and wax will start to form on the pipeline walls and grow over time, thus restricting the flow [30] (figure 1.02). Some oils have a WAT which is as high as 50°C. Pressure drop may cause the light ends such as methane, ethane and other nonhydrocarbon gases to go out of the solution. These light ends function as solvents for the wax and when they disappear from the solution, the wax precipitates [6, 22, 32].

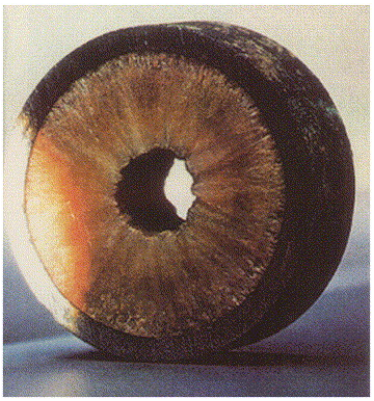

Figure 1.02 *Paraffin depositional problesm [12].*

There are several ways to control wax deposition and gelling, examples of some wax control strategies are [6]:

- Insulation
- Mechanical removal
    - Pigging
    - Downhole wireline cutters
- Heating
    - Downhole
    - Flowline
- Wax dissolvers
- Wax inhibitors, pour-point depressants (PPD) and dispersants

1.3 What is asphaltene?

Asphaltenes are considered to be among the heaviest components in crude oil. They are insoluble in light saturated hydrocarbons such as pentane and heptane, but they are soluble in aromatic solvents such as benzene, toluene and xylene [6, 28, 33]. Figure 1.03 shows the molecular structures of these components.

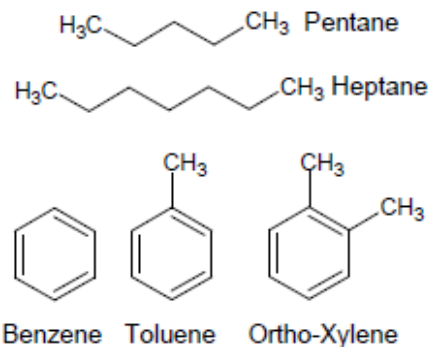

Figure 1.03 *Molecular structures of pentane and heptane in which asphaltenes are not soluble and molecular structures of benzene, toluene and o-xylene in which asphaltenes are soluble.*

Asphaltenes are often referred to as the «unsaturated» fraction of the crude oil which by definition is the fraction of crude oil that may contain some or all of the following [6, 17, 33-35]:

- A high molecular weight
- Polar groups where there is a separation of the electrical charge within the molecule or molecular groups which lead to an electrical dipole or multipole.
- Alkanes which include single bonding hydrocarbon chains and ring structures.
- Alkenes which include double bonding in the alkane chain or ring structure, also called unsaturated because they contain fewer hydrogens per carbon than alkanes.
- Alkynes which include triple bonding in the alkane chain or ring structure, also called unsaturated because they contain fewer hydrogens per carbon than alkanes
- Polyaromatic structures which are ring structures structurally related to benzene.

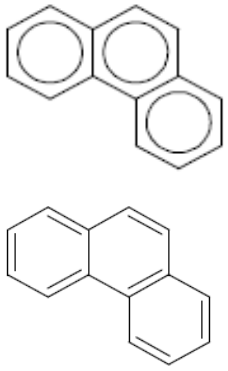

Figure 1.04 *Examples of aromatic structures.*

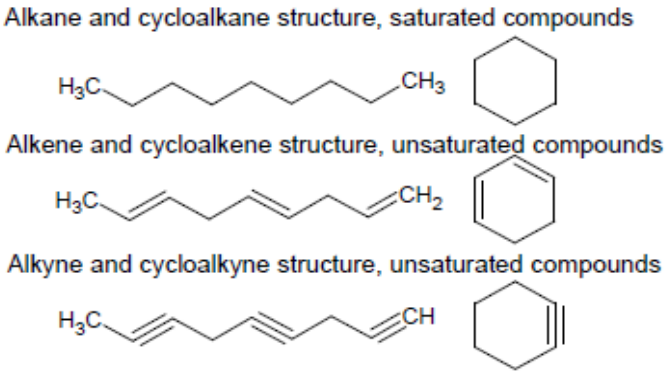

Figure 1.05 *Examples of alkane, alkene and alkyne structures.*

Figure 1.04 and 1.05 shows an example of molecular structures of some of the components which may be present in an asphaltene molecule.

- Various heteroatoms such as sulphur, nitrogen, oxygen and metals such as nickel, vanadium and iron may fill holes and gaps in the asphaltene molecule. The metals form complexes and can give electrical charge to the molecule which may affect the asphaltene deposition.

Figure 1.06 shows a proposed asphaltene molecular structure extracted from Bangestan oil.

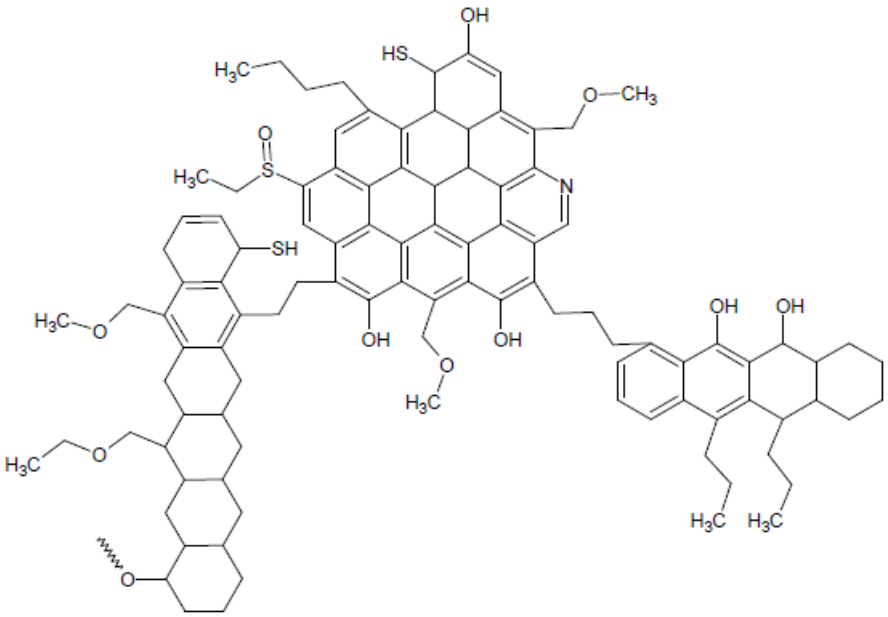

Figure 1.06 *A proposed molecular structure for an asphaltene sample extracted from Bangestan (Iranian) oil [13, 14].*

1.3.1 The asphaltene molecule and its structure

The asphaltene composition is very diverse, therefore a lot of effort has gone into different researches and experiments to understand and predict the chemical and physical properties of asphaltenes [36].

An average asphaltene molecule contains a condensed aromatic system which is formed as a flat sheet. Sulphide, ether, aliphatic chains or naphthenic ring linkages may be connected to this system. Transition metals like vanadium, nickel and iron fill up holes and gaps in the molecule [37].The aromaticity means that the electrons are delocalized within a system, in

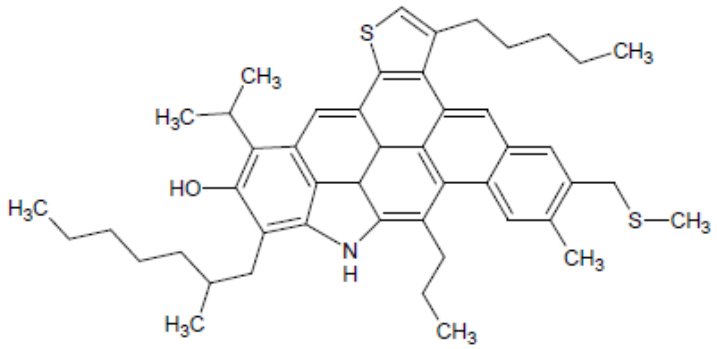

Figure 1.07 *Representative structure and typical molecular weight of a proposed "continental" asphaltene molecule [6].*

this case an aromatic fused ring system, which stabilizes the asphaltene molecule sheet. Figure 1.07 shows a molecular model of a so called continental asphaltene molecule, which mainly consists of a large central aromatic region with peripheral alkanes [5].

A simple archipelago asphaltenes structure is shown in Figure 1.08, the archipelago are actually quite complex aggregates because some of the molecules may act as bridges, connecting them together. The bridging and tangling of the asphaltene aggregates is the cause of many different molecular conformations which do not occur with the continental type asphaltene [5].

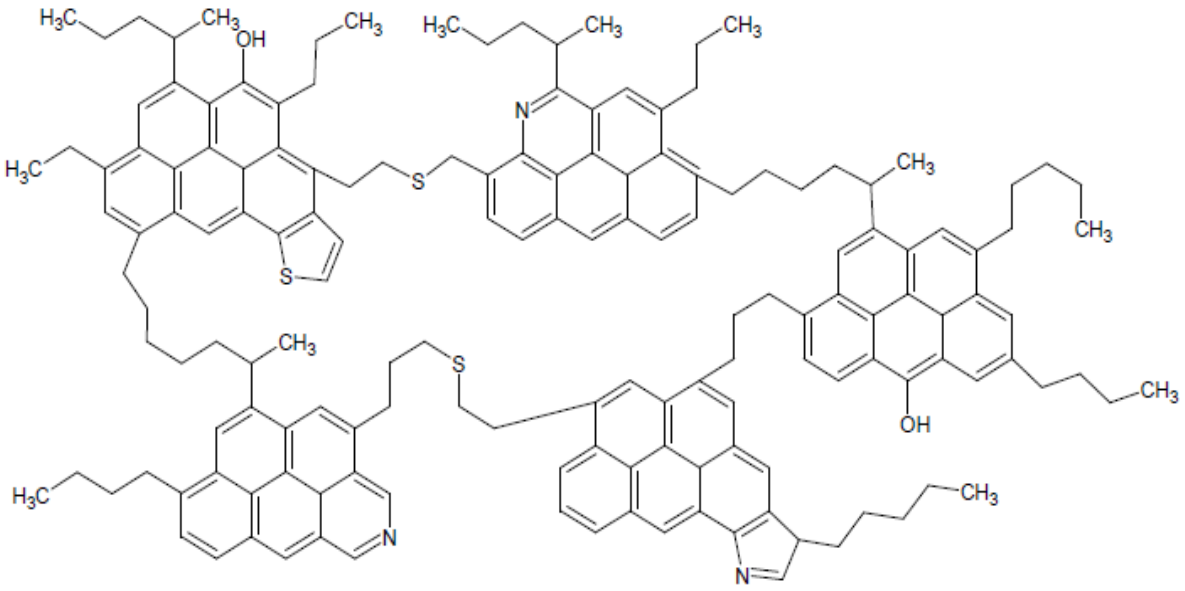

Figure 1.08 *Representative structure of a proposed "archipelago" asphaltene molecule [6].*

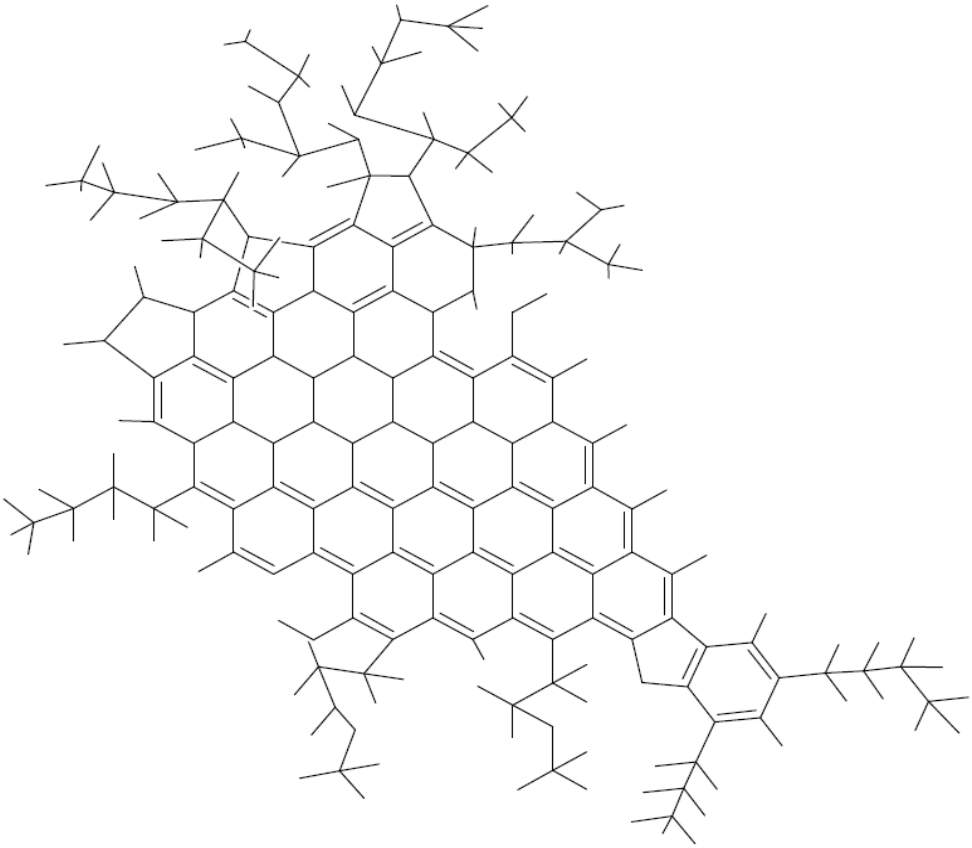

Figure 1.09 *Model molecule of a Venezuelan crude oil sample [5].*

Figure 1.09 shows a top view of a model asphaltene molecule from a Venezuelan crude oil sample [5] as an average model molecule. This is a continental type with a large central aromatic region surrounded by several aliphatic groups.

The original concept of the asphaltene – resin micelle developed the concept of the asphaltene – asphaltene combination to form a stack similar to graphite-like stacks as figure 1.10 and 1.11 shows [9, 11].

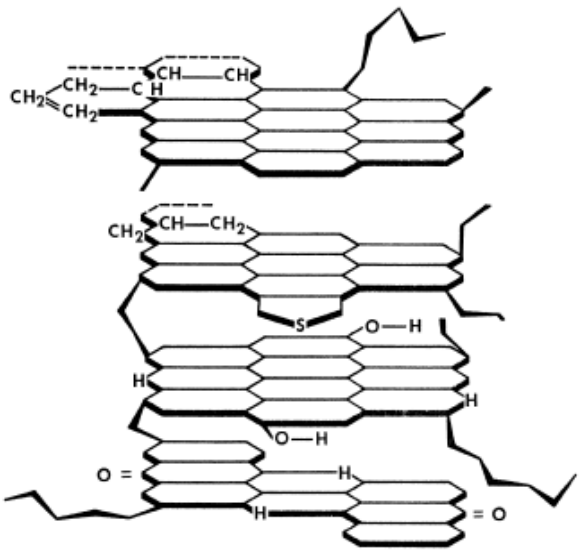

Figure 1.10 *Concept of the stack-type asphaltene micelle [9].*

According to the observations made by an electron spin resonance (ESR) of a Venezuelan crude oil sample, there is a possibility for a vanadium atom in a vanadyl compound to bind to the asphaltenes through the heteroatoms nitrogen, sulphur, oxygen, as figure 1.11 suggests. The vanadyl chelates can also be trapped between the aromatic sheets, especially if there are defect sites in the sheet [38].

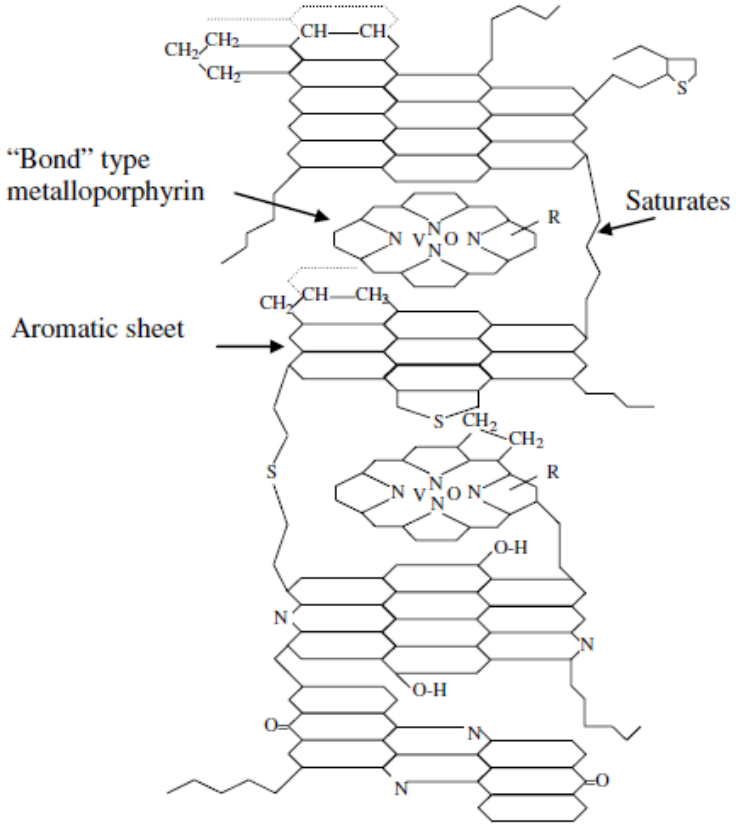

Figure 1.11 *A hypothetical asphaltene molecule interacting with metalloporphyrins [11].*

Mullins, 2010 [39] suggests in the modified Yen model (figure 1.12) that asphaltene nanoaggregates formed from single asphaltene molecules can form a single, disordered stack of polycyclic aromatic hydrocarbon (PAH) with surrounding alkanes, possibly similar to the stacks in figure 1.10 and 1.11. The nanoaggregates (~6 asphaltene molecules) can further form clusters (~8 nanoaggregates) which are not much bigger than the single nanoaggragates and they stay suspended in the crude oil if there are no instabilities affecting the system.

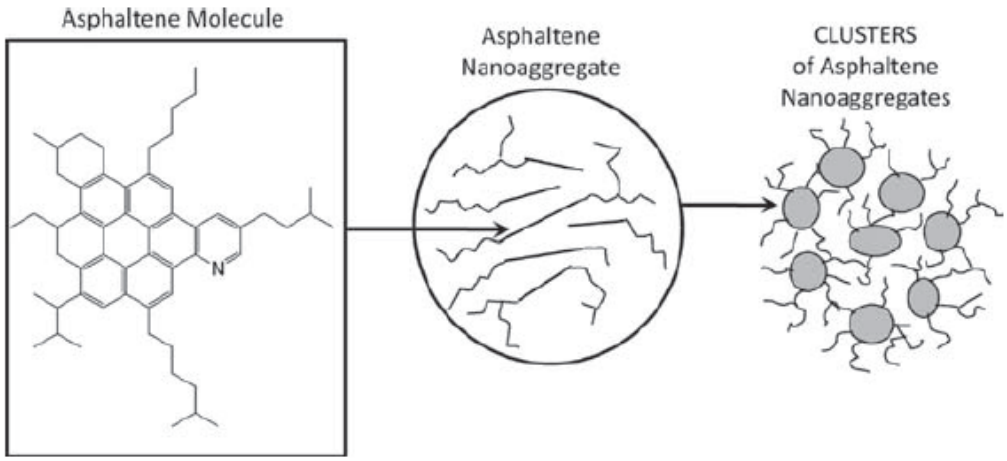

Figure 1.12 *The modified yen model [37].*

The stability of asphaltenes may be destabilized by for example pressure drop, high shear, crude blending, gas or liquid injection and acid stimulations among others, which often results in deposition problems [6, 40]. The amount of asphaltene deposits typically increases as the pressure drops, when the pressure is between the reservoir pressure and the bubble point of the reservoir oil, deposition of asphaltenes begins [41]. Often the oils in the reservoir contain some natural gas in solution. The bubble point is the temperature and pressure conditions where the first gas bubble comes out of solution.

1.3.2 Resins

Resins also called maltenes [33] are lower molecular weight polycyclic polar groups which have a more aliphatic side-chain character (hydrocarbon chains or rings, saturated or unsaturated, but non-aromatic). The aromaticity is less within the resins compared to asphaltenes. Resins are believed to be precursor molecules of the asphaltenes or that asphaltenes are maturation products of resins. Resins and asphaltenes which have been examined show structural similarities [8, 42], however the resins have a lower molecular weight. Figure 1.13 and 1.14 shows the model structures of resins obtained from spectroscopic data of a Venezuelan crude oil sample. The structure was found by using computational methods of molecular mechanics [8].

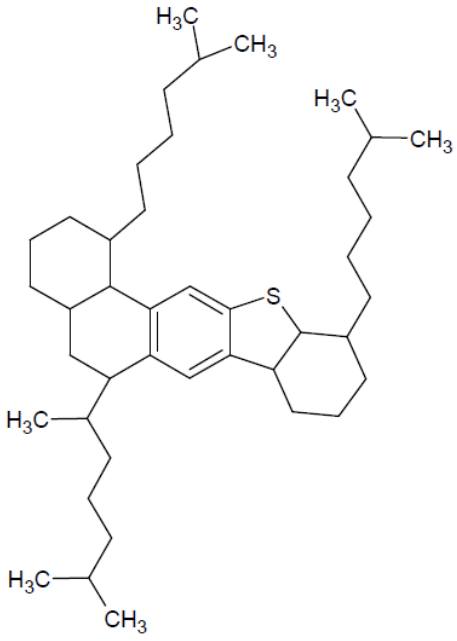

Figure 1.13 *Venezuelan crude oil residues [8].*

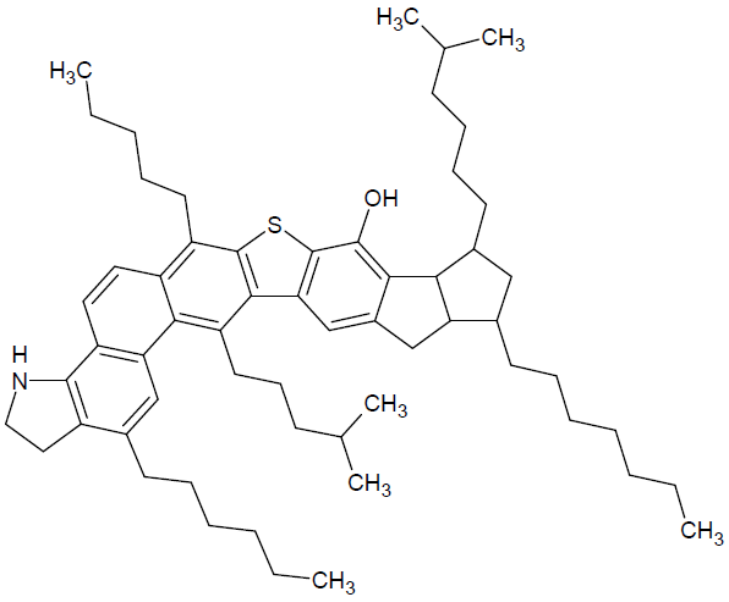

Figure 1.14 *Venezuelan crude oil residues [8].*

Unlike paraffins, asphaltenes are suspended colloidals in the crude oil and the resins surrounds asphaltene molecules forming a stabile micelle [20]. Hydrogen bonding studies have shown that resin – asphaltene interactions are preferred as long as resins and asphaltenes are present together. Resins are said to be a characteristic of asphaltene dispersion, the asphaltenes are incompatible with the oil fraction (saturates and aromatics) so when the resins (polar aromatics) which are compatible with the oil fraction surrounds the asphaltenes, they become stable [9] (figure 1.15). When unfavorable solvent conditions occurs the resins will desorb from the asphaltenes which cause precipitation of large asphaltene aggregates [43].

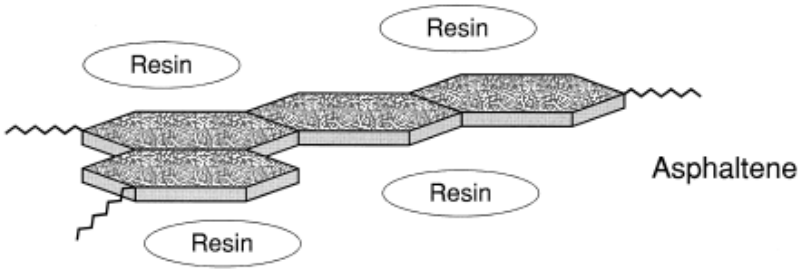

Figure 1.15 *Resin - asphaltene micelle concept [9].*

However, the resins in themselves will not form damaging deposits and they are also heptane-soluble [6, 43]. In general resins are soluble in the liquids in which asphaltene is precipitated [37]. Figure 1.16 below, show a space-filling structure of a resin molecule which is attached to an asphaltene molecule (the dark structure is the resin, the light structure is the asphaltene) [8].

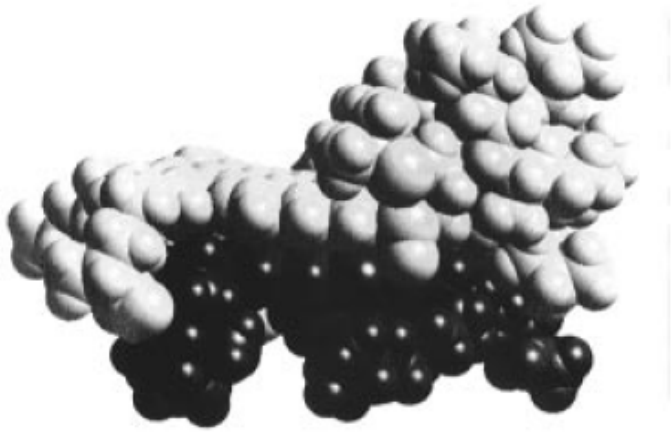

Figure 1.16 *A space-filling structure of a model asphaltene molecule (white) and a model resin (black) [8].*

1.4 Control of asphaltene deposition

There are different ways of controlling asphaltene deposition, as mentioned earlier, both nonchemical techniques and chemical techniques. The focus in this thesis will be chemical treatment of asphaltenes.

1.4.1 Nonchemical asphaltene control

Some of the nonchemical methods which have been recommended to prevent and clean asphaltene deposits are [6]:

- To operate outside the asphaltene formation envelope (AFE). This involves adjusting the operating conditions such as temperature, pressure or flow to prevent conditions which cause asphaltene deposition.
- To avoid blending of different crude streams, where blending is a common cause of asphaltene deposition, for example light nonasphaltic crude may precipitate asphaltene in heavier crudes.
- Physical removal of asphaltene deposits include [17, 27]:
    - Wireline cutting
    - Pigging which scrapes tubes and piping surfaces, this may also cause some tube/pipe material loss.
    - Hydroblasting is an abrasive/erosive cleaning technique which uses a high pressure water stream to remove deposits.
    - Drilling

1.4.2 Chemical asphaltene control – dispersants and inhibitors

In general there are two methods for controlling asphaltene deposits chemically [6]:

- Asphaltene dispersants (ADs) and asphaltene inhibitors (AIs)
- Asphaltene dissolvers (solvents or deasphalted oil)

The ADs and AIs are two different classes of additives which can prevent asphaltene deposition. AIs are in general polymers (or resins) and ADs are in general nonpolymeric surfactants, however many AI polymeric surfactants function as ADs, but ADs do not function as AIs [6].
These two classes work in different ways:

- AIs prevents the aggregation of asphaltene molecules, they increase the stability to allow operation under more severe conditions.
- ADs reduce the particle size and agglomeration behaviour so any precipitated solids are dispersed thus keeping them in suspension in the oil [6, 44].

In order to prevent the aggregation of asphaltene molecules, AIs need to interact with several molecular points for effective inhibition, thus polymers are needed [6].
A dispersant will in general contain an “anchoring” polar group which will attach itself to the asphaltene surface and a “blocking” alkyl group which will block other asphaltene molecules. The polar group will normally contain etheroatoms like: oxygen, nitrogen, phosphorous and so on [45]. The nonpolymeric ADs polar and/or aromatic head groups with long alkyl tails interact with aggregated asphaltene molecules. The polarity of the outside of the aggregate changes with the help of the long alkyl chains, and so the aggregate is more similar to the crude oil, thus it is dispersible in the crude oil [6].
The AIs and ADs are known to be oil-specific meaning that for example a polymeric AI with aliphatic tails and polar heads prevents asphaltene deposition in oil A, but will have no effect in oil B. On the other hand, for example a nonpolymeric amine prevented asphaltene deposition in oil B, but not in oil A [46].
Interaction between AIs or ADs and asphaltenes may be summarized as follows [6]:

- $\pi - \pi$ interaction between unsaturated or aromatic groups and asphaltene molecules. The green arrow in figure 1.17 shows sigma bond formed by the end-on overlap of the sp^2 orbitals. The red arrow shows the pi overlap which is a lateral overlap of the p orbitals with its two neighbours [4].
- Acid – base interactions
- Hydrogen bonding
- Dipole – dipole interactions
- Complexing of metal ions

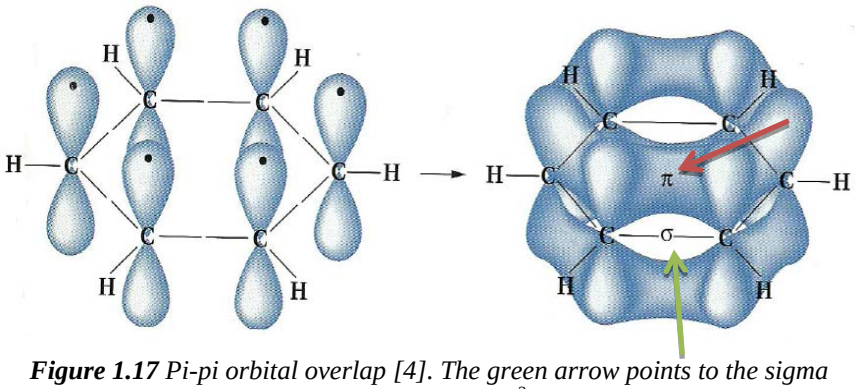

Figure 1.17 *Pi-pi orbital overlap [4]. The green arrow points to the sigma bonding formed by the end-on overlap of the sp^2orbitals. The red arrow points to the pi overlap formed by the lateral overlap of the p orbitals.*

1.4.3 Asphaltene dissolvers

Deposits may need to be removed mechanically as mentioned above. However the use of asphaltene dissolvers or solvents is the only chemical method of removing asphaltene deposits properly. Light aromatic species are commonly used for this purpose for example benzene, toluene and xylene [47] (see figure 1.03 in chapter 1.3), but they are expensive. The latter compounds and are also highly volatile, causing them to easily vaporize and they have low flash points which is the lowest temperature that these compounds can under normal conditions form an ignitable vapour. Toluene and xylene are the most common solvents, however there is a lot of on-going research in finding other alternatives because of environmental restrictions and the high costs of these solvents [48].The solvents attack between the asphaltene molecules and replaces the asphaltene – asphaltene connection with asphaltene – solvent $\pi - \pi$ interactions, thus solubilizing them [6].

One study showed that monocyclic and bicyclic aromatics solved asphaltene better than tricyclic or polycyclic aromatics [49]. It was found in another study that bicyclic molecules such as tetralin and 1-methylnaphthalene (figure 1.18) performed better than mono ring solvents such as toluene and benzene [50].

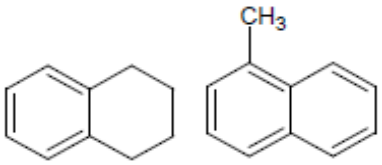

Figure 1.18 *Structures of tetralin and 1-methylnaphthalene [6].*

High temperatures and turbulent conditions will improve the dissolution rate of the deposited asphaltene [6].

Carbon disulphide is a good asphaltene dissolver, aromatic solvents which contain heteroatoms and polar groups should be able to dissolve asphaltenes well, since the asphaltenes also contain heteroatoms which give some polarity [6].

It was shown that the cosolvent polarity can be adjusted to the asphaltene type in the considered field by combining aromatic solvents and additives with polar functional groups [51]. One patent claimed that quinoline and isoquinoline mixed with aromatic solvents, improve the dissolution rates compared to normal aromatics since these compounds are more polar [52]. Another patent claims improved performance if the aromatic solvent is mixed with benzotriazole[53]. A more toxicologically and environmentally friendly claim is alkyl or alkenyl esters which contain isopropyl benzoate which are good dissolvers [54].

1.5 Asphaltene dispersants (ADs) – different classes

Many ADs have been used in the field for many years and even more are still being researched in the laboratories in order to find better performing, more cost efficient, more health safe and environmentally friendly chemicals. The different classes of low molecular weight, nonpolymeric ADs can be summarized as [6]:

- Very low polarity alkyl aromatics
- Alkylaryl sulphonic acids
- Phosphoric esters and phosphonocarboxylic acids
- Sarcosinates
- Ethercarboxylic acids
- Aminoalkylenecarboxylic acids
- Imidazolines and alkylamide-imidazolines
- Alkylsuccinimides
- Alkylpyrrolidones
- Fattyacid amides and their ethoxylates
- Fatty esters of polyhydric alcoholes
- Ion-pair salts of imines and organic salts
- Ionic liquids

1.5.1 Low-polarity nonpolymeric aromatic amphiphiles

The non-polymeric aromatic amphiphile types of molecules with low polarity do not interact strongly with the asphaltene molecules, however they interact mainly by $\pi - \pi$ interactions between the aromatic rings of naphthalene and the asphaltene monomers. A two ring naphthyl group seems to give a better $\pi - \pi$ interaction than a single phenyl group. These interactions prevent the asphaltene monomers from stacking and flocculating. Figure 1.19 shows a naphthalene based AI. Hexadecylnaphthalene (figure 1.20) is suggested to be an AI rather than an AD because its mechanism is thought to prevent precipitation instead of dispersing precipitates [6].

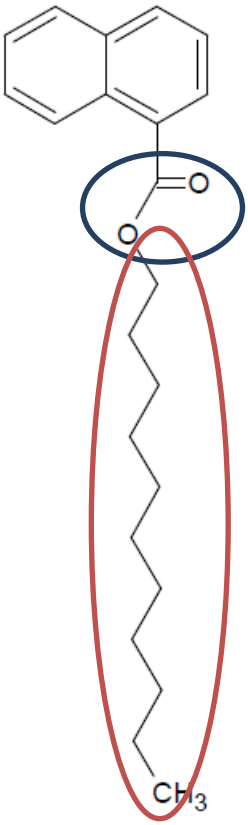

Figure 1.19 *Naphthalene based AIs. The blue group may be for example an ester, ether or amide group. The red group is a long alkyl chain [6].*

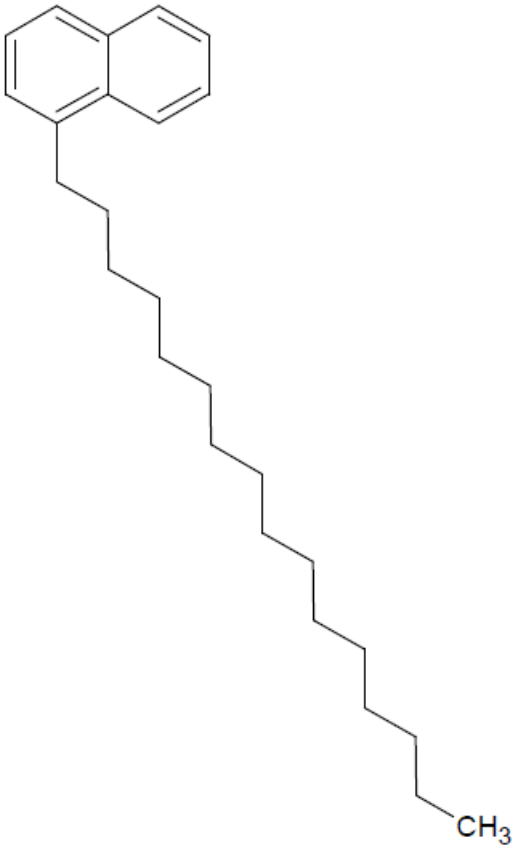

Figure 1.20 *Structure of 1-hexadecylnaphthalene [3].*

A mixture of light aromatic hydrocarbon solvents (for example xylene, toluene etc.) and quinoline or isoquinoline worked better as an asphaltene dissolver than these aromatics worked alone [55]. Dimethyl formamide and N-methyl pyrrolidone (NMP) dissolve asphaltene better than aromatic solvents [6]. Molecular simulations suggest that asphaltene additives with more polar head groups such as pyridinyl, quinolinyl, tetrahydrofuryl and dimethylamidyl should react better with asphaltene molecules than the less polar head groups such as phenyl or naphthyl [56].

1.5.2 Sulphonic acid-based nonpolymeric surfactant ADs

Figure 1.21 shows dodecyl benzene sulphonic acid (DDBSA) which is one of the most common ADs in this class, the sulphonic acid group is only one of many ways of making the aromatic head group of ADs (and AIs) more polar [6].

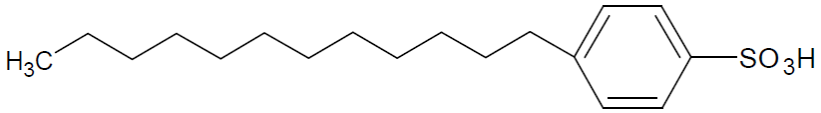

Figure 1.21 *Structure of dodecyl benzene sulphonic acid [6].*

The stabilization of the asphaltene has been found to depend on the head groups of the amphiphiles [57]. This may be explained by the attraction and compatibility with the asphaltenes. For example one study [57] found that the performance of some ADs in decreasing order was DDBSA > nonyl phenol > nonyl benzene di-oxyethylene > nonyl benzene. The hydroxyl group in nonyl phenol creates a more compact planar phenol structure which seems to make a stable $\pi - \pi$ interaction with the asphaltenes. However, the benzene group in the nonyl benzene di-oxyethylene is separated from the hydroxyl group which causes limited $\pi - \pi$ interaction. DDBSA creates effective $\pi - \pi$ interaction with the asphaltenes, in addition the SO_3H group can strengthen the attachment with the asphaltenes because of the polarity, it is more polar than the hydroxyl group [57].
DDBSA have also shown that it sufficiently dissolves asphaltene deposits, and in the same research DDBSA did not show very strong inhibiting effects [58]. This shows that the performance of amphiphiles on the stabilization of asphaltenes depend on for example different types of alkane solvents [57].

An overbased magnesium alkyl aryl aromatic sulphonate is also used to prevent asphaltene deposits in pipelines, however this is used in paraffin hydrocarbon liquids containing small amounts of C_7 asphaltenes [59]. Magnesium (blue arrow) is positively charged by 2+ and the sulphonic groups (red arrows) are each negatively charged with 1-, as figure 1.22 shows.

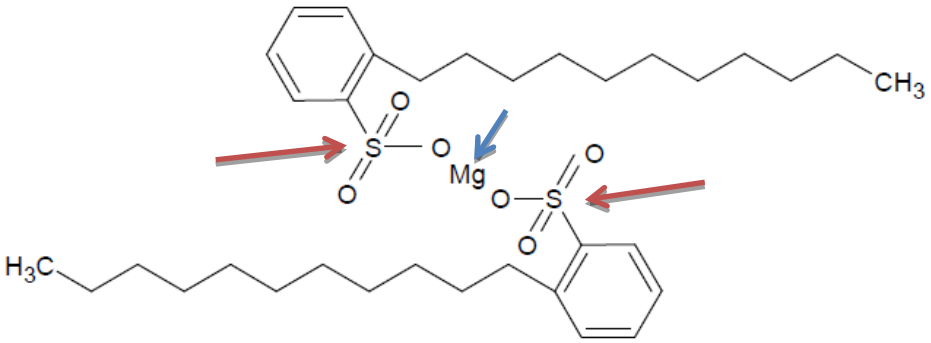

Figure 1.22 *Structure of Dodecyl benzene sulphonic acid magnesium salt (related to Hybase M-401) [1].*

DDBSA has been used as a basis for improvements. It was found that straight carbon chain tails containing over 16 carbons would bond to other AD tails and waxes thus causing crystallisation which decreased solubility in the oil. Also, n-alkyl-aromatic sulphonic acids were known to lose the dispersant effect with time. The improvement solved both these problems where the head group contained sulphonic acid connected to an aromatic group of two fused rings [60-62], see figure 1.23.

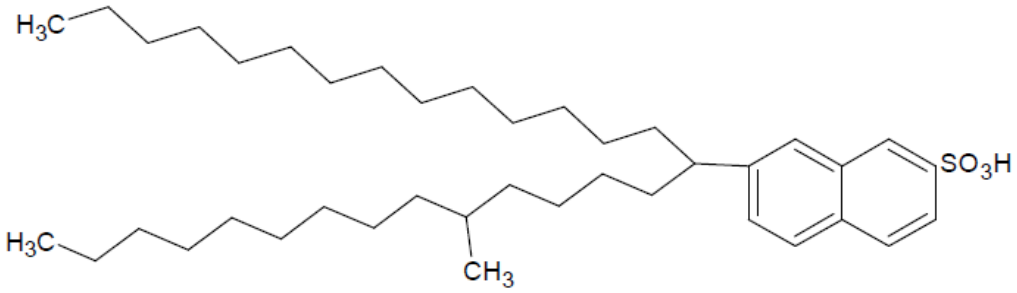

Figure 1.23 *Structure of iso-C15-C15 naphthalene sulphonic acid [6].*

The two tails have preferably a total of 30 carbons or more, and it is even more favourable if the dispersant is a mixture where the tails vary in length. For every 12 carbon there should be a branch of a methyl group or a larger group, which was discovered to effectively increase the solubility of the asphaltenes. This kind of sulphonated alkylnaphthalenes appears to be the best among the sulphonic acid-based monomeric surfactants which has been investigated [60-62].

Other sulphonic acid-based AD has also been tested as asphaltene dispersing agents. For example secondary alkanesulphonic acid with chain lengths of 8 – 22 carbons, the sulphonate group is bound directly to the carbon chain and the aryl group has been removed [63], see figure 1.24.
The alkane sulphonic acids will reduce the amount of precipitation, slow down the precipitation formation rate, form precipitate which is more dispersed and reduce the tendency of the precipitate to deposit on surfaces [63].

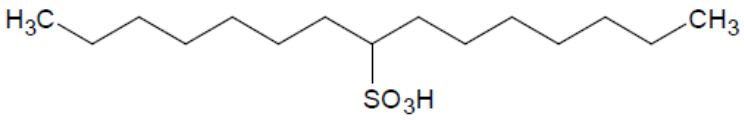

Figure 1.24 *Secondary alkanesulphonic acid [6].*

Hydrocarbon sulphonic acids have also been used in a mixture of for example esters of phosphorous and/or phosphoric acids. This mixture gives a synergistic effect which may provide a superior antifouling protection rather than the effect of the components separately [64].

1.5.3 Non polymeric surfactant ADs with acidic head groups

The additives ability to adsorb to the asphaltene surface is important to stabilize and prevent asphaltene from aggregating and depositing. As mentioned above, DDBSA with the sulphonic acid head group has a suitable affinity for the asphaltene surface, which seemed to work well in stabilizing the asphaltene. Östlund et.al [65] investigated how different amphiphiles adsorbed to asphaltene. They found that amphiphiles which contains basic head groups such as $–NH_2$ had the lowest adsorption of the tested compounds. Compounds which contained –COOH functional groups adsorbed better to the asphaltenes than other sub-groups. This indicates that hydrogen bonding between the acidic additives and the asphaltenes basic sites such as amines and hydroxyl groups are more obvious, than the bonding of basic additives to acidic sites on the asphaltene molecules [6].
Many have further investigated the acid – base interaction between different acidic additives and asphaltenes [65-68]. It was found that phosphono acid or phosphino acid with at least one carboxyl group which is esterified with C_{6-25} alkyl, alkaryl or alkenyl groups, are effective as asphaltene dispersants as well as wax dispersants and scale inhibitors [69].

Aliphatic alcohol-phosphoric acid derivatives which contains C_{10-20} aliphatic alcohol partial esters of phosphoric acids, stabilizes the asphaltenes in bituminous liquids [67].
Ethercarboxylic acids (figure1.25) of the given formula (I) below can also be used to prevent precipitation and/or deposition of asphaltenes.

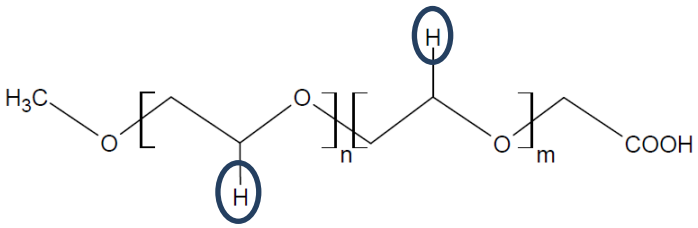

Figure 1.25 *Example of an ethercarboxylic acid, the circled groups can be either H or Me [6].*

I. $RO(CH_2CHR_1O)_x(CH_2CHR_2O)_yCH_2CO_2H$

The R can be C_{6-22} –alkyl, or –alkenyl, C_{6-20} –alkylaryl, R_1 and R_2 are independent of one another and can be H or methyl groups. X and Y are also independent of one another and can be a number between 0 – 20, the total of X and Y is 1 – 20.
The preferred composition is C_{9-18} – alkyl or –alkenyl, the R groups is H and x and y are a total of 1.5 – 8[66].

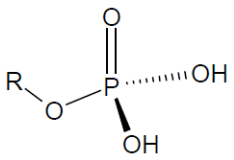

Figure 1.26 *Structure of phosphoric monoester, R is an alkyl or an alkylaryl group [6].*

Most of the phosphoric esters (figure 1.26) and carboxylic acids do not contain aromatic groups, meaning that these additives cannot interact via π – π overlap with the asphaltenes. Both do however contain very acidic protons which may bind to amines or hydroxyl groups in the asphaltene molecule via hydrogen bonding [6]. A preferred structure of esters of phosphoric acid blended with fatty acid oligo-dialkanolamides is shown in figure 1.27 [6, 14]. Both π – π interactions and hydrogen bonding can take place between this AD and the asphaltene molecules.

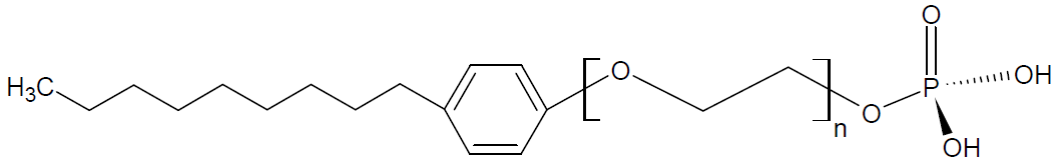

Figure 1.27 *Preferred phosphoric ester of alkylphenylethoxylates AD [6].*

Sarcosinate surfactants are patented as asphaltene dispersants. A general structure is seen in figure 1.28, where R_1 is $C_{7\text{-}21}$ alkyl or alkenyl, and R_2 is a H or $C_{1\text{-}22}$ alkyl group [70].

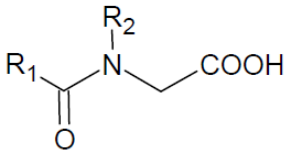

Figure 1.28 *General structure of a sarcosinate AD [6].*

Another class of amphiphiles containing an acidic head group are the reaction products of amines and unsaturated organic acids. These ADs will increase demulsibility, reduce sediment formation, reduce surface fouling and corrosion in addition to dispersing the asphaltene [6, 71]. General structures of these are shown in figure 1.29.

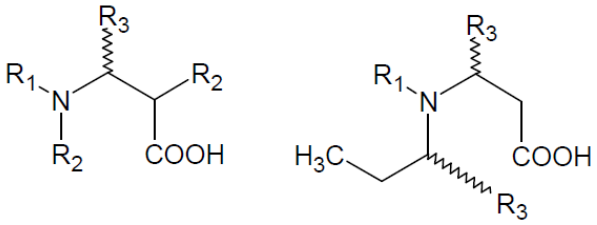

Figure 1.29 *General structures of reaction products of amines and unsaturated organic acids [6].*

1.5.4 Amide and imide nonpolymeric surfactant ADs

Several nonionic amphiphiles with amide or imide groups (figure 1.30) have been claimed as AD's and some are used commercially [6]. The *N,N*-dialkylamides and alkylpyrrolidones (figure1.31) are some of the simplest in the amide classes and contains a single amide group and no other functional group. The 5-ring structure in the alkylpyrrolidones resembles the pyrrolic groups found in the asphaltenes [6].

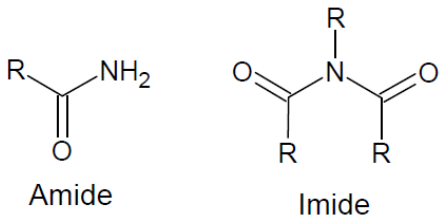

Figure 1.30 *Structure of amide and imide.*

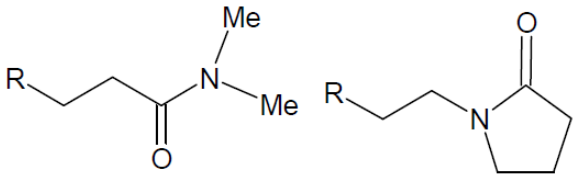

Figure 1.31 *N,N-dialkylamides and alkylpyrrolidone ADs, The R groups are preferably larger than C_8 [6].*

Some dispersants of industrial interest are: polymetacrylates, polyisobutylene succinimides, and polyisobutylene succinates (figure 1.32). For example polyisobutylene succinimides may help to stabilize and/or allow the asphaltenes to repeptize [6, 45].

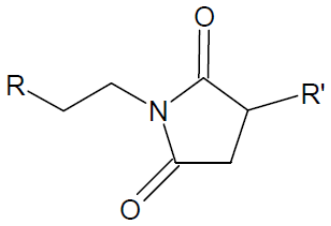

Figure 1.32 *A general structure of alkylsuccinimides [6].*

The imide head group can create hydrogen bonds via either of the carbonyl groups. Mukkamala & Banaval, 2006 [2] claimed a compound which is created from the reaction between alkyl amine ($C_{16\text{-}22}NH_2$) and polyisobutylene succinic anhydride (PIBSA) as an AD. The product takes the formula shown in figure1.33.The R^1 is an alkyl with $C_{10\text{-}22}$ and R^2 is an alkyl with $C_{50\text{-}70}$. This compound will in addition to disperse asphaltene, increase demulsibility, reduce viscosity, reduce deposition formation, reduce surface fouling and reduce corrosion[2]. Both carboxyl groups and amide groups should be included in the reaction product as well as one or more alkyl chain tails to get the best effect [72].

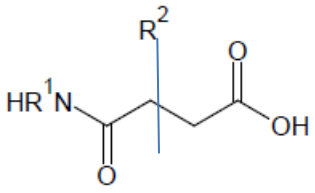

Figure 1.33 *Alkyl amine reactions with PIBSA [2]*

The Flowsolve 110 and 120 series are products of JD Horisons, these additives are developed to inhibit/disperse asphaltenes for oil field applications [73]. The Flowsolve series are based on polyisobutylene succinic anhydride (PIBSA) which is further reacted with different functional groups such as alcohols and amines with aromatic and polar groups. The PIBSA are made from isobutylene and maleic anhydride [74].

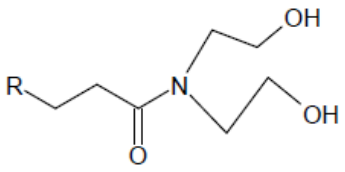

Figure 1.34 *Fatty acid diethanolamides [6].*

Blends of phosphoric esters of alkylphenylethoxylates and fatty acid diethanolamines are effective ADs [14]. Figure 1.34 shows the structure of diethanolamides, which can form hydrogen bonds with asphaltene via the three functional groups.
More advanced blends of alkylarylsulphonic acids, condensation products of fatty acids and emulsifiers have been patented as ADs. This mixture will remove solid asphaltene residues from the surface of formation and production or refining equipment, it will also prevent asphaltenes from precipitating [75].

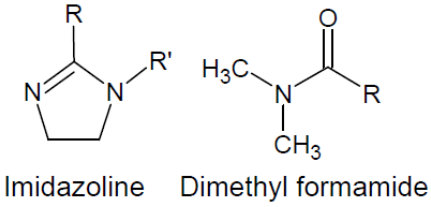

Figure 1.35 *Imidazoline and dimethyl formamide [6].*

Condensation products of fatty acids to form N-substituted imidazolines (NSI) mixed with dimethyl formamide (DMF) (figure 1.35) and aromatic solvents are claimed to dissolve and disperse asphaltenes [76]. The unsaturated imidazoline rings form π – π orbital overlap with the aromatic rings in asphaltene [6].
The π – π interaction will be similar for the following compounds 1) and/or 2). 1) is the condensation of at least one cyclic anhydride and at least one linear N-alkyl-polyamine, 2) a reaction product of an ethylated amine with at least one carboxylic acid. Some examples are

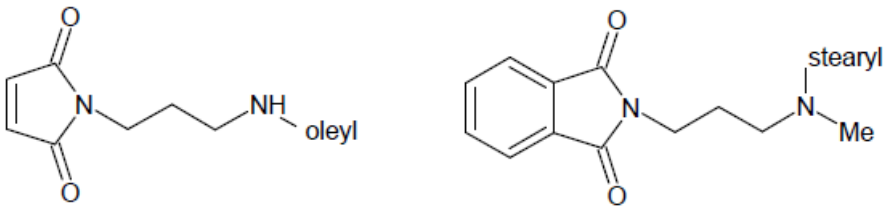

Figure 1.36 *The structure of the reaction product of N-oleyl-diamino-1,3-propane with maleic anhydride(left). Structure of the reaction product of phthalic anhydride with N-stearyl methyl-1-diamino-1,3-propane (right) [6].*

the reaction of N-oleyl-diamino-1,3-propane with maleic anhydride (figure 1.36 left) and the reaction of phthalic anhydride with N-stearyl methyl.-1-diamino-1,3-propane (figure 1.36 right) [6, 77]. These are claimed to prevent flocculation of asphaltenes.

1.5.5 Alkylphenols and related ADs

Alkylphenols are known as an environmental hazard and cannot be used in certain regions. These compounds are known to interfere with the hormone systems of marine animals. However, these ADs have been used commercially for downstream applications [6]. There has been much investigation around monomeric alkylphenols (figure 1.37) as ADs. It is believed that the mildly acidic phenolic head group resembles parts of the asphaltene structures.

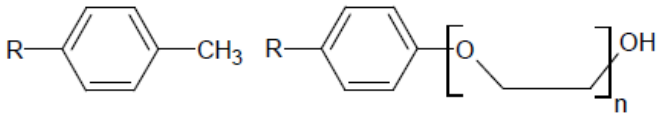

Figure 1.37 *The structure of 4-alkylphenols and 4-alkylphenyl ethoxylates [6].*

One study suggests that an increase in the alkyl tail size will enhance the performance of the alkylphenols [78]. Dodecylphenol (DDP) is the best AD in this class [6]. It was suggested that a short chain amphiphile will not be able to create a steric stabilization layer and will then coprecipitate with asphaltenes. However, a long chain may cover the surface of the asphaltene better, thus produce a more effective steric stabilization against asphaltene flocculation. If the chain length is too long, it may lead to a poor interaction with the asphaltene surface [35, 78].

Another study showed that making the head of the amphiphile more polar will reduce the performance as an asphaltene inhibitor (AI) [6, 10]. The tested components were p-(n-nonyl) phenol (NP), p-(n-dodecyl) phenol (DP) and p-(n-nonyl) phenol ethoxylate (NPE), see figure 1.38 which shows the structure of each of these. The NP> DP> NPE was the results where NPE had the more polar head of the amphiphiles [10, 35].

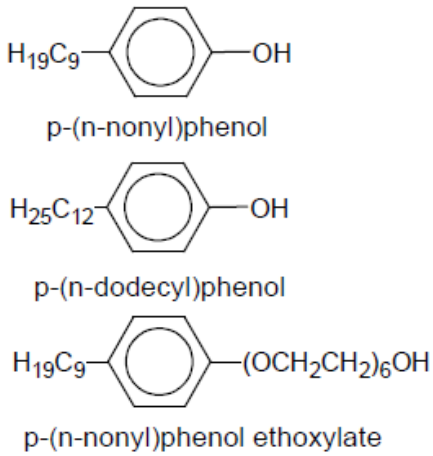

Figure 1.38 *Structures of p-(n-nonyl) phenol (NP), p-(n-dodecyl) phenol (DP) and p-(n-nonyl) phenol ethoxylate (NPE) [10].*

Alkylphenols contains a π-interacting aromatic ring and a hydrogen bonding polar group, giving this class the activity of ADs. The two mentioned features can be found in ether carboxylic phenyl ester amphiphiles which are incorporated with a phenyl ring attached to a polar chain made of an ester group and one or more alkoxylate chains [6].

1.5.6 Ion pair surfactant ADs

Oil-soluble ion-pair surfactants may possibly bind to the metals in asphaltenes which can improve their adsorption. These ADs were claimed in the early nineties. A mixture of alkylarylsulphonic acid and alkylimidazoline will form an anion-cation ion pair when the acid proton is lost to the imidazoline [6].

An oil soluble salt, which is a reaction product of an imine mixed with an acid preferably carboxylic, phosphoric or sulphonic acid will probably exist as ion pairs (figure 1.39).

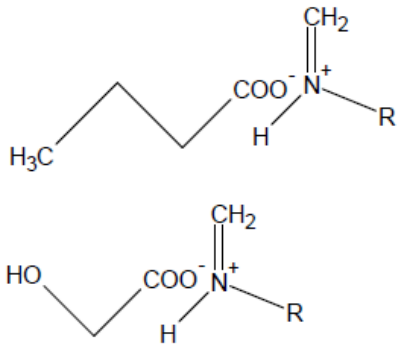

Figure 1.39 *Ion pair salt reaction products of imines and organic acids [6].*

This compound is said to disperse asphaltenes, increase demulsibility, reduce sediment formation, reduce surface fouling and reduce corrosion [6, 79].

Another ion pair AD consists of the reaction product of an imidazoline compound with two $C_{9\text{-}21}$ alkyl groups or one $C_{9\text{-}21}$ alkenyl group together with an organic acid with at least two carbons and at least one –OH group or at least one additional carboxyl group.

1.6 Asphaltene inhibitors (AIs) – different classes

AIs have successfully been squeezed in problem wells which have prevented premature failure due to asphaltene plugging in the tubing. Also continuous injection treatments have solved problems with asphaltene plugging. However, it does not help with deposition in the formation, which may be one of the most damaging places for asphaltene to deposit [80, 81]. The use of squeeze treatment requires that the inhibitor stick to the rock which will give a longer AI squeeze treatment lifetime. The different classes of oligomeric (2-12 monomer units) and polymeric (>12 monomer units) AIs can be summarized as [6]:

- Alkylphenol/aldehyde resins and similar sulphonated resins
- Polyolefin esters, amides, or imides with alkyl, alkylenephenyl, or alkylenepyridyl functional groups
- Alkenyl/vinyl pyrrolidone co polymers
- Graft polymers of polyolefins with maleic anhydride or vinylimidazole
- Hyperbranched polyester amides
- Lignosulphonates
- Polyalkoxylated asphaltenes

1.6.1 Alkylphenol-aldehyde resin oligomers

Several reports have been made on polyalkylphenol resins as effective AIs. It seems the performance depend on the polymerization procedure when making these additives. The alkylphenol-aldehyde resin oligomers (figure 1.40) are regularly used in the oil industry and are among the most investigated polymeric AIs [6].

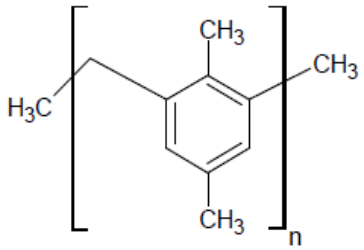

Figure 1.40 *Alkylphenol formaldehyde resin AI [6].*

A study was made where nonylphenol (NP), nonylphenolic formaldehyde resin (NPR) and native resins (NR) were compared as AIs, in decreasing order. The results were NPR>NR>NP. The adsorption mechanism was explained in two steps. First, the amphiphiles adsorb to the asphaltene surface individually then the amphiphiles aggregates in the surface whereas the interactions between the amphiphiles become predominant [82, 83]. A more theoretical study suggested that stability between the dipole moment and the polarizability of the amphiphile is necessary in order to obtain maximum adsorption energy of the amphiphiles onto the asphaltenes [83].

Different improvements on the normal alkylphenol-formaldehyde resin AIs have been patented. For example sulphonated alkylphenol formaldehydes have been used as AIs [84, 85]. These structures resemble DDBSA units joined together, so the polymer has several areas for acid-base and hydrogen bonding interaction to asphaltene. Alkylphenol formaldehyde resins treated with polyamines were found to give a better performance than alkylaryl sulphonic acid based products in caustic-treated petroleum crude oil [86].

Some additives which give a synergistic effect, thus improving the AI performance, have also been used. Alkylphenol formaldehyde resins and oxalkylated amines have shown better effect together than the compounds alone [87]. A blend of nonyl phenol-formaldehyde resins and hydrophilic-lipophilic vinylic polymer showed an improved performance compared to the resins used alone [88]. Another patent specified the hydrophilic monomers which should be mixed with alkylphenol-formaldehyde resin. The monomers mentioned should consist of (meth) acrylic acid, (meth) acrylic-acid salts and (meth) acrylic acid alkoxylate esters [89, 90].

1.6.2 Polyester and polyamide/imide AIs

AI polyesters and polyamides/imides have for some time been used by several service companies [91]. Reactions with acrylic and/or maleic anhydride monomers will usually give the ester groups in polyester and the amide groups in polyamide. When used in squeeze applications, unesterified monomers of the abovementioned types allows the incorporation of free carboxylic groups which will adsorb better to the formation. Examples of typical esters are (meth) acrylate copolymers, styrene/maleate ester and alkene/maleate ester copolymers (figure 1.41), all which are commercial AIs. To make polyamides, the ester groups can be substituted with amide groups [6].

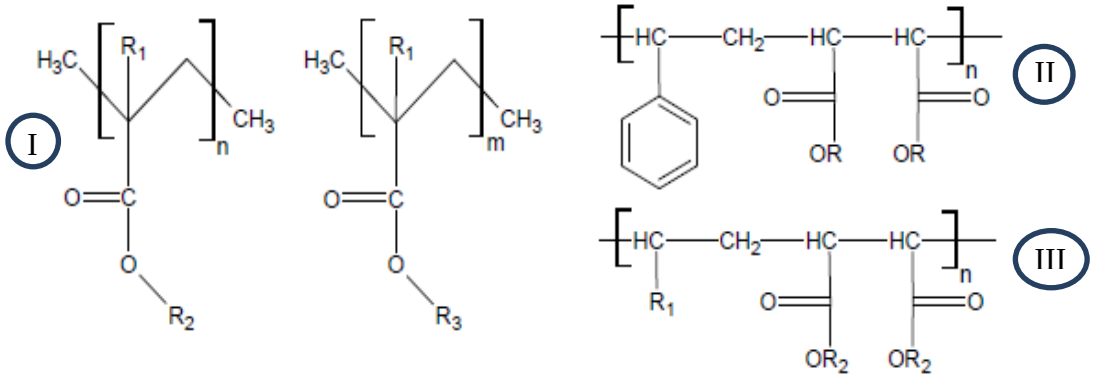

Figure 1.41 *Structures of I - (meth)acrylate, II - styrene/maleate diester and III - alkene/maleate diester copolymers [6]*

If the copolymer contains hydrophilic monomers, the polarity will increase and give stronger hydrogen bonding interactions with the asphaltenes [89, 92]. A hydrophilic-lipophilic copolymer with the major content being lipophilic has been claimed as an AI, for example lauryl (meth) acrylate/hydroxyethyl (meth) acrylate copolymers [89].
Polymers or polyesters have been claimed as AIs. They are made of partially derivatizing polycarboxylic acids with amines or alcohols containing ring structures such as aromatic or heterocyclic rings [93]. Two examples are p-nonylphenyl methacrylate and p-dodecylphenyl methacrylate shown in figure 1.42. The R group (red circle) has nine (nonyl) to twelve (dodecyl) carbons.

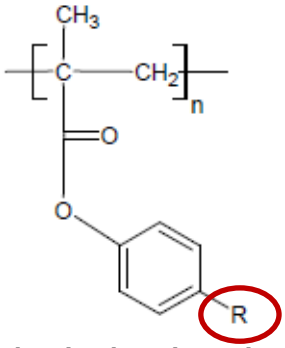

Figure 1.42 *4-alkylphenylmethacrylate polymer AIs. The R group (red circle) has nine (nonyl) to twelve (dodecyl) carbons [6].*

Another class of polyesteramides which may be used to solve asphaltenes are hyperbranched polyesteramides (figure 1.43). They have alkyl groups pointing out in every direction in a three dimensional, dendrimeric structure and are made by (self-) condensation reactions between cyclic anhydrides and di- or trialkanolamines.

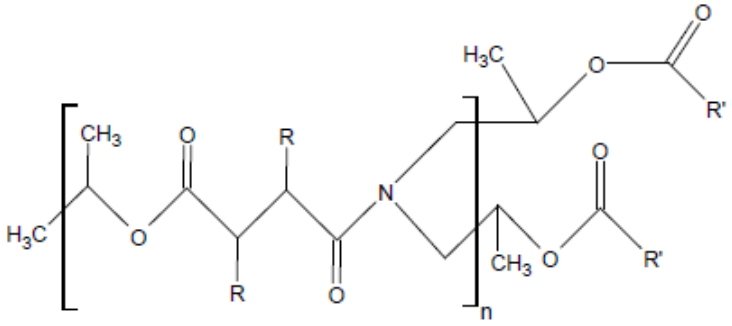

Figure 1.43 *Stuctural units and the end groups in hyperbranched polyesteramide AIs [6].*

A preferred example is a mixture of succinic anhydride and di-isopropanolamine [94]. The R groups can be either H or hydroxyl and the R' groups are long alkylchains.

1.6.3 Other polymeric AIs

The use of graft copolymers as AIs has been patented [95-97]. Graft copolymers consist ordinarily of a linear backbone of one composition and another composition which is randomly distributed branches as shown in figure 1.44. There are in general three methods for preparing graft copolymers [98]:

- Grafting onto, this requires a complementary functionality on the graft unit and the backbone.
- Grafting through, this method use polymer chains with copolymerizable moiety at the end of the chains.
- Grafting from, this method use a backbone with reactive sites that is capable of initiating a polymerization.

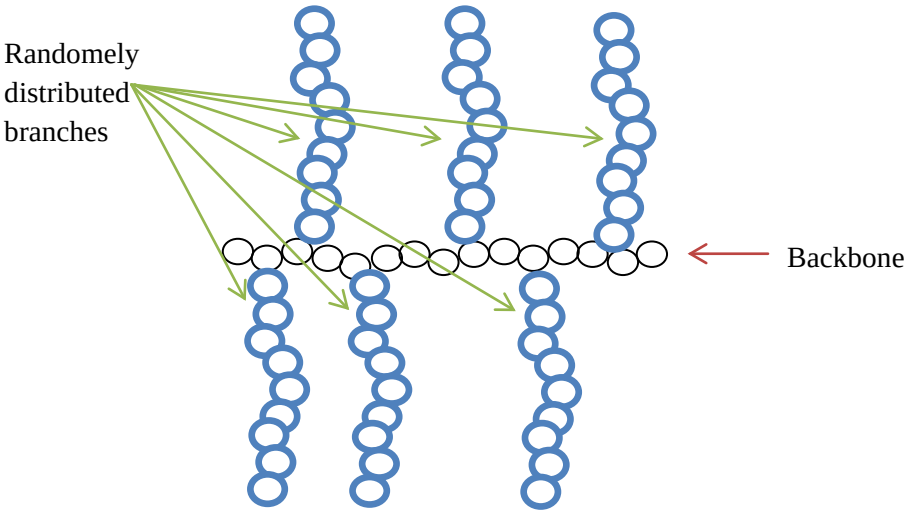

Figure 1.44 *Grafting polymer.*

The patented graft polymers are made by grafting a vinylicmonomer containing oxygen or nitrogen atoms with a polyolefin. Examples of the vinylic monomers which can be used are N-vinylimidazole and 4-vinylpyridine [95-97] (figure1.45).The R group is preferably an alkyl chain.

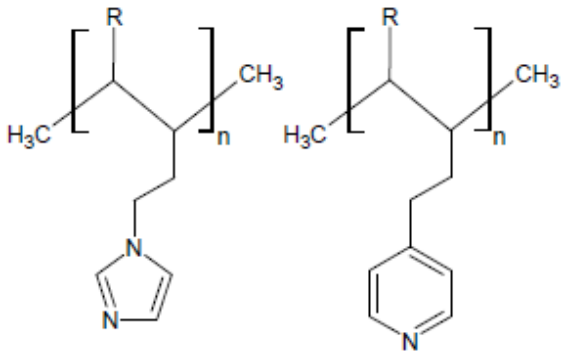

Figure 1.45 *Graft polymer AIs imidazole pendant or pyrimidine rings [6].*

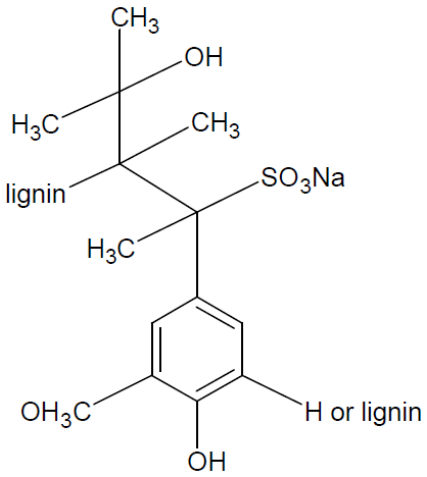

Figure 1.46 *The partial structure of a lignosulphonate [6].*

The lignosulphonates (figure 1.46) have been used in squeeze treatments. It adsorbs to the formation surface so the asphaltene is not able to adsorb to the surface itself.
One patent claims that biodegradable molecules or a mixture of biodegradable molecules can stabilize asphaltenes in crude oil. Molecules containing tetrapyrrolitic patterns such as chlorophyll-based molecules extracted from plant leaves have been suggested [6, 99].

1.7 References

1. *Chemical Book.* [cited 2012 11.05]; Chemical information, structures etc.]. Available from: http://www.chemicalbook.com/.
2. Mukkamala, R. and R.M. Banavali, *Compounds containing amide and carboxyl groups as asphaltene dispersants in crude oil*, 2006, Google Patents.
3. *ChemSpider*, 2012, Royal Society of Chemistry.
4. Hart, H., *Organic chemistry: a short course*2007, Boston: Houghton Mifflin. XXIV, 577 s.
5. Murgich, J., *Molecular simulation and the aggregation of the heavy fractions in crude oils.* Molecular Simulation, 2003. **29**(6-7): p. 451-461.
6. Kelland, M.A., *Production Chemicals for the Oil and Gas Industry*, CRC Press, Boca Raton, FL., 2009
7. australia, N.t.o., *Petroleum act*, 2011.
8. Murgich, J., Rodríguez, and Y. Aray, *Molecular Recognition and Molecular Mechanics of Micelles of Some Model Asphaltenes and Resins.* Energy & Fuels, 1996. **10**(1): p. 68-76.
9. Speight, J.G., *The chemical and physical structure of petroleum: effects on recovery operations.* Journal of Petroleum Science and Engineering, 1999. **22**(1–3): p. 3-15.
10. León, O., E. Contreras, and E. Rogel, *Amphiphile adsorption on asphaltene particles: adsorption isotherms and asphaltene stabilization.* Colloids and Surfaces A: Physicochemical and Engineering Aspects, 2001. **189**(1-3): p. 123-130.
11. Rana, M.S., et al., *A review of recent advances on process technologies for upgrading of heavy oils and residua.* Fuel, 2007. **86**(9): p. 1216-1231.
12. Venkatesan, R., et al., *The strength of paraffin gels formed under static and flow conditions.* Chemical Engineering Science, 2005. **60**(13): p. 3587-3598.
13. Sayyad Amin, J., et al., *Investigating the effect of different asphaltene structures on surface topography and wettability alteration.* Applied surface science, 2011. **257**(20): p. 8341-8349.
14. Von Tapavicza, S., et al., *Use of selected inhibitors against the formation of solid organo-based incrustations from fluid hydrocarbon mixtures*, 2002, Google Patents.
15. Odland, P.J., *Subsea production systems*, in *Offshore field development*2010: Stavanger.
16. Kaczmarski, A.A. and S.E. Lorimer, *Emergence of Flow Assurance as a Technical Discipline Specific to Deepwater: Technical Challenges and Integration into Subsea Systems Engineering*, in *Offshore Technology Conference*2001: Houston, Texas.
17. Frenier, W.W. and M. Ziauddin, *Formation, removal, and inhibition of inorganic scale in the oilfield environment*2008, Richardson, Tex.: Society of Petroleum Engineers. x, 230 s.
18. Nengkoda, A., et al., *A Current Mapping and Predicting of Indonesia Flow Assurance Challenges Based on Fluid Physical Characteristics*, in *SPE Asia Pacific Oil and Gas Conference and Exhibition*2011, Society of Petroleum Engineers: Jakarta, Indonesia.
19. Akbarzadeh, K., et al., *The Importance of Wax-Deposition Measurements in the Simulation and Design of Subsea Pipelines.* SPE Projects, Facilities & Construction, 2010. **5**(2): p. pp. 49-57.
20. Addison, G.E., *Identification and Treating of Downhole Organic Deposits*, in *SPE Production Operations Symposium*1989, 1989 Copyright 1989, Society of Petroleum Engineers, Inc.: Oklahoma City, Oklahoma.
21. Yang, X. and P. Kilpatrick, *Asphaltenes and Waxes Do Not Interact Synergistically and Coprecipitate in Solid Organic Deposits†.* Energy & Fuels, 2005. **19**(4): p. 1360-1375.

22. Carnahan, N.F., *Paraffin Deposition in Petroleum Production.* SPE Journal of Petroleum Technology, 1989. **41**(10): p. 1024-1025, 1106.
23. Lichaa, P.M. and L. Herrera, *Electrical and Other Effects Related to the Formation and Prevention of Asphaltene Deposition Problem in Venezuelan Crudes*, in *SPE Oilfield Chemistry Symposium*1975, 1975 Copyright 1975: Dallas, Texas.
24. Becker, J.R., *Crude oil waxes, emulsions, and asphaltenes*1997, Tulsa, Okla.: PennWell Books. IX, 276 s.
25. Stephenson, W., *Producing asphaltenic crude oils: problems and solutions.* Petroleum Engineer International, 1990. **24**.
26. Sheu, E.Y., O.C. Mullins, and F.P.S. Meeting, *Asphaltenes: fundamentals and applications*1995: Plenum Press.
27. Nalco/Exxon Energy Chemicals, L.P., *Oil field chemicals Training manual Part 7 Asphaltenes*, 1997.
28. Yen, T.F. and G.V. Chilingarian, *Asphaltenes and asphalts*1994, Amsterdam: Elsevier. b.
29. McCain, W.D., *Properties of Petroleum Fluids (2nd Edition)*1990, Tulsa, OK, USA: Pennwell Books.
30. Aiyejina, A., et al., *Wax formation in oil pipelines: A critical review.* International Journal of Multiphase Flow, 2011.
31. Kriz, P. and S.I. Andersen, *Effect of Asphaltenes on Crude Oil Wax Crystallization.* Energy & Fuels, 2005. **19**(3): p. 948-953.
32. Misra, S., S. Baruah, and K. Singh, *Paraffin Problems in Crude Oil Production And Transportation: A Review.* SPE Production & Operations, 1995. **10**(1): p. 50-54.
33. Speight, J.G., *The chemistry and technology of petroleum*1999, New York: Marcel Dekker. XIV, 918 s.
34. Srivaslava, A., et al. *Quantification Of Asphaltene Flocculation During Miscible CO Flooding In The Weyburn Reservoir*. 1993.
35. Chang, C.L. and H.S. Fogler, *Stabilization of asphaltenes in aliphatic solvents using alkylbenzene-derived amphiphiles. 1. Effect of the chemical structure of amphiphiles on asphaltene stabilization.* Langmuir, 1994. **10**(6): p. 1749-1757.
36. King, S.R. and C.R. Cotney, *Development and Application of Unique Natural Solvents for Treating Paraffin and Asphaltene Related Problems*, in *SPE Mid-Continent Gas Symposium*1996, 1996 Copyright 1996, Society of Petroleum Engineers, Inc.: Amarillo, Texas.
37. Mullins, O.C., et al., *Structures and Dynamics of Asphaltenes: Edited by Oliver C. Mullins and Eric Y. Sheu*1998: Plenum Press.
38. Yen, E.C.T.a.T.F., *Association of vanadium chelates in petroleum asphaltenes as studied by ESR.* Fuel, 1969. **43**: p. 191-208.
39. Mullins, O.C., *The Modified Yen Model†.* Energy & Fuels, 2010. **24**(4): p. 2179-2207.
40. Marques, L.C.C., J.B. Monteiro, and G. González, *Asphaltenes flocculation in light crude oils: A chemical approach to the problem.* Journal of dispersion science and technology, 2007. **28**(3): p. 391-397.
41. Jamaluddin, A.K.M., et al., *A Comparison of Various Laboratory Techniques to Measure Thermodynamic Asphaltene Instability*, in *SPE Asia Pacific Improved Oil Recovery Conference*2001, 2001,. Society of Petroleum Engineers Inc.: Kuala Lumpur, Malaysia.
42. Koots, J.A. and J.G. Speight, *Relation of petroleum resins to asphaltenes.* Fuel, 1975. **54**(3): p. 179-184.
43. Mullins, O.C., *Asphaltenes, heavy oils, and petroleomics*2007, New York: Springer. XXI, 669 s.

44. Oschmann, H.J., *New Methods for the Selection of Asphaltene Inhibitors in the Field.* SPECIAL PUBLICATION-ROYAL SOCIETY OF CHEMISTRY, 2002. **280**: p. 254-263.
45. FERRARA, M., *HYDROCARBON OIL-AQUEOUS FUEL AND ADDITIVE COMPOSITIONS*, 1995, WO Patent WO/1995/020,637.
46. Marugán, J., et al., *Characterization of the Asphaltene Onset Region by Focused-Beam Laser Reflectance: A Tool for Additives Screening†.* Energy & Fuels, 2008. **23**(3): p. 1155-1161.
47. Del Bianco, A. and F. Stroppa, *Effective hydrocarbon blend for removing asphaltenes*, 1995, Google Patents.
48. Jamaluddin, A.K.M. and T.W. Nazarko, *Process for removing and preventing near-wellbore damage due to asphaltene precipitation*, 1995, Google Patents.
49. Charles W. Benson, R.A.S.a.I.C.H., *Tailoring aromatic hydrocarbons for asphaltene removal.* royal society of chemistry no.97, 1991. **97**: p. 215-233.
50. Canonico, L.B., et al., *A comprehensive approach for the evaluation of chemicals for asphaltene deposit removal.* Special Publications of the Royal Society of Chemistry, 1994. **159**: p. 220-233.
51. Minssieux, L., *Removal of asphalt deposits by cosolvent squeeze: Mechanisms and screening.* SPE Journal, 2001. **6**(1): p. 39-46.
52. Delbianco, A. and F. Stroppa, *Composition effective in removing asphaltenes*, 1997, Google Patents.
53. Lawson, M.B. and K.J. Snyder, *Method for dissolving asphaltic material*, 1977, Google Patents.
54. *MAINTENANCE OF OIL PRODUCTION AND REFINING EQUIPMENT*, 2001, WO Patent WO/2001/074,966.
55. Delbianco, A. and F. Stroppa, *Composition effective in removing asphaltenes*, 2003, EP Patent 0,737,798.
56. Takanohashi, T., S. Sato, and R. Tanaka, *Molecular dynamics simulation of structural relaxation of asphaltene aggregates.* Petroleum Science and Technology, 2003. **21**(3-4): p. 491-505.
57. Chang, C.-L. and H.S. Fogler, *Asphaltene Stabilization in Alkyl Solvents Using Oil-Soluble Amphiphiles*, in *SPE International Symposium on Oilfield Chemistry*1993, 1993 Copyright 1993, Society of Petroleum Engineers, Inc.: New Orleans, Louisiana.
58. Rocha Junior, L.C., M.S. Ferreira, and A.C. da Silva Ramos, *Inhibition of asphaltene precipitation in Brazilian crude oils using new oil soluble amphiphiles.* Journal of Petroleum Science and Engineering, 2006. **51**(1): p. 26-36.
59. Dickakian, G.B., *Antifoulant additive for light end hydrocarbons*, 1990, Google Patents.
60. Varadaraj, R. and C.H. Brons, *Branched alkyl-aromatic sulfonic acid dispersants for dispersing asphaltenes in petroleum oils*, 2003, Google Patents.
61. Wiehe, I.A., et al., *Branched alkyl-aromatic sulfonic acid dispersants for solublizing asphaltenes in petroleum oils*, 2000, Google Patents.
62. Wiehe, I.A. and T.G. Jermansen, *Design of synthetic dispersants for asphaltenes.* Petroleum Science and Technology, 2003. **21**(3-4): p. 527-536.
63. Miller, D., A. Vollmer, and M. Feustel, *Use of alkanesulfonic acids as asphaltene-dispersing agents*, 1999, Google Patents.
64. Miller, R.F., *Method for minimizing fouling of heat exchangers*, 1984, Google Patents.
65. Östlund, J.A., et al., *Functional groups in fractionated asphaltenes and the adsorption of amphiphilic molecules.* Colloids and Surfaces A: Physicochemical and Engineering Aspects, 2004. **234**(1): p. 95-102.

66. Miller, D., et al., *Ethercarboxylic acids as asphaltene dispersants in crude oils*, 2000, Google Patents.
67. Stout, C.A., *Method of inhibiting precipitation of asphaltenes*, in *Canadian patent*1983: USA.
68. Auflem, I., T. Havre, and J. Sjöblom, *Near-IR study on the dispersive effects of amphiphiles and naphthenic acids on asphaltenes in model heptane-toluene mixtures.* Colloid & Polymer Science, 2002. **280**(8): p. 695-700.
69. WOODWARD, G., *NOVEL PHOSPHONOCARBOXYLIC ACID ESTERS*, 2004, WO Patent WO/2004/002,994.
70. MILLER, D., et al., *USE OF SARCOSINATES AS ASPHALTENE DISPERSANTS*, 1998, WO Patent WO/1998/016,595.
71. Mukkamala, R., *Amine-unsaturated acid adducts as asphaltene dispersants in crude oil*, 2003, EP Patent 1,359,206.
72. Banavali, R. *Reducing viscosity of asphaltenic crudes via chemical additives*. in *Proceedings of the Chemistry in the oil industry VIII Symposium: an international symposium*. 2003. Staffordshire: Royal Society of Chemistry.
73. Dunlop, D.J. *JD Horizons, solutions in chemistry*. 1999 [cited 2012 19.05]; Today JD Horizons primary business activity is centred on the development and marketing of proprietary chemicals technology for oil industry markets with special emphasis on oilfield chemicals and flow assurance applications. Flowsolve products.]. Available from: http://www.jdhorizons.com/.
74. Kelland, M.A., *Flowsolve products*, 2012, Eirin L. Abrahamsen: Stavanger.
75. Alain Lesimple, C.-P.H., Didier Groffe, Wolfgang Breuer, *Asphaltene inhibitors*, 2001.
76. Becker, H.L. and B.W. Wolf, *Asphaltene removal composition and method*, 1996, Google Patents.
77. Bernasconi, C., A. Faure, and B. Thibonnet, *Homogeneous and stable composition of asphaltenic liquid hydrocarbons and additive useful as industrial fuel*, 1986, Google Patents.
78. Hu, Y.F. and T.M. Guo, *Effect of the structures of ionic liquids and alkylbenzene-derived amphiphiles on the inhibition of asphaltene precipitation from CO 2-injected reservoir oils.* Langmuir, 2005. **21**(18): p. 8168-8174.
79. Mukkamala, R., *Oil-soluble imine-acid reaction products as asphaltene dispersants in crude oil*, 2003, Google Patents.
80. Cenegy, L.M., *Survey Of Successful World-wide Asphaltene Inhibitor Treatments In Oil Production Fields*, in *SPE Annual Technical Conference and Exhibition*2001, Copyright 2001, Society of Petroleum Engineers Inc.: New Orleans, Louisiana.
81. Allenson, S.J. and M.A. Walsh, *A Novel Way to Treat Asphaltene Deposition Problems Found in Oil Production*, in *International Symposium on Oilfield Chemistry*1997, 1997: Houston, Texas.
82. León, O., et al., *The Influence of the Adsorption of Amphiphiles and Resins in Controlling Asphaltene Flocculation.* Energy & Fuels, 2001. **15**(5): p. 1028-1032.
83. Rogel, E., E. Contreras, and O. Leon, *An experimental theoretical approach to the activity of amphiphiles as asphaltene stabilizers.* Petroleum Science and Technology, 2002. **20**(7-8): p. 725-739.
84. Behler, A., *Use of sulphonated alkyl phenol formaldehydes in the stabilization of ashphaltenes in crude oil*, 2002, Google Patents.
85. BEHLER, A., W. BREUER, and M. HOF, *USE OF SULPHONATED ALKYL PHENOL FORMALDEHYDES IN THE STABILIZATION OF ASHPHALTENES IN CRUDE OIL*, 2003, WO Patent WO/2003/054,348.

86. Manek, M.B. and K.N. Sawhney, *Alkyl substituted phenol-polyethylenepolyamine-formaldehyde resins as asphaltene dispersants*, 1996, Google Patents.
87. Miller, D., et al., *Synergistic mixtures of alkylphenol-formaldehyde resins with oxalkylated amines as asphaltene dispersants*, 2001, Google Patents.
88. Stephenson, W.K., B.D. Mercer, and D.G. Comer, *Refinery anti-foulant-asphaltene dispersant*, 1992, Google Patents.
89. Stephenson, W.K. and M. Kaplan, *Asphaltene dispersants-inhibitors*, 1991, Google Patents.
90. Stephenson, W.K., Walker, J.S., Krupay, B.W. and Wolsey-Iverson, S.A., *Desalting adjunct chemistry*, in *Smart & Biggar*, U. Nalco chemical company, Editor 2004: Canada. p. 45.
91. H.Anfindsen, P.f., and A. M. Mathisen in *9th international oilfield chemical symposium* 1995: Geilo, Norway.
92. W. Stephenson, J.W., B. Krupay and S. Wolsey-Iverson, 1993.
93. Sheetal Handa, P.K.G.H., William James Ferguson, *Asphaltene precipitation inhibiting polymer for use in oils*, 1998. p. 28.
94. CORNELISSE, P. and W. Marinus, *METHOD FOR SOLUBILISING ASPHALTENES IN A HYDROCARBON MIXTURE*, 2002, WO Patent WO/2002/102,928.
95. Boden, F.J., et al., *Polar grafted polyolefins, methods for their manufacture, and lubricating oil compositions containing them*, 1997, Google Patents.
96. Boden, F.J., et al., *Polar grafted polyolefins, methods for their manufacture, and lubricating oil compositions containing them*, 2004, Google Patents.
97. Boden, F.J., et al., *Polar grafted polyolefins, methods for their manufacture, and lubricating oil compositions containing them*, 1999, Google Patents.
98. Davis, K.A. and K. Matyjaszewski, *Statistical, Gradient, Block and Graft Copolymers by Controlled/Living Radical Polymerizations*2002: Springer.
99. ROUET, J., D. GROFFE, and M. SALAUN, *ASPHALTENE-STABILISING MOLECULES HAVING A TETRAPYRROLIC PATTERN*, 2008, WO Patent WO/2008/084,178.

Chapter 2 Design of experiments (DoE)

A mixture of asphaltene dispersants will hopefully give a synergistic effect that can be used to solve some of the deposition problems mentioned in chapter 1. Design of experiments is used as a method or technique for finding an optimal asphaltene dispersant mixture.
Experiments are often separated into three different stages: planning, performance and analysis of the results, the experimental design involves a lot of statistics in the mentioned stages [3]. To design an experiment involves an overview of the number of experiments which is needed to be completed to find an optimal formulation. There are several complex mathematical models involved in these type of processes, so computer software are often used as a tool to create optimal designs which can handle different combinations of mixture components, processing factors (for example time or temperature) and categorical variables (such as supplier and material type) [4]. DoE techniques provide an idea of how the mixtures work together and can then optimize the formulation at a minimum effort and expense [5].

The focus in this thesis will be on mixture design which is the design used for the experiments with the asphaltene dispersants.

2.1 Mixture design

Mixture design can be used when mixing together multiple components. For example when baking a cake, different ingredients are used in different proportions depending on the cake. Or when mixing a fruit juice, different types of juice in different proportions can be mixed. When the proper mixture is found, different properties are of interest. A cake can be fluffy or compact, the fruit juice can have different degrees of flavour depending on the amount of for example grape juice, apple juice and orange juice which is added to the mixture.
One reason for mixing together compounds like this is to investigate if there is a product which is more desirable and can give better properties than the compounds alone.

The mixture problem characteristic is that the response depends on the proportion of the ingredients, not the amount of ingredients. The studied property is assumed to be a real-valued function and is called the response. This leads to two requirements which need to be fulfilled if the mixture simplex is to be used [3].

1. The summation or equality constraint:
$$\sum_{i=1}^{q} X_i = 1$$
This requirement explains that the sum of the components, q, needs to be constant for all experiments, for example 0-100% or fractions between 0 and 1. X_i is the symbol for a component *i* and its proportion in the mixture [2].
2. The nonnegativity constraint:
$$X_i \geq 0 \qquad i = 1, 2, \ldots, q$$
This requirement explains that the components in the mixture cannot have a negative value.

2.2 Simplex lattice method

The simplest of all simplex method is the basic simplex which is always a regular geometrical figure. A simplex is defined as any given number of dimensions that is bounded by the least possible number of hyper planes [6]. This means that for example a simplex with two factors is a triangle, a simplex with three factors is a tetrahedron and a simplex with four factors or more is a hyperpolyhedron [7], this is the case when the factors are independent.
Simplex coordinate system is commonly used with mixture simplexes [8]. In mixture design the factors depend on each other because the total mixture amount will always be the same (the summation or equality constraint), thus a mixture space for a q-component mixture is always a q – 1 dimensional simplex. So a two dimensional factor space is a one dimensional mixture space which means a two component mixture is a single line, a three component mixture is a two dimensional triangle and a four component mixture is a tetrahedron. The simplex lattice models is expressed by the form {q, m} where q is the number of components and m indicates how many line segments each side in the simplex is divided into. Figure 2.01 show some examples of different simplexes [2].

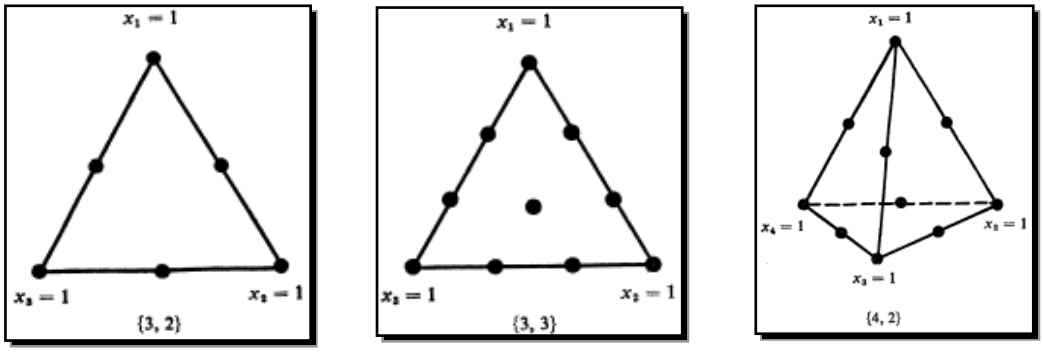

Figure 2.01 *a) shows a three component quadratic simplex, b) shows a three component cubic simplex and c) shows a four component quadratic simplex [2].*

Figure 2.01a) have three vertices (three pure components) and the sides are divided into two line segments, thus it is called a {3, 2} simplex. Similar with figure 2.01b), it has three vertices but the sides now consists of three line segments, so it is called a {3, 3} simplex. Figure 2.01c) is a {4, 2} simplex and has four vertices (four components), the sides are divided into two line segments.
Each point represents an experiment; the number of experiments depends on the number of components and the behaviour of the mixture [9].
The figure 2.02 on the next page shows a simplex coordinate system with three components and three data points are inserted. The orange arrows show the components increasing direction in the coordinate system which is counter clockwise. At the vertices the mixture will consist only of one component. On each axis the mixture will consist of two components as the blue point shows. This data point consists of 45% of component A, 0% of component B and 55% of component C. When the data points are within the simplex (triangle), then the mixture will contain all three components, as the red and green data points show. The green data point consists of 24% of component A, 42% of component B and 34% of component C. The red data point consists of 50% of component A, 30% of component B and 20% of component C.

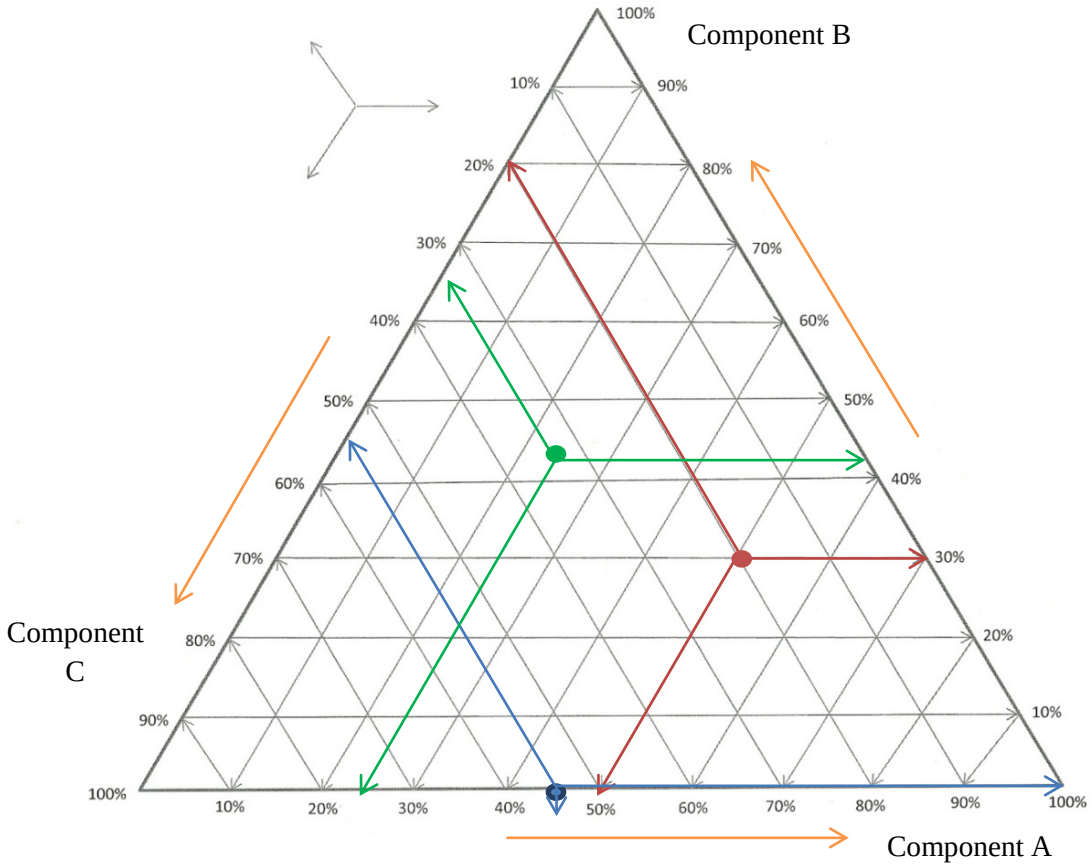

Figure 2.02 *An example of a three component simplex with three data points inserted.*

2.3 Response surface

The response for each of the mixtures is the measured value in the experiment, for example viscosity, turbidity, solubility etc. Figure 2.03 below shows an example of a response surface with three components. The red points are the actual responses which are above the predicted surface and the light pink points are the actual responses which are under the predicted surface.

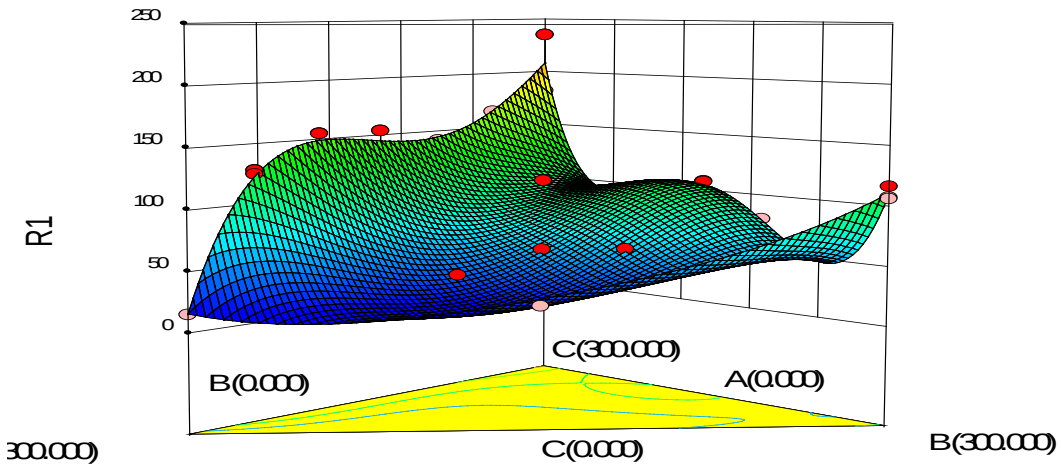

Figure 2.03 *Example of a 3D response surface.*

The blue colour on the surface indicates low predicted response values, green indicates medium predicted response values and red indicates high predicted response values. Mathematical models, so called polynomials, are used to describe these types of response surfaces. The polynomials which are the most commonly encountered in mixture model forms in technical articles, books and software are the Scheffé canonical polynomials [3].

2.4 Models

A response surface may be described by mathematical equations, polynomials. Depending on the number of points, the degree of the polynomial is decided. For example in a two component design, the normal polynomials are of first, second and third degree for the response [10]. In a three component design the normal polynomials will be of second, third and fourth degree which express the response [9].

2.4.1 Linear model for a two component system

A linear model is the simplest model with two coefficients (β_1 and β_2).
The polynomial for a linear model [3, 10]:

$$Y = \sum_{i=1}^{q} \beta_i X_i \qquad \text{(general form)}$$

$$Y = \beta_1 X_1 + \beta_2 X_2 \qquad (2.01)$$

The total number of mixture components are represented with q and X_i is the component *i* and its proportion in the mixture.
A minimum of two mixtures is necessary in order to solve equation (I) although more points are recommended in order to reveal deviations. Figure 2.04 shows a graphical representation of a linear polynomial model.

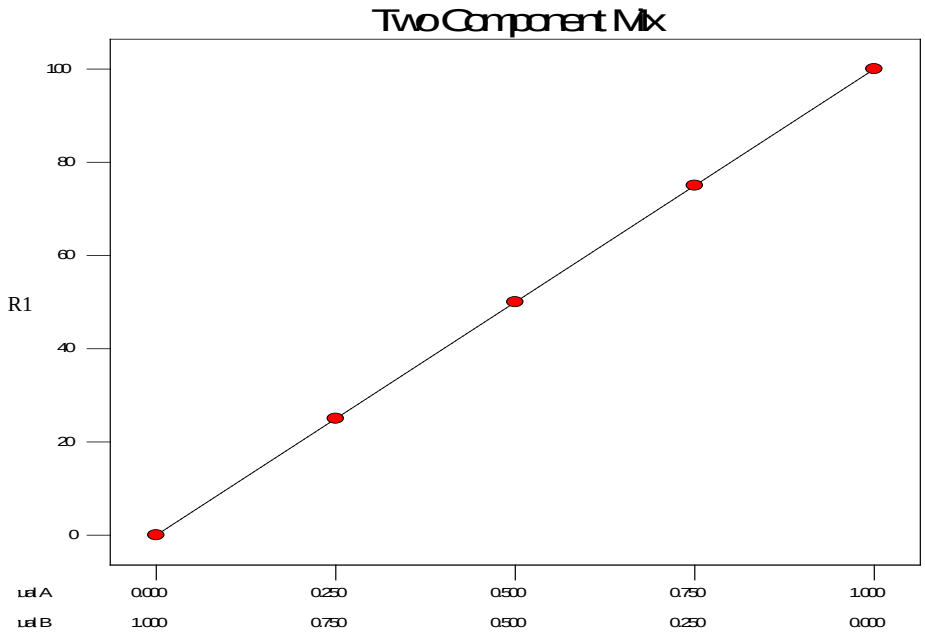

Figure 2.04 *An example of a two component, linear model.*

2.4.2 Quadratic model for a two component system

This model takes into account the second order interaction between the components. This plot can show if the mixture of the components are synergistic or antagonistic. This means that if a high value is desired, blending the components will give a higher value than the components give alone which is a synergistic effect (figure 2.05). Or if blending the components give a lower value than the components give alone the effect is antagonistic (figure 2.06) [3].

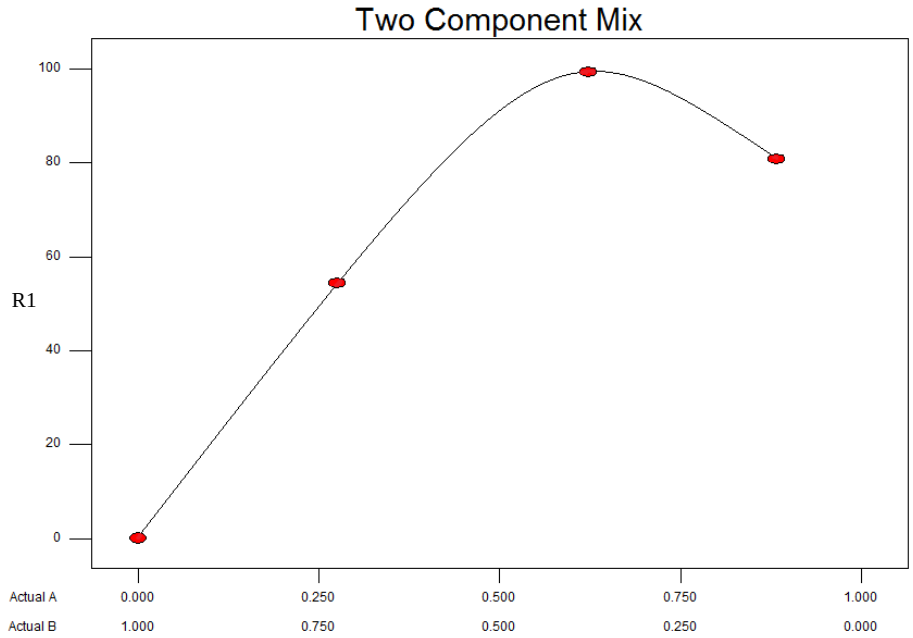

Figure 2.05 *An example of a quadratic model with two components, giving a synergistic effect.*

The polynomial for a quadratic model:

$$Y = \sum_{i=1}^{q} \beta_i X_i + \sum_{i<j}^{q-1} \sum_{j}^{q} \beta_{ij} X_i X_j \qquad \text{(general form)}$$

$$Y = \beta_1 X_1 + \beta_2 X_2 + \beta_{12} X_1 X_2 \qquad (2.02)$$

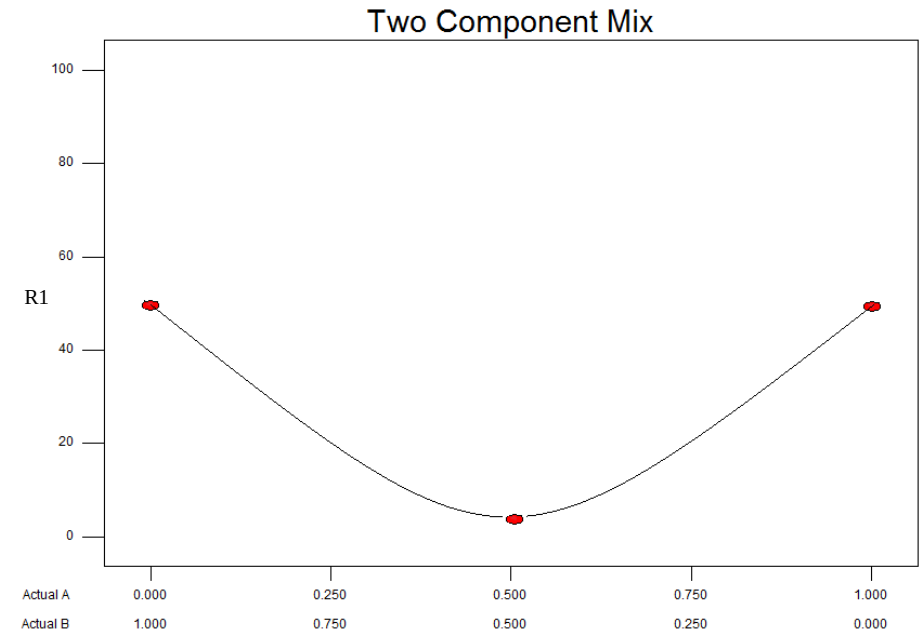

Figure 2.06 *An example of a quadratic model with two components, giving an antagonistic effect.*

2.4.3 Cubic model for a two component system

The cubic model takes into consideration the third order interaction between the components. The polynomial for a cubic model [3, 10]:

$$Y = \sum_i^q \beta_i X_i + \sum \sum_{i<j}^q \beta_{ij} X_i X_j + \sum \sum_{i<j}^q \gamma_{ij} X_i X_j (X_i - X_j) + \sum \sum \sum_{i<j<k}^q \beta_{ijk} X_i X_j X_k \quad \text{(general form)}$$

$$Y = \beta_1 X_1 + \beta_2 X_2 + \beta_{12} X_1 X_2 + \gamma_{12} X_1 X_2 \quad (2.03)$$

Figure 2.07 shows a graphical representation of a typical cubic polynomial model with two components.

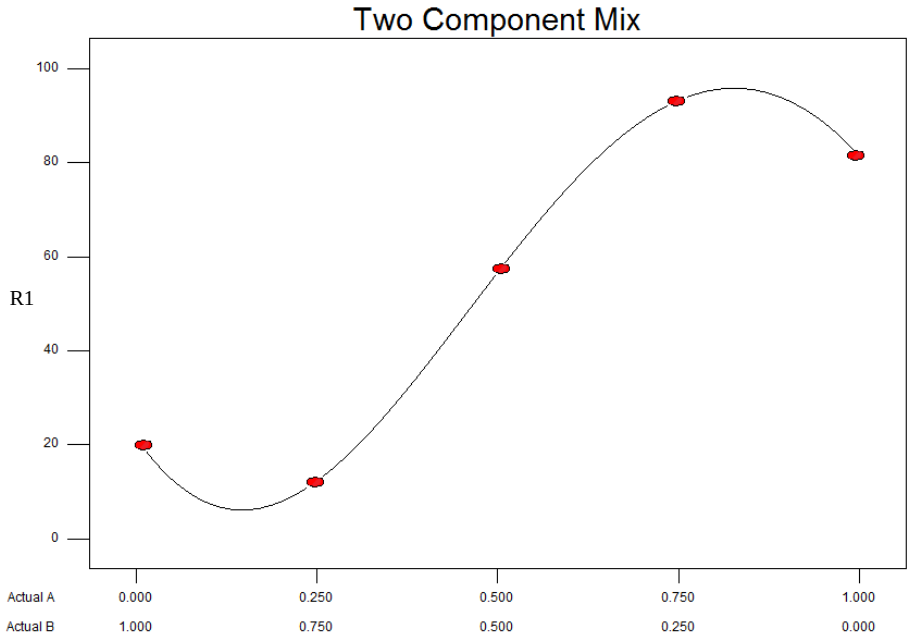

Figure 2.07 *An example of a two component, cubic model.*

In a system with three components, the conditions for the models will be similar to the system with two components. A minimum of experiments need to be performed to be able to use the different models. The polynomials which are the most used in a three component system are [3]:

- Linear model

  $Y = \sum_{i=1}^q \beta_i X_i$ (general form)

  $Y = \beta_1 X_1 + \beta_2 X_2 + \beta_3 X_3$ (2.04)
- Quadratic model

  $Y = \sum_{i=1}^q \beta_i X_i + \sum_{i<j}^{q-1} \sum_j^q \beta_{ij} X_i X_j$ (general form)

  $Y = \beta_1 X_1 + \beta_2 X_2 + \beta_{12} X_1 X_2$ (2.05)

- Cubic model

$$Y = \sum_i^q \beta_i X_i + \sum\sum_{i<j}^q \beta_{ij} X_i X_j + \sum\sum_{i<j}^q \gamma_{ij} X_i X_j (X_i - X_j) + \sum\sum\sum_{i<j<k}^q \beta_{ijk} X_i X_j X_k \quad \text{(general form)}$$

$$Y = \beta_1 X_1 + \beta_2 X_2 + \beta_{12} X_1 X_2 + \gamma_{12} X_1 X_2 \quad (2.06)$$

- Quartic

$$Y = \sum_i^q \beta_I X_i + \sum\sum_{i<j}^q \beta_{ij} X_i X_j + \sum\sum_{i<j}^q \gamma_{ij} X_i X_j (X_i - X_j) + \sum\sum_{i<j}^q \delta_{ij} X_i X_j (X_i - X_j)^2 + \sum\sum\sum_{i<j<k}^q \beta_{iijk} X_i^2 X_j X_k + \sum\sum\sum_{i<j<k}^q \beta_{ijjk} X_i X_j^2 X_k + \sum\sum\sum_{i<j<k}^q \beta_{ijkk} X_i X_j X_k^2 + \sum\sum\sum\sum_{i<j<k<l}^q \beta_{ijkl} X_i X_j X_k X_l \quad \text{(general form)}$$

$$Y = \beta_1 X_1 + \beta_2 X_2 \beta_3 X_3 + \beta_{12} X_1 X_2 + \beta_{13} X_1 X_3 + \beta_{23} X_2 X_3 \gamma_{12} X_1 X_2 (X_1 - X_2) + \gamma_{13} X_1 X_3 (X_1 - X_3) + \gamma_{23} X_2 X_3 (X_2 - X_3) \quad (2.07)$$

These types of polynomials are used in Design Expert to describe the different models.

2.5 Design expert 8.0

Before a system can be modelled, the premises for using the simplex lattice method must be made. The number of components and the total amount should be determined. The software will then calculate the number of experiments which are needed for a complete model.
In this thesis the Mixture Design and Simplex Lattice design were used, thus the focus will be on these subjects as well.

2.5.1 Design of experiment

When designing the experiment, the following points need to be decided:

- Choose the design type:
  The simplex lattice design for mixtures can be used when there are 2-30 components and if the total mixture amount is constant [1]. The lattice method is the method of which points are chosen to be experimented. The first points are the vertices and the following points are the different mixtures.
  An augment design is set to default, this means that more experiment points are calculated to improve the design analysis. Replicates are also needed in the design in order to calculate estimates of pure error. Replicates set the safety margin of the measurements. At the chosen data points in which the replicates were performed, a certain deviation is calculated and for each data point in the model this deviation +/- will be integrated. A replicate needs to be performed as its own experiment point, if a sample of the same run is made it is considered a repeated measurement and will not reflect the complete process error [1]. Design expert will add the replicates automatically, or a number can be inserted manually.
- Choose the number of components to include in the model.
- Choose the degree of the model:
  Linear, quadratic, cubic etc. A higher degree will give more experiment points.
- Choose the number of responses:
  The response is the value which is measured after each experimental run. They need to be numeric and sensitive enough to detect small changes. The main cause of failed DOEs is the poor response measurement.

When all this is decided, the software will provide an experimental plan. This plan will contain the different mixture compositions to be tested, including random replicates. The experiments are also randomized in order to avoid systematic errors.

2.5.2 Analysis of the response data

The analysis of the design model can be examined once the responses have been inserted. If there is more than one set of response data inserted, then multiple nodes will show and an analysis for each of them can be made separately.
The first step is to choose which of the responses is to be analysed.

Transform:
If the ratio between the maximum and minimum response is large, a transformation may be needed. A better model can be attained if the original response data is transformed, the software will give a suggestion if a transformation is needed. The base 10 log is the transformation which is most commonly used. The Box-Cox plot under the diagnostics button will help suggest a transformation after a model is fit [1].

Fit summary:
Regression calculations are done to fit all the polynomial models to the response. Statistical values such as p-values, lack of fit and R-squared values are compared for each of the models. The model with the best fit will be suggested and be selected as default [1].

Model:
Each model can be chosen for further analysis, but the suggested model is selected as default.

ANOVA (analysis of variance):
A more detailed report of the chosen model is shown under this button. The model chosen is the base of different calculations, Design Expert will calculate for example the standard deviation, average, variance and the coefficients of the polynomials are estimated [1].

Diagnostics
Under this tab, a graphical summary for the chosen model is shown under the different diagnostics buttons. The plots will reveal deviations from the model and if there are some points which have very high residual values. See the explanation of the plots in chapter 2.5.3 [1]. Statisticians had originally set the term “residuals” as “error”, but this gave the management people the impression that too much mistakes were made [11]. Studentized residuals imply that a residual is divided by that residuals’ estimated standard deviation.
The different colours in the diagnostic plots indicate the value of the responses. Red indicates a high response value, green indicates a medium response value and blue indicates a low response value.

Model Graphs:
Various graphs can be examined to help interpret the selected model. Trace, two component, contour and 3D surface graphs are generated for a mixture of three components.

Optimization

One response or multiple responses can be optimized simultaneously. There are different ways of finding an optimization goal of interest [1].

- Numerical optimization:
  A goal is set for one or more responses then solutions with optimal conditions are calculated. Response goals such as maximize, minimize, target and range can be selected.
- Graphical optimization:
  Upper and lower limits are set, when there are multiple responses which meet the requirements simultaneously, then a highlighted overlaying graph will appear, showing the “sweet spots”.
- Point prediction:
  The mixture composition can be changed by using slide bars for each of the components. For each mixture composition, the predicted response value will show and the most favourable composition can also be chosen.

2.5.3 Diagnostics plots

The diagnostics plots and influence plots can reveal certain deviations and trends in the model. Examples of the plots shown in Design Expert will be shown here and will briefly be explained.

Normal plot

The normal probability plot of the suggested model show if the residuals are normally distributed. The data points will then follow a straight line as shown in figure 2.08, which indicates that there are no abnormalities. There will often be some scatter of the data, but if the data points form an "S-shaped" curve as shown in figure 2.09, it indicates that a transformation may give a better analysis. If the data points are normally distributed, they will follow the red line shown in the figures [1].

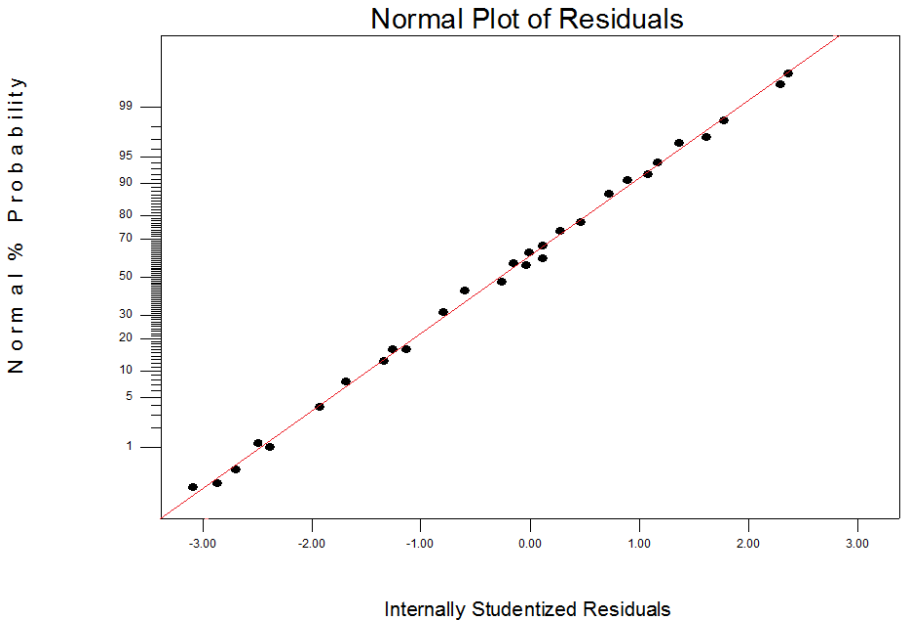

Figure 2.08 *A normal probability plot which shows no abnormalities.*

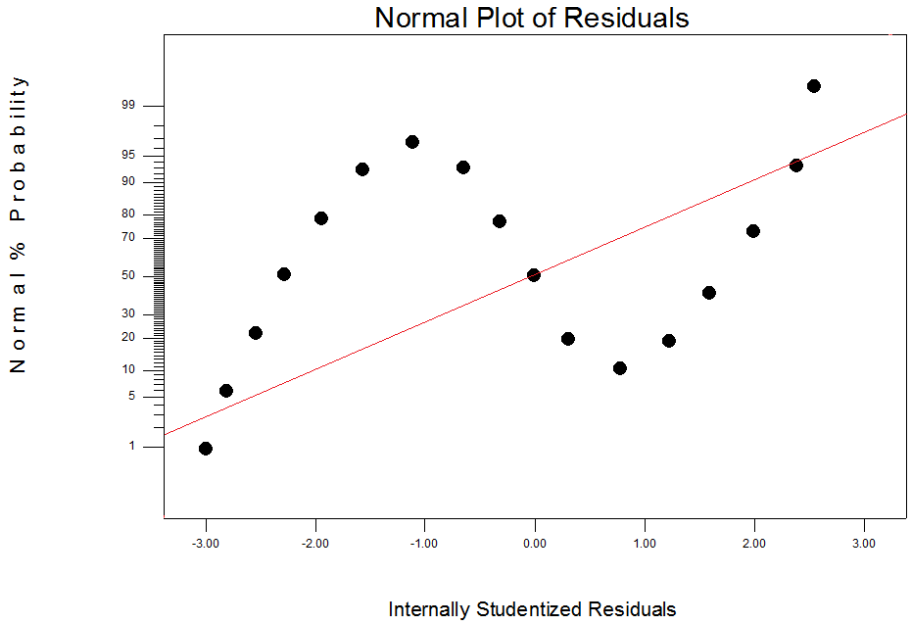

Figure 2.09 *A normal probability plot showing an s-shaped curve.*

Residual vs. predicted

The residuals plotted against the predicted values tests the assumption of constant variance. If this is the case, the data points should be a random scatter as figure 2.10 shows. If the data points take the shape of a megaphone (expanding pattern) as shown in figure 2.11 and 2.12, then a transformation is needed. If the points are close to the line y = 0, then the model is a better fit. The red lines y = +/-3 are the boundary values of the model. Values outside these boundaries indicate the model is not good or major errors have occurred and re-tests need to be considered for the points in question [1].

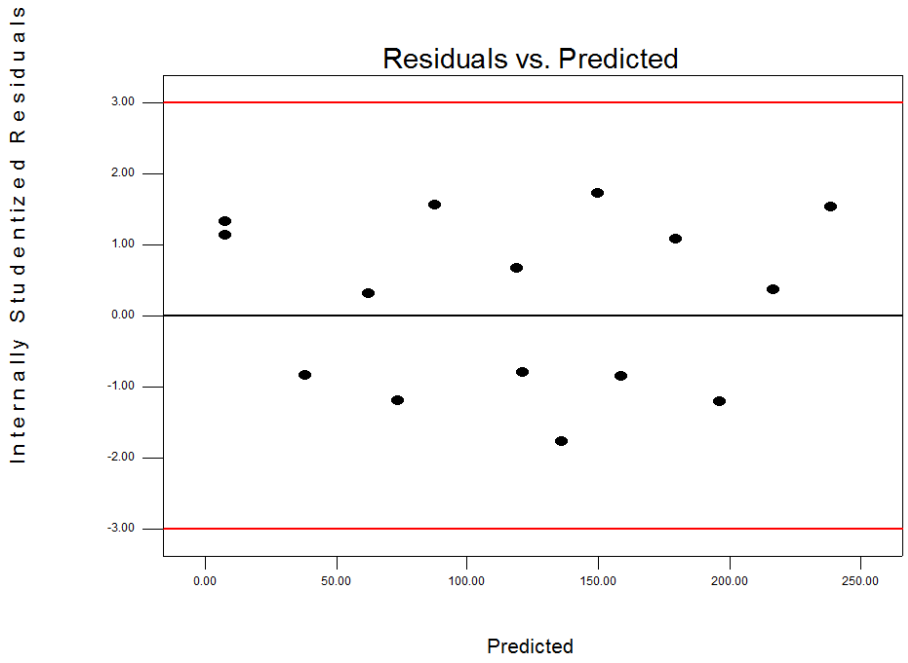

Figure 2.10 *An example of how the residuals vs. predicted plot should look like.*

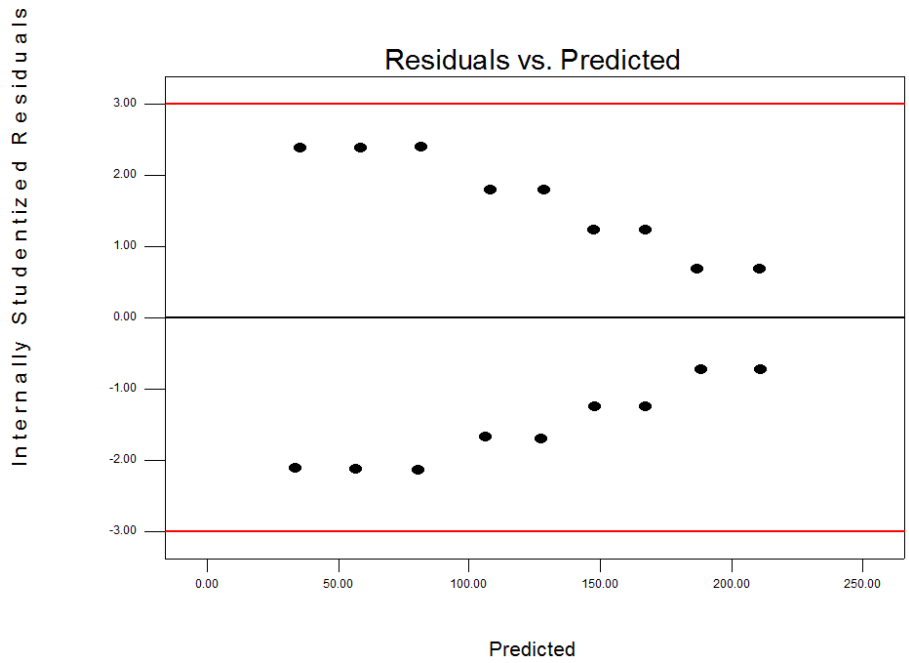

Figure 2.11 *An example of how the residuals vs. predicted plot should not look like.*

Figure 2.11 and 2.12 shows how the Residual vs. Predicted plots should not be. These patterns indicate that the variance increases/decreases with the predicted response values, thus the variance is not constant.

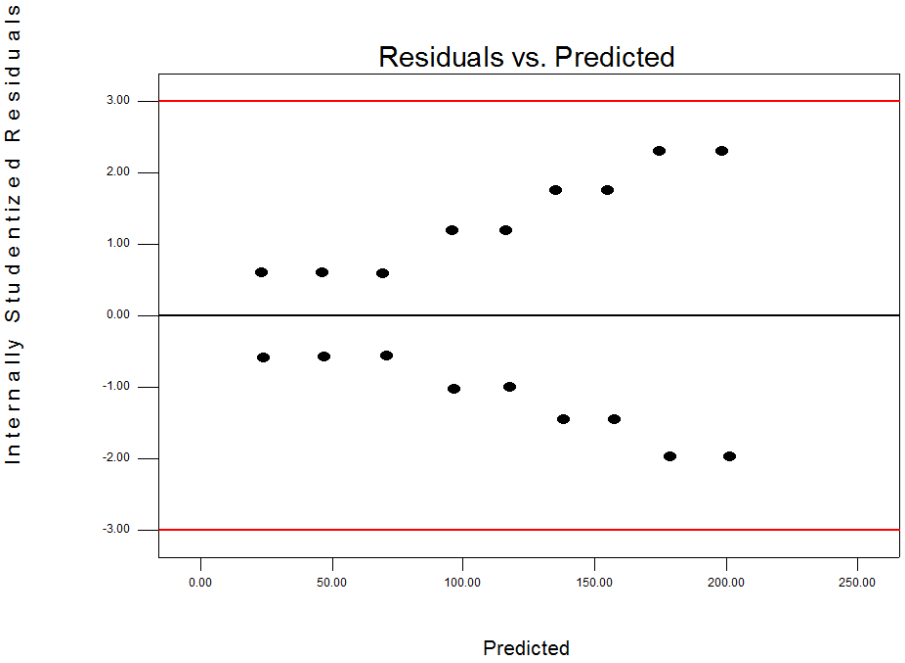

Figure 2.12 *An example of how the residuals vs. predicted plot should not look like.*

Residual vs. run

The residuals plotted against the run number shows experimental deviations over time for each experiment number. This graph (figure 2.13) may be able to expose some suspicious variables if there are any points which stand out. The residuals should be randomly scattered.

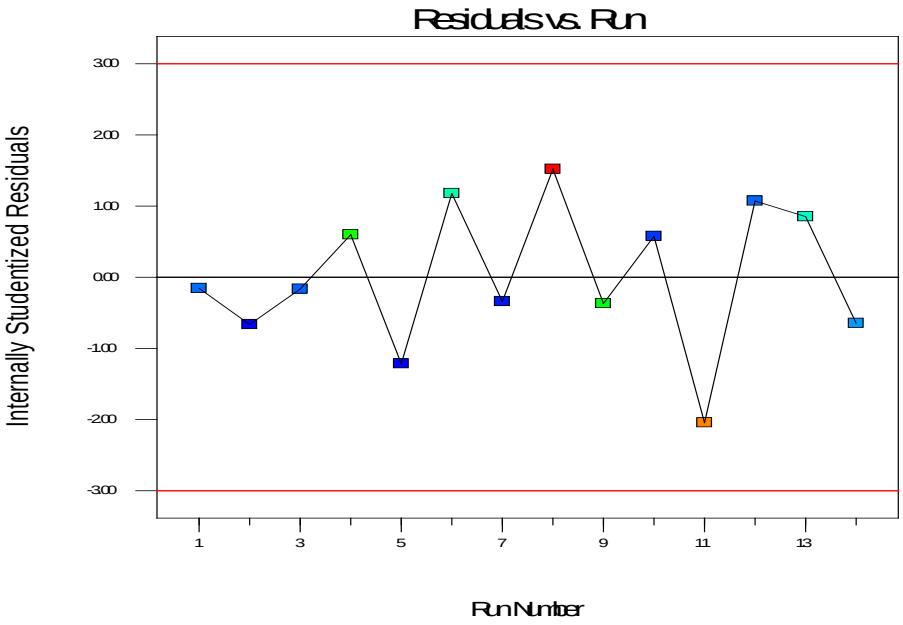

Figure 2.13 *An example of a randomly scattered residuals vs. run number plot [1].*

Any obvious pattern in the plot is caused by time-related variables. The software will randomize the run numbers, which will prevent such systematic variations. For example the person whom is performing the experiments can get tired toward the end of the day and may begin to “slack off”. Or the person whom is performing the experiments may get more precise with time so the residuals will be less scattered [1, 11].

Predicted vs. actual

This graph (figure 2.14) shows a plot of the predicted response values versus the actual response values. The graph may help to identify a value or a group of values which are difficult for the model to predict. The data points should be evenly distributed on each side of the 45^{o} line. If the data points fit the model perfectly, they will lie directly on the 45^{o} line. If there are data points which are obviously distinguished from the other data points, there may be errors in the input response data which is one of the most common mistakes. If this is not the case, then a transformation may be needed or the model should be reconsidered (add replicates, remove or add experiments) [1, 10].

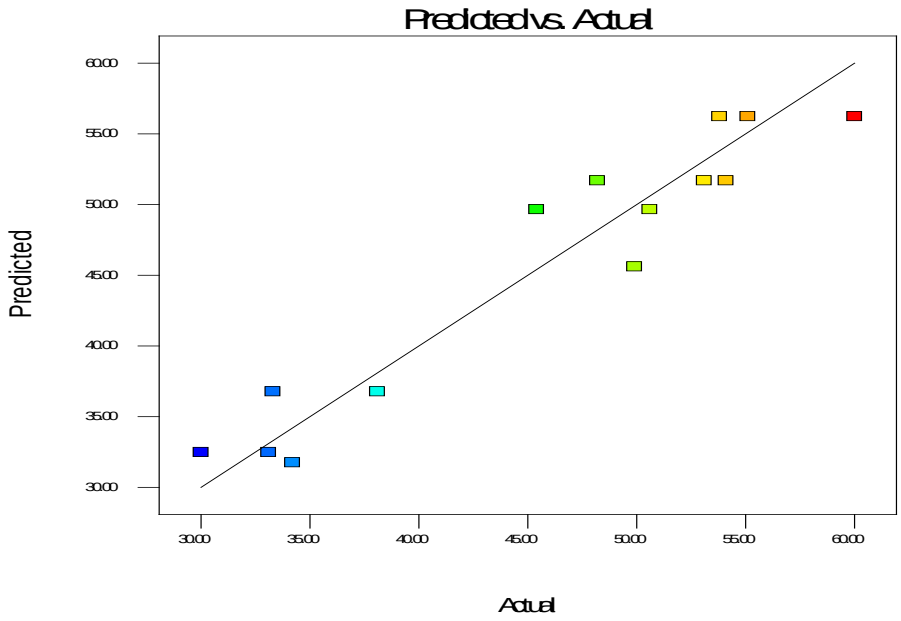

Figure 2.14 *An example of a predicted vs. actual plot.*

Box-Cox Plot

This plot (figure 2.15) helps to select the correct transformation, which is recommended based on the lambda (λ) value found at the minimum point of the curve. This lambda (λ) value gives the minimum sum of residuals and the least deviations from the model. Lambda (λ) is the value in which the response data should be raised to the power of.

The red lines are the limits set by Design Expert. The blue line shows the current data without transformation. And the green line shows the data with transformation. As long as the green line is within the boundaries, then a transformation is not needed [1, 10].

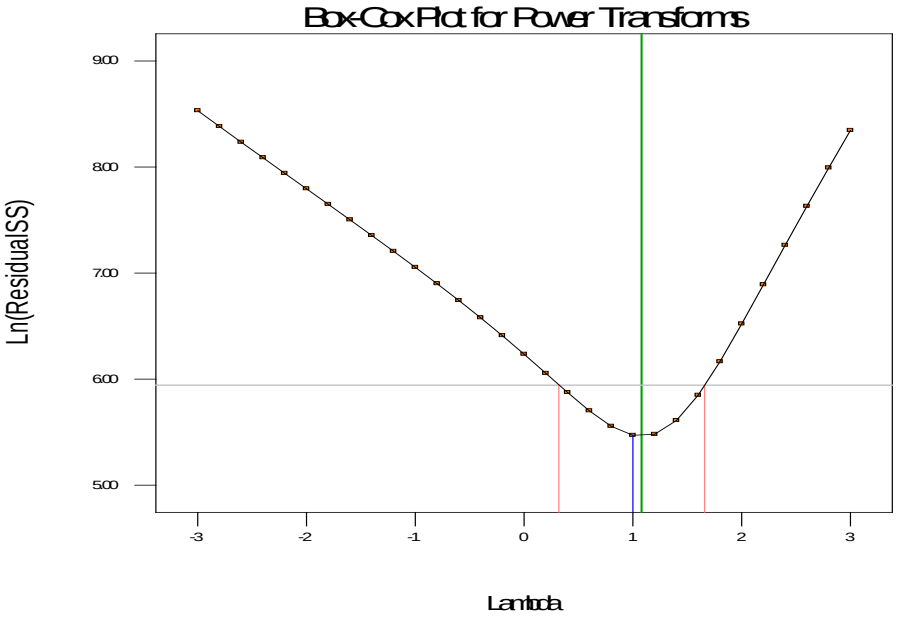

Figure 2.15 *An example of a box-cox plot, the plot indicates that no transformation is needed.*

Residuals vs. factor

This is a plot of residuals versus each of the factors in the system. By comparing the graphs for each component, it is possible to find which of them affects the normal plot [10]. This plot should show a random scatter, obvious curvature may indicate a systematic contribution of the independent factor that is not accounted for by the model.

However, in a mixture design the components (“factors”) are always related to one another, which means that changes to one component will balance the other two components so the total amount is always equal (the summation or equality constraint). Thus it is too difficult to determine each components effect on the system [3]. Figure 2.16 shows a plot of residuals vs. component C in the mixture design.

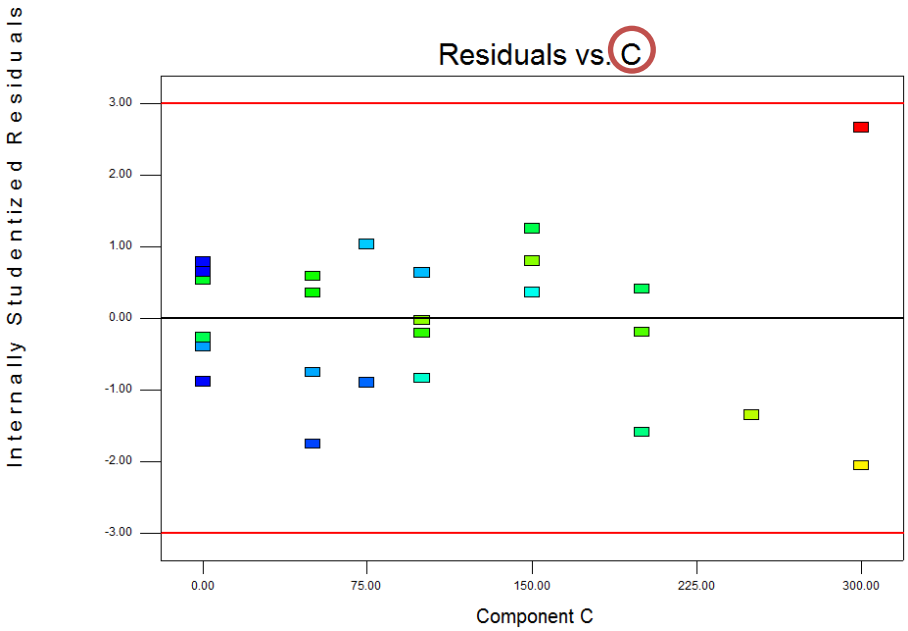

Figure 2.16 *An example of a residual vs. factor plot, where the data points are randomly scattered.*

2.5.4 Diagnostic influence

When a model is fitted, it is of the highest interest that it fits most of the data, the following graphical plots gives a better overview on whether one or more data points differs from the others. Design Expert measures the influence, potential or actual values of individual runs. The plots can for example be used to examine the influence of the model when a data point is deleted [1].

Externally studentized residuals

This plot helps to detect data points which differ from the model. The data points that are outside the given boundaries (red lines) do not fit well by the current model, which indicate that the input data may be wrong or the model may be wrong. If the data points are correct, check if something unusual may have happened during the run, also check the model to see if a transformation will fit all the data points better. A replicate is recommended rather than removing a data point. If a cause is found to the deviant data point, then it may be acceptable to remove it, if not then it should be kept in the data set [1, 3]. Figure 2.17 shows an externally studentized residual plot, all the data points are within the boundaries. Run number 3 is very close to the upper limit so this point should be examined.

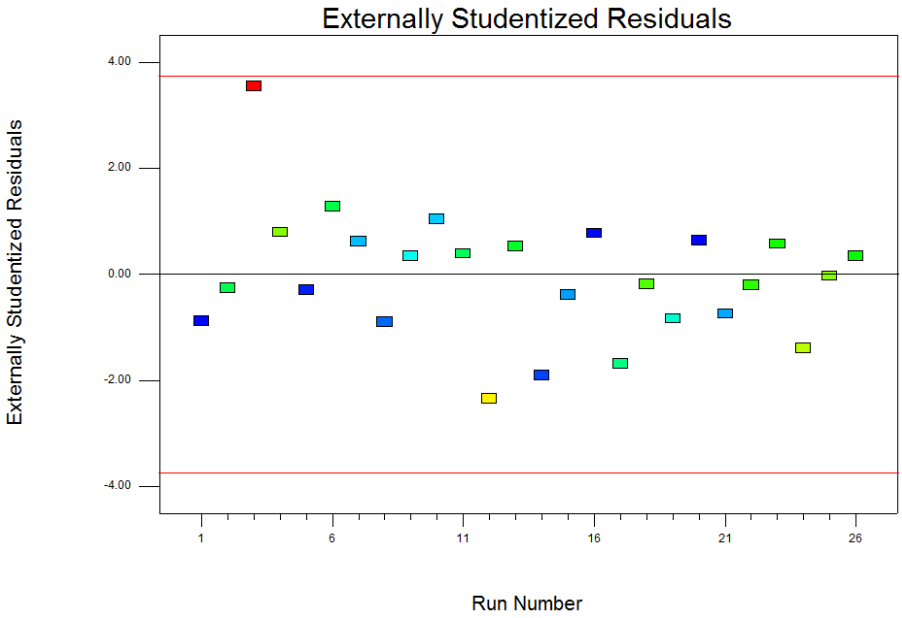

Figure 2.17 *An example of an externally studentized residuals plot.*

Leverage

The leverage value indicates a data points' potential to influence the model and it is a numerical value between zero and one. A value of one means that the predicted value has no residuals and that it is exactly equal to the actual value. A high leverage point is not desired because the data point(s) in which there is a problem with (unexpected error) will influence the model strongly [1]. The data points in figure 2.18 are all within the boundary.

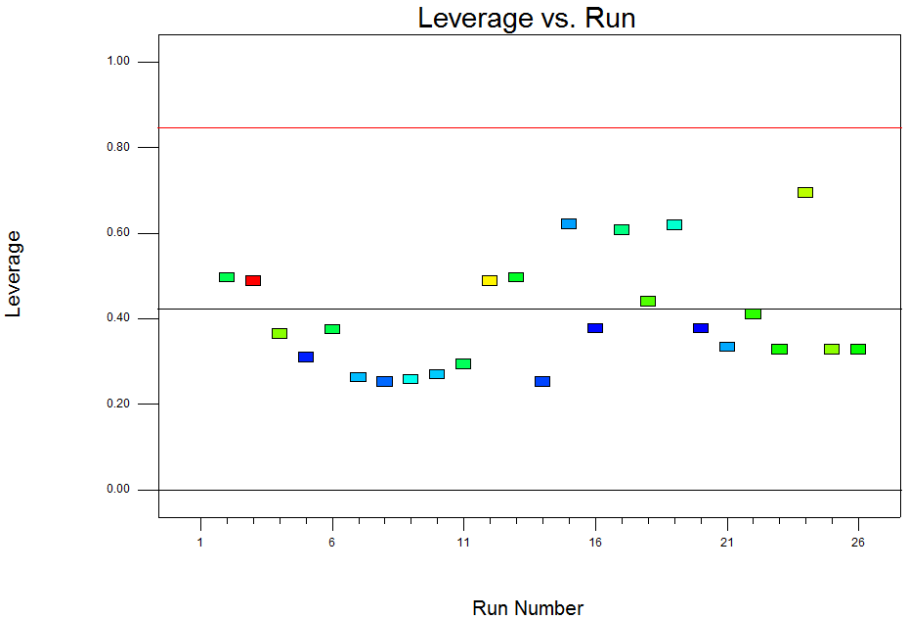

Figure 2.18 *An example of leverage vs. run plot.*

DFFITS

When a data point is deleted, there will be a change in the predicted values (change in the model), the difference in fits (DFFITS) is calculated by measuring the change that occurs in the model if a data point is removed. If the DFFITS is large then it will strongly influences the fitted model [1]. Figure 2.19 shows that all the data points are within the boundaries and no changes are needed.

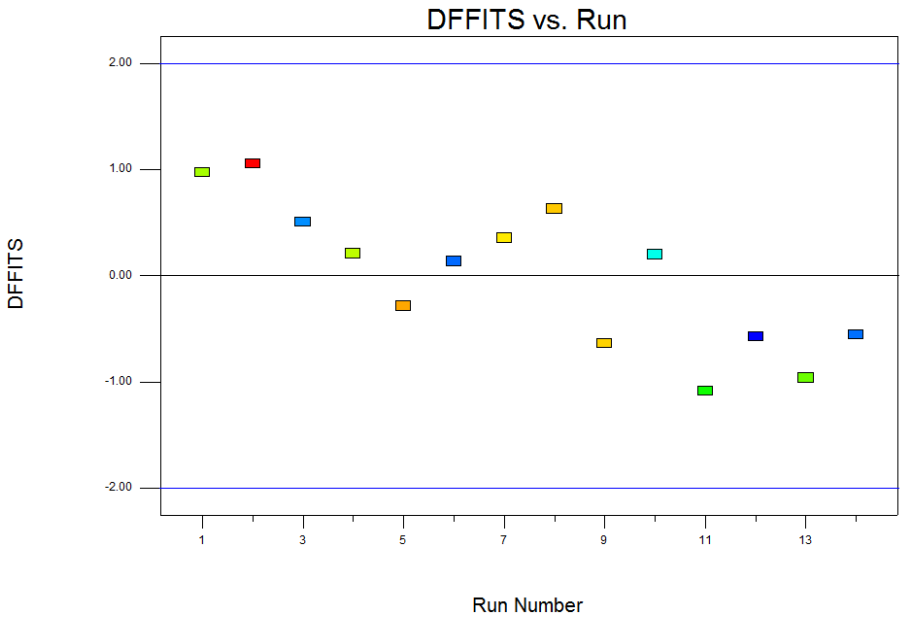

Figure 2.19 *An example of a DFFITS vs. run plot.*

DFBETAS

For example the linear Scheffé polynomial $Y = \beta_1 X_1 + \beta_2 X_2 + \beta_3 X_3$ (2.04), the difference in betas (DFBETAS) is the measured changes in the model related to each coefficient (β_i) if a data point is deleted [1, 10]. An outlying data point may indicate that the model is affected by this result and that the model will slope in that direction. Figure 2.20 shows a DFBETAS plot where all the data points are well within the boundaries.

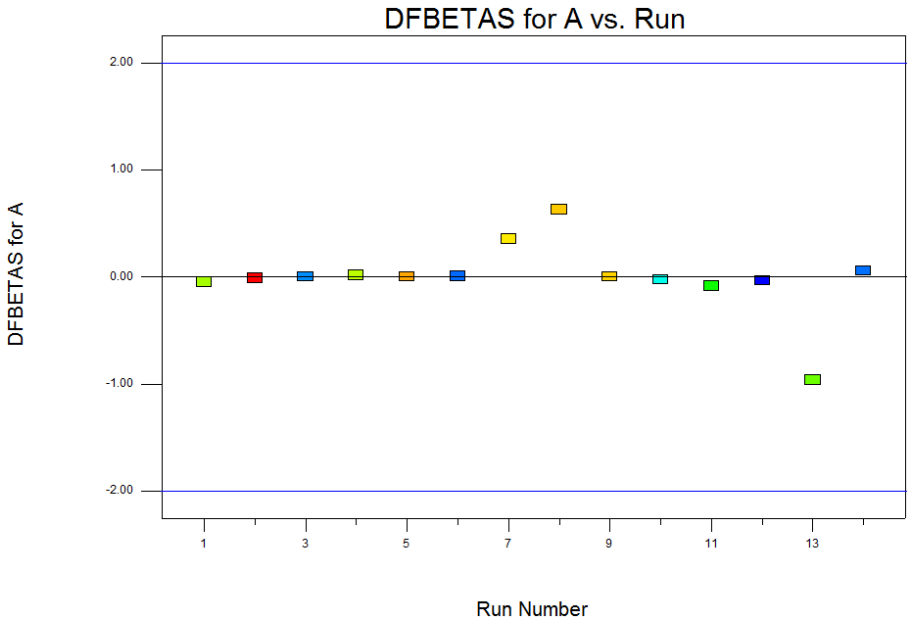

Figure 2.20 *An example of a DFBETAS plot.*

Cook's Distance

If a data point is deleted, cook's distance gives a measure of how much the regression changes. Data points with high leverage and large studentized residuals are related to large values in this plot. Large values should be investigated because they could be caused by errors with input data, an incorrect model or very deviant data points [1]. Figure 2.21 shows a plot for Cook's distance for a data set.

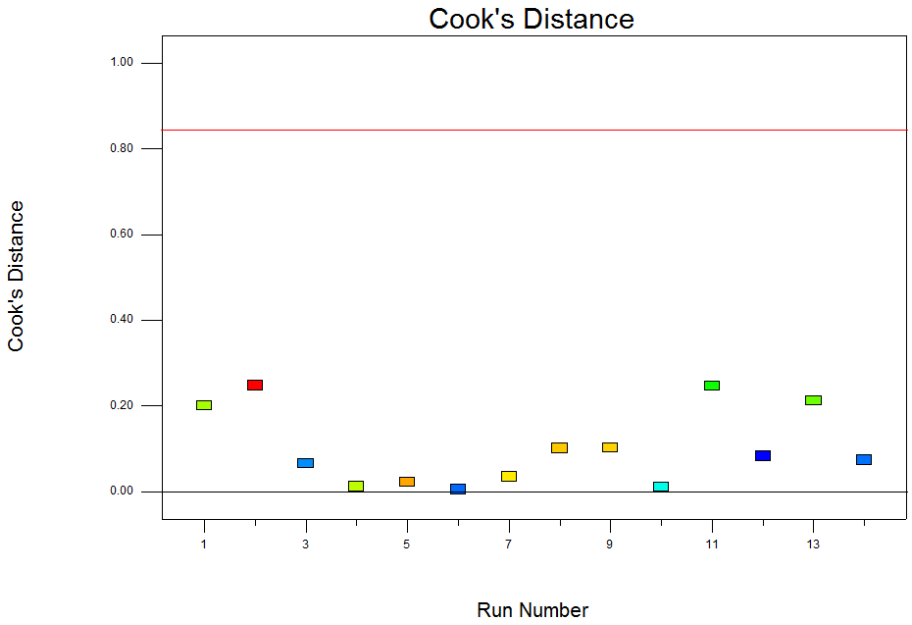

Figure 2.21 *An example of a Cook's distance plot.*

Report (Case Statistics)

The report shows the specific values which are used in most of the diagnostic graphs. In general it is easier to detect trends and deviants in the graphs than by reviewing the raw data [1].

2.6 References

[1] I. D. E. Stat-Ease. Topic Help [Online].

[2] H. Scheffé, "Experiments With Mixtures," *Journal of the Royal Statistical Society. Series B (Methodological),* vol. 20, pp. 344-360, 1958.

[3] W. F. Smith, *Experimental Design For Formulation*: Society for Industrial and Applied Mathematics, 2005.

[4] M. J. Anderson and P. J. Whitcomb, "Computer aided tools for optimal mixture design: This case study looks at formulating a clearcoat using design-of-experiment software," *Paint and Coatings Industry,* vol. 15, pp. 68-72, 1999.

[5] M. J. A. and and P. J. Whitcomb, "Mixture DOE uncovers formulations quicker," *Rubber & Plastics News,* pp. 16-18, october 21 2002.

[6] "The Oxford Dictionary of Foreign Terms in English," in *simplex adjective & noun*, J. Speake, Ed., ed: Berkley Books, Oxford Univercity Press, 1999.

[7] R. E. Bruns, I. S. Scarminio, and B. De Barros Neto, *Statistical Design--chemometrics*: Elsevier, 2006.

[8] J. A. Cornell, *Experiments with Mixtures: Designs, Models, and the Analysis of Mixture Data*: John Wiley & Sons, 2011.

[9] J. W. Gorman and J. E. Hinman, "Simplex Lattice Designs for Multicomponent Systems," *Technometrics,* vol. 4, pp. 463-487, 1962.

[10] K. Woie, "Modellering og optimalisering av formuleringer ved hjelp av eksperimentell design.," Bachelor, Biological chemistry, University of Stavanger, Stavanger, 2008.

[11] I. D. E. Stat-Ease, "DE8-UserGuide.exe," 11.06.2010 ed. Minneapolis: Stat-Ease, Inc., 2010.

[12] R. A. Fisher, Sir,, "Development of the Theory of Experimental Design," *Proceedings of the International Statistical Conferences, (Washington),* pp. 434-439, 1947.

[13] A. Atkinson, A. Donev, and R. Tobias, *Optimum Experimental Designs, with SAS*. Cary, NC, USA: Oxford University Press, 2007.

Chapter 3 Asphaltene test methods – theoretical background

The dispersant mixtures will at first be going through a screening test which is done in this thesis. Four methods were examined to evaluate the asphaltene dispersant mixtures:

- Deposit level test
- Turbidity measurements
- Spot test
- UV-Vis spectroscopy

A simple and quick method is of interest for the screening tests since it will save time and money. If any interesting and useful results are found they will be further tested with more advanced methods and equipment which are more costly and time consuming.

3.1 Deposit level test

When selecting a crude oil to test on, it is good to know how much asphaltene will deposit in the test tubes and how light or dark the supernatant is before a dispersant is applied. Enough deposit is needed in order to know that when a dispersant is used, some of it can be dispersed and some is left to be measured (deposit volume). The supernatant should not be too dark because it will be very difficult to read the deposit level and when a dispersant is added the supernatant will be much darker compared to when a dispersant is not added.
Other observations can also be noted such as deposit consistency (for example solid or soft, loose and "slushy" or compact) and supernatant appearance (light or dark colour, cloudy or clear).
Figure 3.01 shows examples of graded centrifuge tubes which is suitable for the measurement of asphaltene deposit levels.

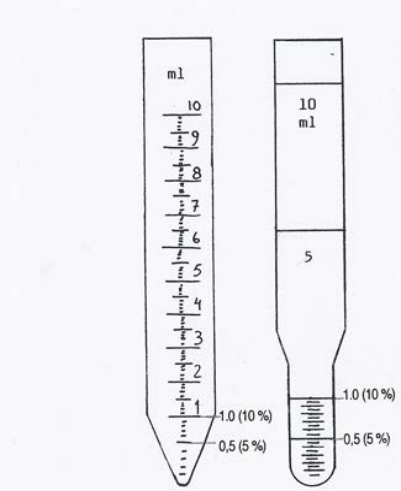

Figure 3.01 *Hotspin centrifuge tubes (http://hotspin.se/hotspin 19.06.12).*

3.2 Turbidity measurements

In drinking water treatment plants, the turbidimeter is one of the most used instruments to quantify the water clarity. The turbidity is measured in nephelometric turbidity units (NTU). The particles in the sample scatter and absorb light which prevents its transmission. The turbidimeters (figure 3.02) measure the amount of scattered light at specified angles [3, 4]. The turbidity do not say anything about the particle size or number of particles, but it is

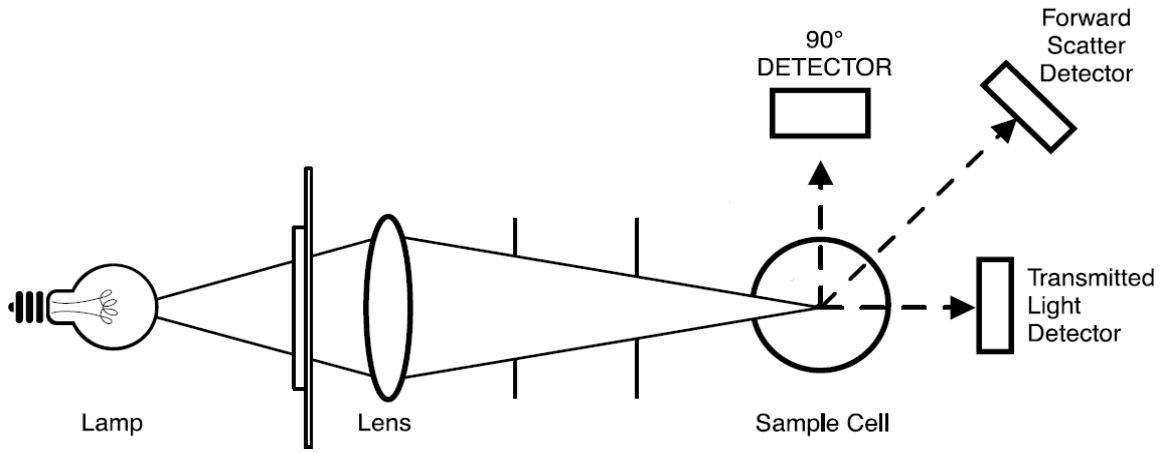

Figure 3.02 *Principal of operation of a 2100N HACH turbidimeter [2].*

affected by size, concentration and type (shape, material, optical characteristics) of the particles present [3]. For example air bubbles in the solution are a cause of error, because it will be mistaken for a particle and it affects the incoming light. High turbidity shows that the water is cloudy, normally because of a high content of fine particulate material [5].
This method is used to measure the suspended asphaltene particles in the supernatant. A high turbidity value indicates an effective dispersant. A low value indicates an effective flocculent which will cause deposition of the asphaltenes.

3.3 Spot test

The asphaltene onset flocculation can be detected by photography or by spotting a small amount of the solution on a filter paper. Automated methods using optical absorption spectroscopy is more frequently used for onset flocculation detection and product screening of suitable asphaltene inhibitors because of high speed, low cost and non-destructive testing [6-8].

The spot test is an easy method that gives an approximate measurement of how much precipitant is needed to destabilize the asphaltenes in a certain amount of crude oil [7]. A weakness of the method is that solid contaminants may interfere to give inaccurate results [9]. Figure 3.03 show three different spot tests on two different filter papers, Whatman no.1 (left) and no.4 (right). The spot in the middle (see the red arrows) is a positive spot which means the test has proven asphaltene deposition. The two other uniform spots (see the blue and green arrows) are negative spots which show that there is no asphaltene deposition in the solutions. The colour or size of the rings is not that important, the key feature is if the spot divides into two rings, an inner- and outer ring.

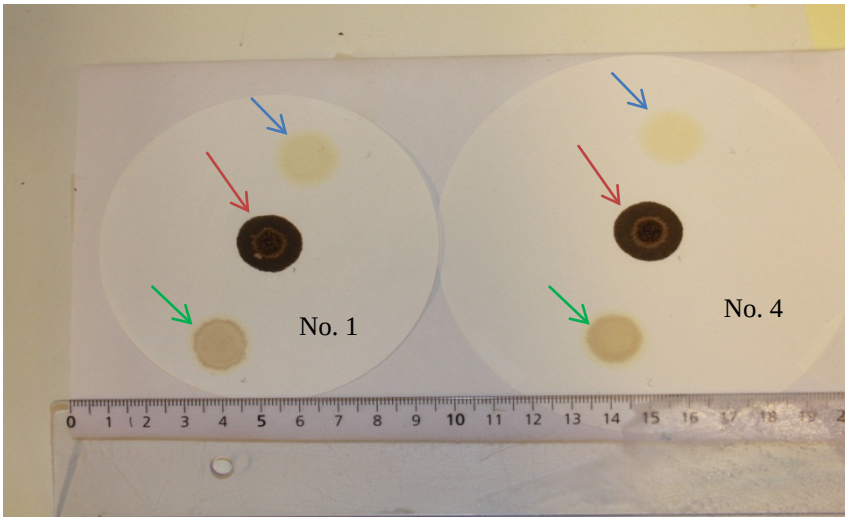

Figure 3.03 *Three different spots made on whatman no.1 filter paper (left) and Whatman no.4 filter paper (right).*

The tests can be compared to the reference spot description [10] as shown in table 3.01. A weak feature with this test is that it is very subjective; even with a reference spot description interpretation of the results will often vary.

Table 3.01 Reference Spot Description

Reference Spot No.	Characterizing Features
1	Homogenous spot (no inner ring)
2	Faint or poorly defined inner ring
3	Well defined thin inner ring, only slightly darker than the background
4	Well-defined inner ring, thicker than the ring in reference spot No. 3 and somewhat darker than the background
5	Very dark solid or nearly solid area in the centre. The central area is much darker than the background

The spot test method was examined in order to determine if it could be used to rank the performance of different asphaltene dispersants.

3.4 UV-Vis spectroscopy

This method is based on the ability of atoms and molecules to absorb or emit electromagnetic radiation in the ultraviolet (UV) region. All organic compounds absorb ultraviolet light although sometimes very short wavelengths. Even though IR (infrared), NMR (nuclear magnetic resonance) and mass spectrophotometers have taken over for some of the UV related tasks, UV is still widely used for its ability to measure the extent of multiple bond or aromatic conjugation within molecules. Non-bonding electrons on oxygen, nitrogen and sulphur may also contribute in extending the conjugation of the multiple-bond system. The study of especially aromatic and heteroaromatic systems is highly dependent on empiricism, but within this area UV-Vis spectroscopy may be able to provide data which is unobtainable from any other spectroscopic method [11].
Atoms or molecules which absorb radiation (figure 3.04) in the UV-Vis region will experience an energy absorbing transition [12].

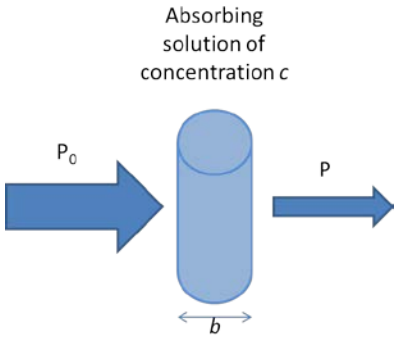

Figure 3.04 *Reduction of a radiating beam by an absorbing solution. The radiation of P_0 is more powerful than the radiation of P [1].*

The analyte (components in a sample to be determined) species will obtain a higher energy level (excited state) when absorbing the radiation, the time spent in the excited state is very brief ($10^{-8} – 10^{-9}$s). However, the absorbed electromagnetic radiation can be measured, or as the analyte species returns to its normal state, the ground state, the emitted electromagnetic radiation can be measured [1].

The sample is kept in a container, a cuvette, when it is measured. As figure 3.05 shows, considerable radiation losses may occur such as reflection and scattering at the cuvette walls and within the sample. To compensate for this, the power of beam passing through the sample is compared to a beam passing through an identical cuvette containing only the solvent or a reagent blank [1].

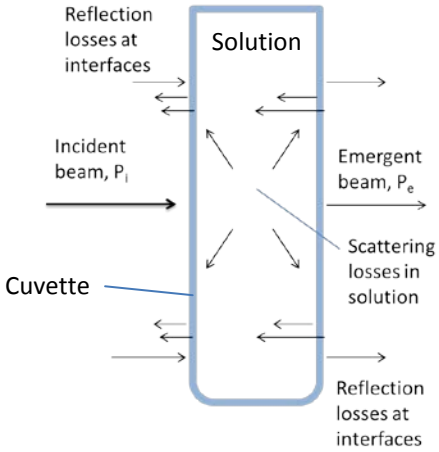

Figure 3.05 *Scattering and reflection losses within a solution inside a typical glass cell (cuvette) [1].*

The absorption (or emission) results can be plotted graphically by a spectrum. An absorption spectrum plots absorbance versus wavelength as shown in figure 3.06. It is also possible to measure the absorbance at a fixed wavelength, instead of scanning along an interval which is done in the spectrum (figure 3.06).

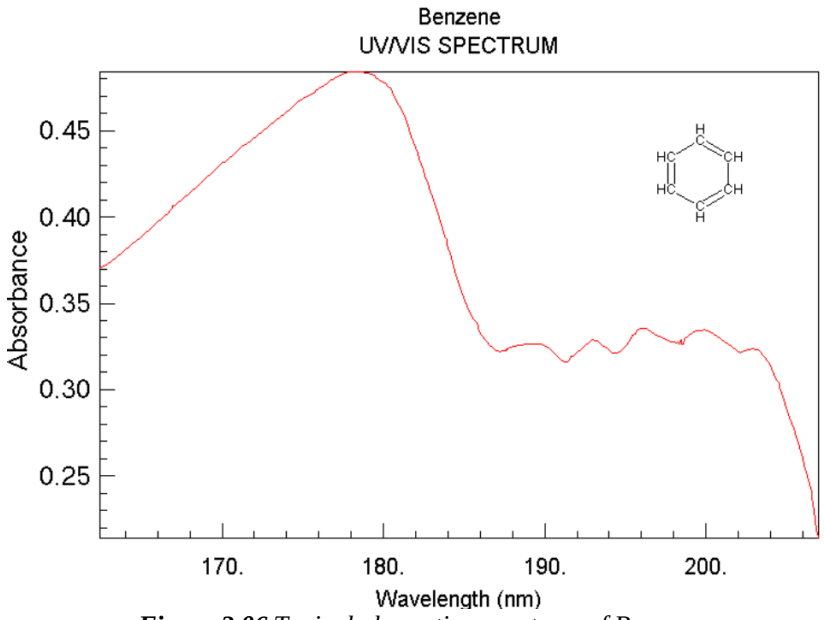

Figure 3.06 *Typical absorption spectrum of Benzene.*

UV-Vis spectroscopy has been used to measure the effects of asphaltene dispersants [7]. The absorbance was measured at 440 nm, an effective inhibitor will give high absorbance readings. The measurement of turbidity was examined in order to determine if it could be used to rank the performance of different asphaltene dispersants.

3.5 References

[1] D. A. Skoog, *Fundamentals of analytical chemistry*. Belmont, Calif.: Thomson Brooks/Cole, 2004.

[2] H. Company, "2100 Series Laboratory Turbidimeters Data Sheet ", 3 ed, 2010.

[3] E. E. Hargesheimer, N. E. McTigue, C. M. Lewis, and A. R. Foundation, *Fundamentals of Drinking Water Particle Counting*: AWWA Research Foundation and American Water Works Association, 2000.

[4] G. Tchobanoglous, F. L. Burton, Metcalf, Eddy, and H. D. Stensel, *Wastewater Engineering: Treatment and Reuse*: McGraw-Hill, 2004.

[5] E. A. a. B. E. Løfsgaard, "Nok, godt og sikkert drikkevann offshore - En veileder i utforming av drift av drikkevannsanlegg på offshoreinnretninger," Folkehelseinstituttet, 2009.

[6] A. T. Pauli, "Asphalt compatibility testing using the automated Heithaus titration test," *Journal Name: Preprints of Papers, American Chemical Society, Division of Fuel Chemistry; Journal Volume: 41; Journal Issue: 4; Conference: 212. national meeting of the American Chemical Society (ACS), Orlando, FL (United States), 25-30 Aug 1996; Other Information: PBD: 1996*, pp. Medium: X; Size: pp. 1276-1281, 1996.

[7] A. Yen, Y. R. Yin, and S. Asomaning, "Evaluating Asphaltene Inhibitors: Laboratory Tests and Field Studies," presented at the SPE International Symposium on Oilfield Chemistry, Houston, Texas, 2001.

[8] I. N. E. a. A. P. Losev, "On the Nature of UV/Vis Absorption Spectra of Asphaltenes," *Petroleum Science and Technology*, vol. 25, pp. 55-66, 2007.

[9] S. Asomaning, "Test methods for determining asphaltene stability in crude oils," *Petroleum Science and Technology*, vol. 21, pp. 581-590, 2003.

[10] A. International, "Standard test method for cleanliness and compatibility of residual fuels by spot test," in *D4740*, ed, 2002.

[11] W. Kemp, Ed., *Organic Spectroscopy*. London: Maclillian Press LTD, 1991, p.^pp. Pages.

[12] D. A. Skoog, S. R. Crouch, and F. J. Holler, *Principles of instrumental analysis*. Belmont, Calif.: Thomson, 2007.

Chapter 4 Asphaltene deposit level test

The first method to be examined was the asphaltene deposit level test where the deposit levels of blank tests (only pentane and crude oil solution) and dispersant tests (pentane, crude oil solution and dispersant) were compared. Different crude oils and concentrations of the crude oils were tested to evaluate how much asphaltene will deposit in the tubes and which concentration would be suitable for the dispersant tests. In the first tests, some of the parameters were varied in order to examine which settings should be used as a standard procedure such as shake time, agglomeration time, centrifuge velocity (rpm) and centrifuge time.

The experiments were performed as similarly as possible each time so when comparing the results, the conditions should have been the same. The equipment used was mainly the type 2 centrifuge tubes (figure 4.01). Type 1 centrifuge tubes were also used at first, but often the deposit levels were uneven and difficult to read.

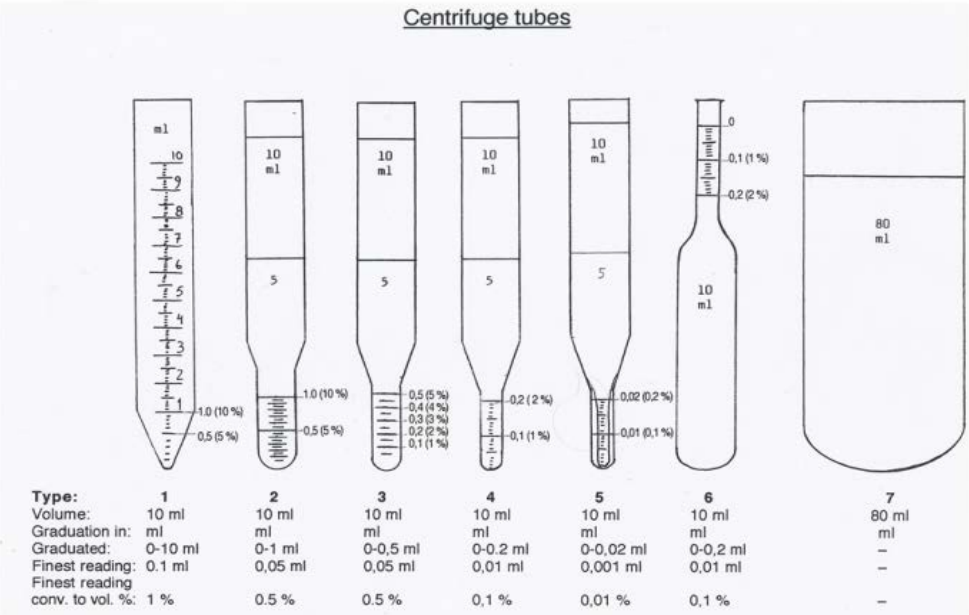

Figure 4.01 *Different types of Hotspin centrifuge tubes (http://hotspin.se/hotspin 19.06.12).*

Pentane was used to promote the deposition of asphaltene.

The crude oils were diluted with xylene since it is difficult to work with if it is very viscous, and dilution with an aromatic solvent will often help to increase the accuracy and reproducibility of the tests [1].

At first the deposit levels to be used in the dispersant tests were decided, by making a series of blank tests with different crude oil concentrations. The procedures for how the samples were prepared is described in chapter 4.1.1 for the blank tests and chapter 4.2.1 for dispersant tests and they were based on the asphaltene dispersant test (ADT) procedure by M.B. Manek [1], only with some differences:

- Pentane was used instead of hexane.
- The crude oil amount to be used was decided by the volume deposit, not the per cent deposit.
- The solutions were shaken for two minutes rather than one minute.
- Instead of letting the samples agglomerate for two hours, they were left for thirty minutes.
- The samples were centrifuged instead of settling by gravity.

4.1 Blank tests

The crude oils used in the experiments were diluted with xylene. The crude oil solutions are:

- Crude MO II 50:50 xylene
- Crudo-Metapetroleum 50:50 xylene
- Hier D02A 80:20 xylene

Different amounts of crude oil solution were used, so the amount is not specified in the procedure, but they are shown in the table of results.
The results were performed as similarly as possible in order to get reproducible and accurate results for comparison.

4.1.1 Procedure

Pentane (10 ml) was added to each centrifuge tube.
The desired concentration of crude oil solution was added to the centrifuge tubes.
The centrifuge tubes were shaken for 2 minutes to agitate the asphaltene stability, the bottom of the centrifuge tubes were held slightly upwards (figure 4.02) and were shaken sideways, not too fast, so the liquid in the narrow bottom of the tubes would be properly mixed.

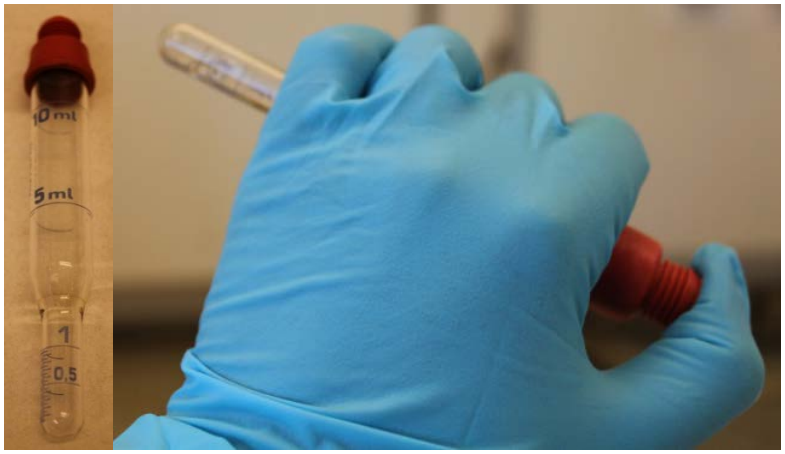

Figure 4.02 *A centrifuge tube (Nr. 2) with the cap (left). How the centrifuge tube is positioned when shaken (right).*

After shaking, the centrifuge tubes were left for 30 minutes in order to let the asphaltenes agglomerate.
They were then centrifuged at 1500 rpm (revelations per minute) for 5 minutes.
The deposit level was evaluated, and noted.

4.1.2 Results and discussion

Observations made of the experiments are commented shortly in the table, such as if anything out of the ordinary happened, if something went wrong during the experiment run or if changes were made to the standard procedure.
The results are listed in table 4.01 which shows the measured deposit levels of different concentrations of crude oil MO II solution in pentane.

Table 4.01 *Deposit levels of different crude oil MO II concentrations.*

Crude oil MO II 50:50 xylene			
Date	Concentration crude oil [µl]	Deposit level [ml]	Comments
26.01.2012	100	0,04	Centrifuged at 2000rpm for 5 minutes.
	200	0,04	
	300	0,04	
	400	0,05	
	500	0,06	
	1000	0,06	
	2000	0,18	
	3000	-	Difficult to read because of the dark supernatant. The deposit followed when the supernatant was poured off.

The deposit levels of the highest concentrations were very low, they should be between 0,05 ml and 1 ml, preferably closer to 1 ml, since that is the part of the centrifuge tube (nr.2 tube) which is graded and will give more accurate readings. The supernatant of the 3000µl crude oil MO II was so dark that the deposit level could not be read unless the supernatant was poured off. That should be avoided since the deposit may also be poured off, or the deposit could loosen and be smeared in the tube and give inaccurate readings.
The results given in table 4.01 indicate that a very high concentration of crude oil was needed to get enough deposit.
Figure 4.03 shows the deposit levels of 500µl and 1000µl crude oil MO II solution. As the figure shows, the supernatant of the 1000µl crude oil concentration was very dark, and the deposit level was difficult to read if the lighting is bad.

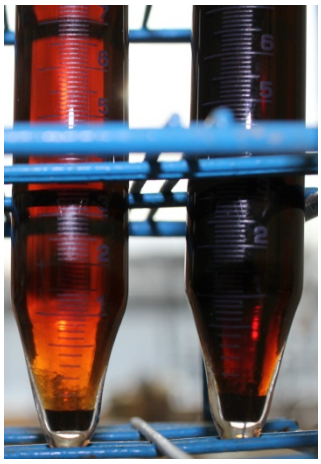

Figure 4.03 *Deposit levels of 500µl and 1000µl of crude oil MO II (50:50 xylene) 30.01.12.*

Table 4.02 on the next page, shows the results of the measured deposit levels of different concentrations of Crudo-Metapetroleum solution in pentane.
There were satisfying amounts of asphaltene deposits in all of the used concentrations, so different parameters were varied to examine the effects.
Since the tubes are so small, they should be shaken for at least 2 minutes in order to agitate the asphaltene stability properly, 1 minute is somewhat short.
When the tubes are left so the asphaltenes can agglomerate, the agglomeration time was varied between 30 minutes and 120 minutes in order to examine if there were any difference in the deposit levels. The four first tests performed 01.02.12 did not show much difference when comparing the 30 minutes and 120 minutes agglomeration time, thus 30 minutes was set as a standard.
All the different concentrations of Crudo-Metapetroleum oil are well within the desired range of the grades on the centrifuge tube and the supernatant is not too dark even when 500µl crude oil solution was used. Figure 4.04 shows the deposit levels of 100µl, 200µl, 300µl, 400µl and 500µl of Crudo-Metapetroleum crude oil solution.

Figure 4.04 *Deposit levels of (from left to right) 100µl, 200µl, 300µl, 400µl and 500µl of Crudo Metapetroleum crude oil solution (50:50 in xylene) 01.02.12.*

The 500µl Crudo-Metapetroleum tests gave satisfying deposit levels and this concentration was tested several times to examine the accuracy and reproducibility of the results.
Comparison of the 500µl concentration tests indicates that the deposit levels are quite similar with some variations.

Table 4.02 *Deposit levels of different concentrations of Crudo-Metapetroleum*

Crudo-Metapetroleum 50:50 xylene			
Date	Concentration crude oil [µl]	Deposit level [ml]	Comments
31.01.2012	100	0,1	Forgot to shake the tubes after crude oil addition.
	200	0,2	
	300	0,3	
	400	0,46	
	500	0,75	
	100	0,1	Shaken for 1 minute. Settled for 120 minutes
	200	0,25	
	300	0,45	
	400	0,5	
	500	0,9	
01.02.2012	250	0,325	
	500	0,7	
	250	0,3	Shaken for 2 minutes after crude oil addition. Settled for 2 hours.
	500	0,65	
	100	0,15	May have dosed too much in the 400µl and 500µl, lost count of doses.
	200	0,28	
	250	0,3	
	300	0,35	
	400	0,7	
	500	0,95	
02.02.2012	500	0,75	
	500	0,65	
	500	0,69	
	500	0,71	
	500	0,7	Uneven deposit level after centrifugation, difficult to read accurately.
	500	0,8	
	500	0,725	
	500	0,75	
	500	0,65	
	500	0,725	
06.02.2012	500	0,71	
	500	0,73	
	500	0,74	
	500	0,7	
	500	0,74	
	500	0,76	
	500	0,74	Spilled some, the cap slipped.
	500	0,76	
	500	0,74	
	500	0,69	

Table 4.03 shows the results of the deposit levels of the different Hier D02A crude oil solution concentrations.

Table 4.03 *Deposit levels of different concentrations of Hier D02A.*

Hier D02A 80:20 xylene			
Date	Concentration crude oil [µl]	Deposit level [ml]	Comments
08.03.12	100	0,05	Light orange and clear supernatant.
	250	0,1	Clear brown supernatant.
	500	0,15	Dark brown clear supernatant.
	1000	0,35	Very dark brown black supernatant, difficult to read the deposit level.

Only four runs were made to decide which concentration should be used in the dispersant testing. 1000µl crude oil solution gave a very dark supernatant, so it was difficult to read the deposit level, 500µl crude oil solution could be used, but the supernatant would probably be too dark once a dispersant was added. 250µl crude oil solution did not give very much asphaltene deposit, however the deposit level could clearly be seen through the supernatant. 100µl did not give enough asphaltene deposit since the grading on the centrifuge tube starts at 0,05ml.

The deposit levels of 100µl, 250µl, 500µl and 1000µl Hier D02A crude oil solution are shown in figure 4.05.

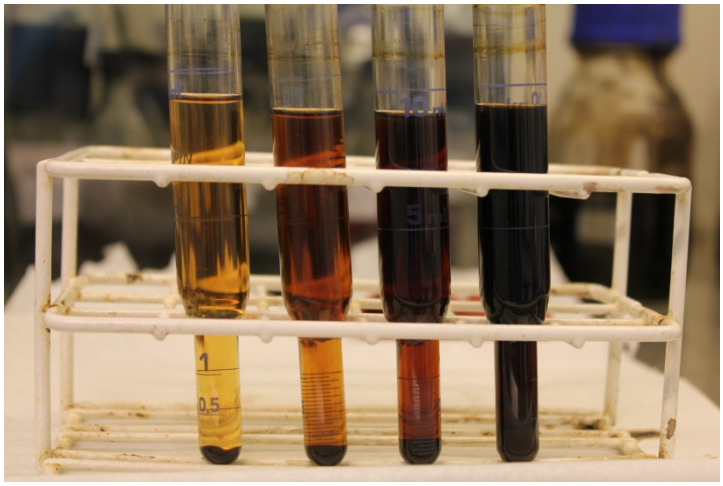

Figure 4.05 *Deposit levels of (from the left to right) 100µl, 250µl, 500µl and 1000µl Hier D02A crude oil solution (80:20 in xylene).*

4.1.3 Conclusion

There were some differences in the asphaltene deposit levels even though the concentrations of crude oil were the same. This is clearly observed in table 4.02 of the tests made with 500µl Crudo-Metapetroleum crude oil solution. However, the crude oil solution concentrations were chosen and will be further tested with dispersants to examine the effects on the deposit levels. The dispersants will be tested on 500µl Crudo-Metapetroleum solution and 250µl Hier D02A solution. Dispersants will not be tested on crude oil MO II because of the low deposit levels even with high crude oil concentrations.

4.2 Testing the effects of asphaltene dispersants on the deposit levels

Commercial asphaltene dispersants were tested to examine the effects on the chosen crude oils (500µl Crudo-Metapetroleum solution and 250µl Hier D02A solution). Three different dispersants were chosen to be tested in different concentrations:

- Hybase M-401 (monomeric, see chapter 1.5.2) 60:40 Exxol D80 (60% active solution).
- Flowsolve 110 (polymeric, see chapter 1.5.4), 50:50 Solvesso 150 ND (25% active solution).
- Flowsolve 113 (polymeric, see chapter 1.5.4), 50:50 Solvesso 150 ND (25% active solution).

The concentration of added dispersant was based on the active dispersant material. The effects of these were examined and compared to the blank tests.

4.2.1 Procedure

This procedure is similar to the procedure for the blank tests, with some additional points such as the addition of the dispersant, and mixing the dispersant in to pentane.

Pentane (10 ml) was added to each centrifuge tube.
The desired dispersant concentration was added to the pentane.
The centrifuge tubes were shaken well 20 times.
The desired concentration of crude oil solution was added to each of the centrifuge tubes.
The centrifuge tubes were shaken for two minutes to agitate the asphaltene stability, the bottom of the centrifuge tubes were held slightly upwards (figure 4.02) and was shaken sideways, not too fast, so the liquid in the narrow bottom of the tubes would be properly mixed.
After shaking, the centrifuge tubes were left for 30 minutes in order to let the asphaltenes agglomerate.
They were then centrifuged at 1500 rpm (revelations per minute) for 5 minutes.
The deposit level was evaluated, and noted.

4.2.2 Results and discussion

Table 4.04 on the next page, shows the results of 500µl Crudo-Metapetroleum solution with Hybase M-401, Flowsolve 110 and Flowsolve 113.

There were some changes in the deposit levels when a dispersant was added to the system compared to the blank tests. The supernatant became very dark when a dispersant was added, which indicates that the asphaltenes are dispersed.

In some of the tests, water separated in the bottom of the centrifuge tubes, so the observed deposit level may not be completely accurate, since it is difficult to read especially when the water level was below 0,05ml.

When Flowsolve 110 was used, the supernatant had to be poured off in order to be able to read the deposit levels. This may give some differences in the results compared to the measurements of Hybase M-401 and Flowsolve 113. Pouring out the supernatant may affect the deposit compactness, it may loosen and some liquid can be mixed in so the deposit level gives a higher reading than it would have given if it could be read directly.

The consistency of the deposit varies, some are soft and others are more compact. Even if the deposit level is the same, it does not say anything about the compactness, which will also play a role in choosing the better dispersant. An evaluation of the deposit consistency will be subjective, and the small amounts can make it difficult to compare and distinguish.

The deposit levels can at the finest be read by every 0,05ml, the second decimal is somewhat uncertain because of the marks on the centrifuge tubes. As the results show, the deposit levels are a bit varying even when the same concentration of the same dispersant is used.

Table 4.04 *Deposit levels of 500µl Crudo Metapetroleum solution mixed with three different dispersants.*

Crudo metapetroleum 50:50 Xylene						
Date	Concentration crude oil [µl]	Concentration dispersant [ppm]			Deposit level [ml]	Comments
		Hybase M-401	Flowsolve 110	Flowsolve 113		
07.02.2012	500	100	0	0	0,5	Some water was observed in the bottom. Not enough to measure.
	500	200	0	0	0,5	
	500	300	0	0	0,45	
	500	400	0	0	0,5	
	500	500	0	0	0,7	
	500	0	0	0	0,65	
	500	100	0	0	0,6	Some water was observed in the bottom. Not enough to measure
	500	200	0	0	0,5	
08.02.2012	500	0	100	0	0,3	The supernatants were so dark that it was not possible to read the deposit level. Had to pour off the supernatant to read the deposit level.
	500	0	200	0	0,3	
	500	0	300	0	0,35	
	500	0	400	0	0,35	
	500	0	500	0	0,35	
	500	0	100	0	0,4	
	500	0	200	0	0,35	
	500	0	300	0	0,35	
	500	0	400	0	0,4	
	500	0	500	0	0,4	
10.02.2012	500	0	50	0	0,35	Centrifuge for 20 minutes at 2500 rpm. Water was observed in the bottom of the three last centrifuge tubes.
	500	0	100	0	0,05-0,4	
	500	0	200	0	0,1-0,45	
	500	0	300	0	0,02-0,35	
13.02.2012	500	300	0	0	0,15-0,45	There were water in the bottom of all these tests, they were centrifuged at 2500 rpm for 10 minutes.
	500	300	0	0	0,15-0,46	
	500	300	0	0	0,1-0,46	
	500	300	0	0	0,15-0,46	
	500	0	300	0	0,04-0,45	
	500	0	300	0	0,05-0,4	
	500	0	300	0	0,05-0,45	
	500	0	300	0	0,1-0,47	
	500	0	0	300	0,1-0,45	
	500	0	0	300	0,15-0,45	
	500	0	0	300	0,15-0,45	
	500	0	0	300	0,2-0,45	

Table 4.05 shows the results of the deposit levels of 250µl Hier D02A crude oil solution with Flowsolve 110 and 113.

Table 4.05 *Deposit levels of 250µl Hier D02A solution mixed with two different dispersants.*

Hier D02A 80:20 xylene					
Date	Concentration crude oil [µl]	Concentration dispersant [ppm]		Deposit level [ml]	Comments
		Flowsolve 110	Flowsolve 113		
08.03.2012	250	100	0	0,1	Very dark supernatant, difficult to read the deposit levels. The deposit levels were too low (below the grading on the centrifuge tube).
	250	200	0	0,09	
	250	300	0	0,08	
	250	400	0	0,06	
	250	0	100	0,08	
	250	0	200	0,09	
	250	0	300	0,08	
	250	0	400	0,07	

The supernatants were very dark, thus difficult to read. Compared to the blank test (table 4.03), there were small observable effects on the deposit level when the dispersants were used, 400µl of Flowsolve 110 gave the best result, the higher concentrations of both dispersants caused a lower deposit level, which is desired.
The consistency of the asphaltene deposit varied also in this crude oil, which cause problems in deciding which dispersant is really better than the other.

4.2.3 Conclusion

This method is not very good in order to reveal small changes in the system, which makes it difficult to rank the dispersants. As the results show, the addition of a dispersant will not give very accurate repeatable results under the same conditions. The level varies so much that it is difficult to compare the different dispersants using the deposit levels.
Often the deposits vary in consistency, when a dispersant is added the deposits were often observed to be softer and more "slushy" compared to the blank tests. So even if the deposit level is the same, it is not very accurate to only consider the volume of the deposit. If the deposits consistency were to be evaluated, it would be a subjective evaluation, which should be avoided.
Another method should be examined to see if better repeatable results may be obtained and if it is possible to detect the small differences.

Measurements of the turbidity seemed to work well and three models were made with turbidity set as a response value (chapter 5).

4.3 References

1. Manek, M.B., *Asphaltene Dispersants as Demulsification Aids*, in *SPE International Symposium on Oilfield Chemistry*1995, Copyright 1995, Society of Petroleum Engineers Inc.: San Antonio, Texas.

Chapter 5 Asphaltene dispersant/inhibitor formulation development through Experimental Design

The turbidity of the supernatants of different mixtures were measured, high asphaltene content in the solution would give a higher reading of the turbidity. This was the second method to be examined. A number of samples were tested and the results were inserted in Design Expert where the models were evaluated. Any interesting interactions in the models in Design Expert were further examined to build the model gradually.
This chapter is the main part of this thesis, turbidity was used as a response to create a model that would hopefully give an optimal mixture formulation of the asphaltene dispersants.

The tests were performed as similarly as possible each time in order to get the most reliable results. The tests should also give repeatable results, if done correctly each time. Of course human errors will always be a factor to be taken into consideration when performing experiments. That is why it is very important to always observe the experiments and take notes of any observed differences.
The experimental plan made in Design Expert randomized the experiments in order to prevent systematic errors, and the different plots in chapter 2.5.3 and 2.5.4 were used as an important tool to discover experiments which deviate strongly from the model.

5.1 The different mixture models

A three component mixture with Crudo Metapetroleum (50:50 in xylene) and different concentrations of A) DDBSA (25% active), B) Hybase M-401 (60% active) and C) Flowsolve 113 (25% active) were used to create a model where the turbidity was chosen as the measured response.
A) Hybase M-401 (60% active) and B) Flowsolve 113 (25% active) were further tested on other crude oils: Hier D02A crude oil (80:20 in xylene) and Jordbær crude oil (50:50 in water). Two component models were created and turbidity was used as the response.

80ml centrifuge tubes (tube nr.7, figure 4.01) were used in order to have enough supernatant to measure the turbidity. Different crude oil concentrations were used for each of the crude oils tested depending on the results given in the deposit level tests in chapter 4:

- The total amount of dispersants was always 300ppm active material. Pentane (76 ml) was used with the Crudo Metapetroleum solution (4 ml).
- The total amount of dispersants was always 300 ppm active material. Pentane (78,8 ml) was used with the Hier D02A crude oil solution (1,2 ml).
- The total amount of dispersants was always 300 ppm active material. Pentane (72 ml) was used with the Jordbær crude oil solution (8 ml).

The designs of experiments were performed as described in chapter 2 and the experiments for all three models were performed by following the same procedure described in chapter 5.2.1.

5.2 Experimental procedure

The procedure was similar to the procedures in chapter 4, but with some differences:

- Centrifuge the samples at 2500rpm for 10 minutes, rather than 1500rpm for 5 minutes.
- The samples were shaken in bottles with screw caps and transferred to the centrifuge tubes, instead of being shaken in the centrifuge tubes. There were not large enough rubber caps to cover the centrifuge tube.

The amounts of pentane, dispersants and crude oil solution were not specified in the procedure because of the different amounts used for each model. The amounts used were specified on the previous.

5.2.1 Procedure

Pentane was added to four 100ml bottles.
The desired dispersant concentrations were then added to the pentane, one dispersant at the time.
The bottles were then shaken well 20 times before the crude oil solution was added to the pentane and dispersant mixtures.
The bottles were shaken for two minutes to agitate the asphaltene stability.
Directly after shaking, the mixtures were transferred to the 80 ml centrifuge tubes and are left for 30 minutes so the asphaltenes could agglomerate.
The tubes were then centrifuged at 2500 rpm for 10 minutes.
After centrifugation the top of each supernatant of each centrifuge tube was transferred to turbidity tubes (approximately 30 ml).
The turbidity of each run was noted and inserted in Design Expert.

5.3 The Crudo Metapetroleum three component model

The procedure for Design Expert in chapter 2 and the experimental procedure on the previous page was followed and performed as similarly as possible each time. The experimental plan was followed by run number and the measured response, turbidity, was plotted into Design Expert when they were ready.

As the experiments were performed, the model was examined as more data points were added and the interesting areas of the model graph were further tested. A detailed analysis was given when the model was complete. The analysis was examined frequently in order to know which experiments deviated from the model and had to be re-tested.

5.3.1 The Crudo Metapetroleum design results and discussion

Table 1 shows the results for the seven first runs of the DDBSA, Hybase M-401 and Flowsolve 113 mixture design.

The standard order of the experiment plan is randomized, so the experiments are done according to the run number (green). The measured turbidity is in the red column, a high turbidity indicates that the dispersant is highly effective.

Table 1 *Shows the experimental plan including the responses of the model.*

Run number	Component A) DDBSA	Component B) Hybase M-401	Component C) Flowsolve 113	Response 1 Turbidity	Comments
-	-	-	-	19,0	Blank test, not a part of the design.
1	300	0	0	14,8	
2	0	300	0	107	
3	0	0	300	235	
4	150	0	150	154	
5	150	150	0	20,4	
6	0	150	150	108	
7	100	100	100	54,6	

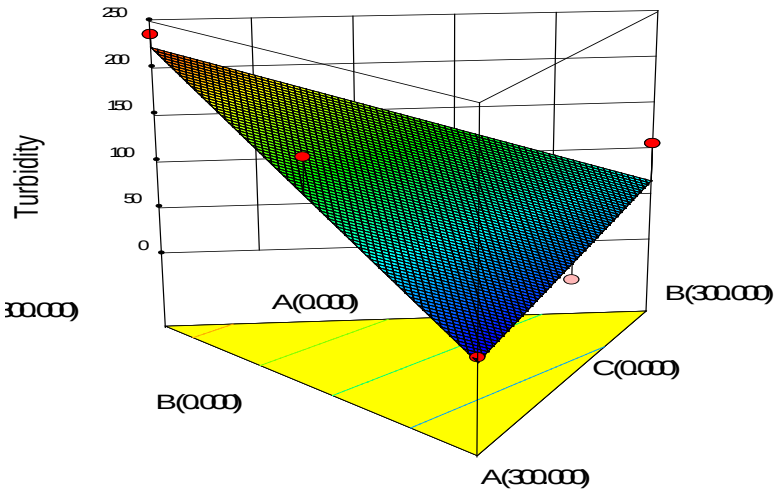

Figure 5.01 *The model graph of the first 7 runs, a linear model.*

The model was built gradually as mentioned. The first seven runs gave a linear model as shown in figure 1. Seven data points are not enough for this kind of model, replicates are needed in addition to more data points, but it gives an overview of the system. As the model graph shows, 300ppm of component C – Flowsolve 113 measured the highest turbidity and 300 ppm Component A – DDBSA measured the lowest turbidity. The analysis of the model (diagnostics and diagnostic influence) shows no abnormalities. Further testing was done in order to improve the model.

Table 2 *Continuation of the experimental results – run 8 – 23.*

Run number	Component A) DDBSA	Component B) Hybase M-401	Component C) Flowsolve 113	Response 1 Turbidity	Comments
8	150	75	75	36,1	
9	75	75	150	72,5	
10	75	150	75	57,6	
11	50	50	200	105	
12	0	0	300	182	
13	0	300	0	116	
14	200	50	50	28,3	
15	100	200	0	48,3	
16	200	100	0	15,2	
17	0	100	200	96,3	
18	100	0	200	142	
19	0	200	100	79,2	
20	200	100	0	13,5	
21	50	200	50	50,2	
22	200	0	100	134	

After adding run number 8-22 (table 2), Design Expert suggested the special cubic model. Figure 5.02 shows the special cubic model of the Crudo-Metapetroleum design so far. Further experiments were done with only DDBSA and Flowsolve 113, since the model graph (figure 5.20) seems to show a slight positive interaction between these dispersants.

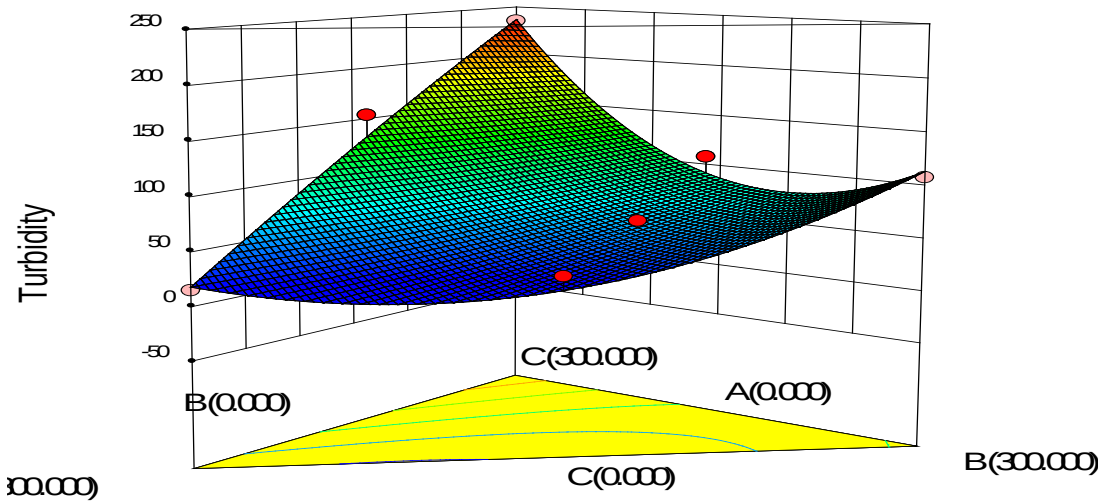

Figure 5.02 *The 3D model graph of 22 experimental runs, special cubic model.*

Table 3 *The results of DDBSA mixed with Flowsolve 113. The last results of the Crudo-Metapetroleum model*

Run number	Component A) DDBSA	Component B) Hybase M-401	Component C) Flowsolve 113	Response 1 Turbidity	Comments
23	250	0	50	128	
24	50	0	250	165	
25	200	0	100	155	
26	250	0	50	125	

Table 3 shows the results of the turbidity measurements of DDBSA mixed with Flowsolve 113. The results show high measured turbidity, however not as high as the measurements from the 300ppm Flowsolve 113 tests. Run number 3 gave the highest measurement of 235 NTU (300ppm Flowsolve 113). Hybase M-401 mixed with DDBSA gave the lowest measured turbidity of 13,5 NTU (Run number 20), the other measurements of these dispersants mixed together were not very high either.

Design Expert gave two suggested models as the best fit, a cubic model and a quartic model, where the analysis of each model needs to be evaluated and compared.

A transformation of both these models were suggested, however it was decided that a transformation should not be used. Even if a transformation is suggested in this case, it does not necessarily mean that it is “better”. It may even cause the interpretation of the model to become more difficult.

Comparison of the cubic and quartic models –model graphs from Design Expert

Both these response surfaces (figure 5.03 and 5.04) shows that the best formulation is Flowsolve 113 as a pure component. The interesting mixture interaction in this model was between Flowsolve 113 and DDBSA, which was further examined in run number 22-26 as mentioned earlier. However this interaction did not give any better results than Flowsolve 113 as the only dispersant.

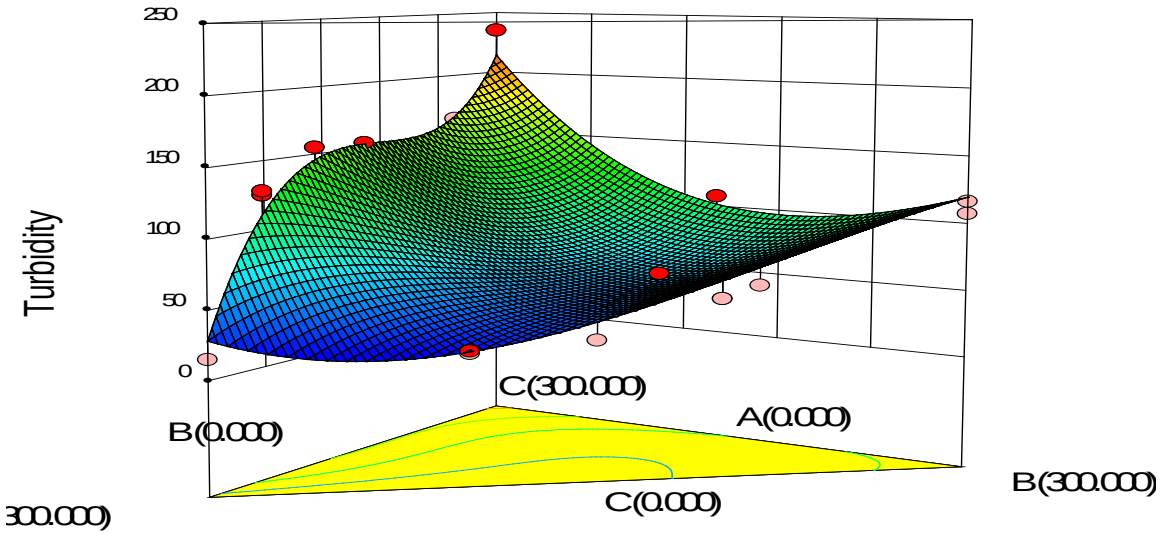

Figure 5.03 *The 3D response surface of the cubic model. A) DDBSA, B) Hybase M-401and C) Flowsolve 113.*

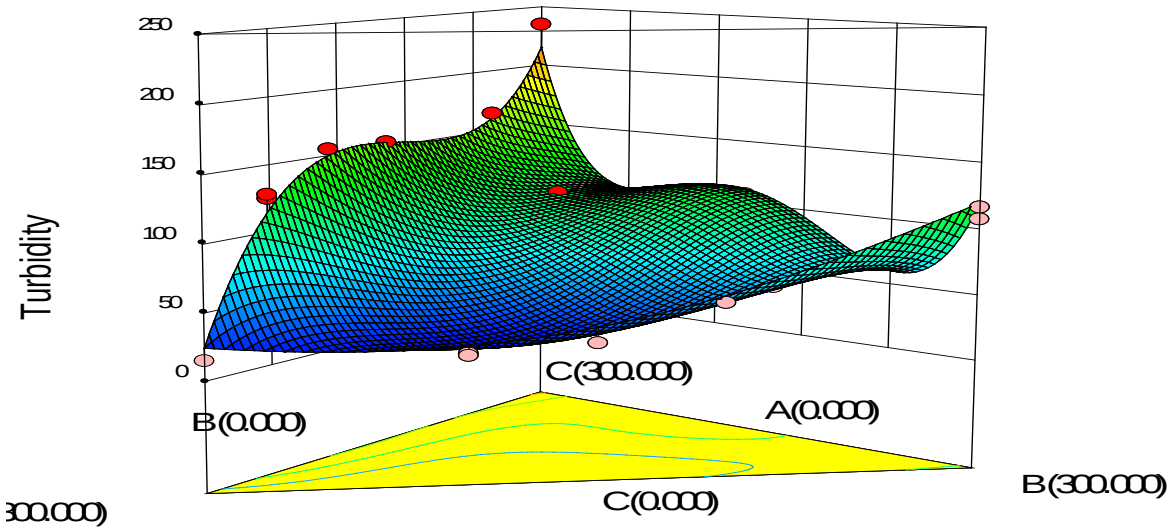

Figure 5.04 *The 3D response surface of the quartic model. A) DDBSA, B) Hybase M-401and C) Flowsolve 113.*

The quartic model (figure 5.04) show some kind of positive reaction of the Hybase M-401 – Flowsolve 113 mixture, but further examination was not done in this model, because the DDBSA – Flowsolve 113 mixture showed better results. The 3D response surface makes it easier to interpret which mixtures are effective as well as which mixtures to stay clear of (the low measurements).

The 3D response surfaces can be rotated in all directions in Design Expert in order to view the whole surface in detail.
The red points are the actual responses which are above the predicted surface and the light pink points are the actual responses which are under the predicted surface (figure 5.03 and 5.04).
The blue colour on the surface indicates low predicted response values, green indicates medium predicted response values and red indicates high predicted response values. The vertices A, B and C are DDBSA, Hybase M-401 and Flowsolve 113 respectively, which can easier be observed in the 2D contour plots (figure 5.05 and 5.06).

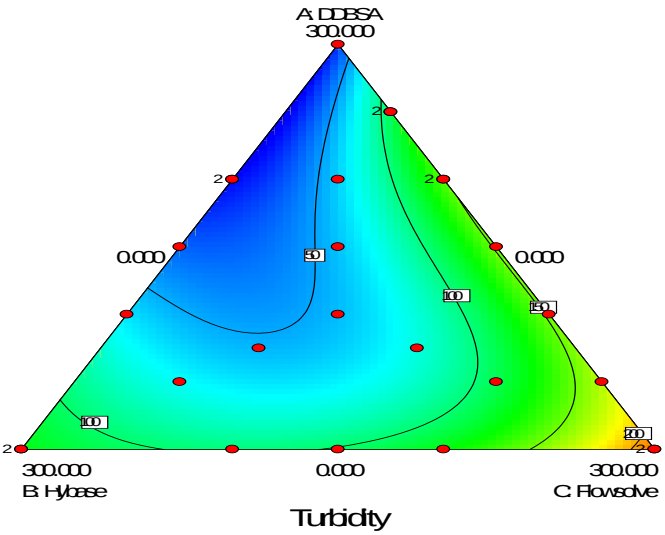

Figure 5.05 *The contour of the cubic model.*

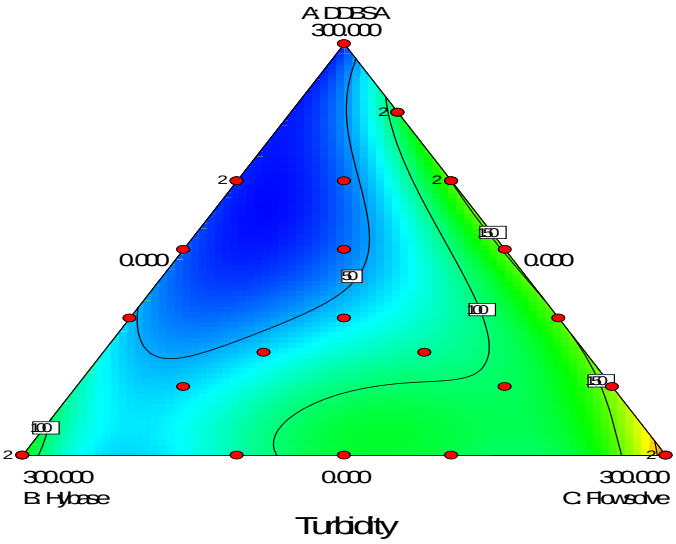

Figure 5.06 *The contour of the quartic model.*

Comparison of the cubic and quartic models – diagnostics from Design Expert

The different diagnostics plots will be compared and commented.

The colours of the different data points in the diagnostics plots represent the value of the measured turbidity. Colours from low values to high values are: dark blue < light blue < green < yellow < orange < red.

Normal plot

As the cubic normal plot show (figure 5.07), there are no obvious S-curved patterns. The cubic plot does not indicate that a transformation was needed. The quartic normal plot shows more curving (the light blue line in figure 5.08) than the cubic plot, which indicates that a transformation could be used. The quartic plot shows two data points that deviated from the rest of the data points while the cubic plot only shows one data point deviating from the rest. The normal plots indicate that the cubic model fits better than the quartic model.

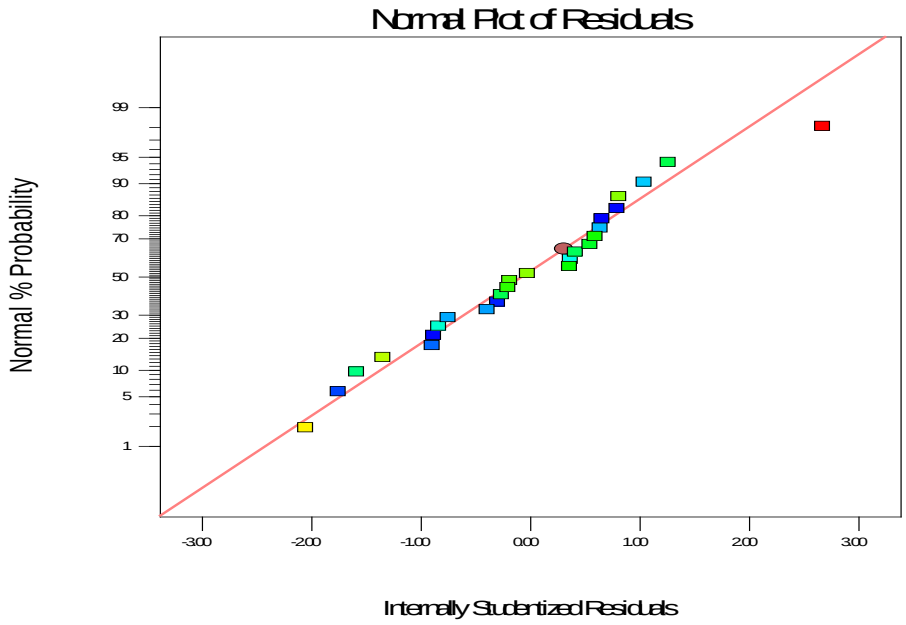

Figure 5.07 *The normal probability plot of the cubic model.*

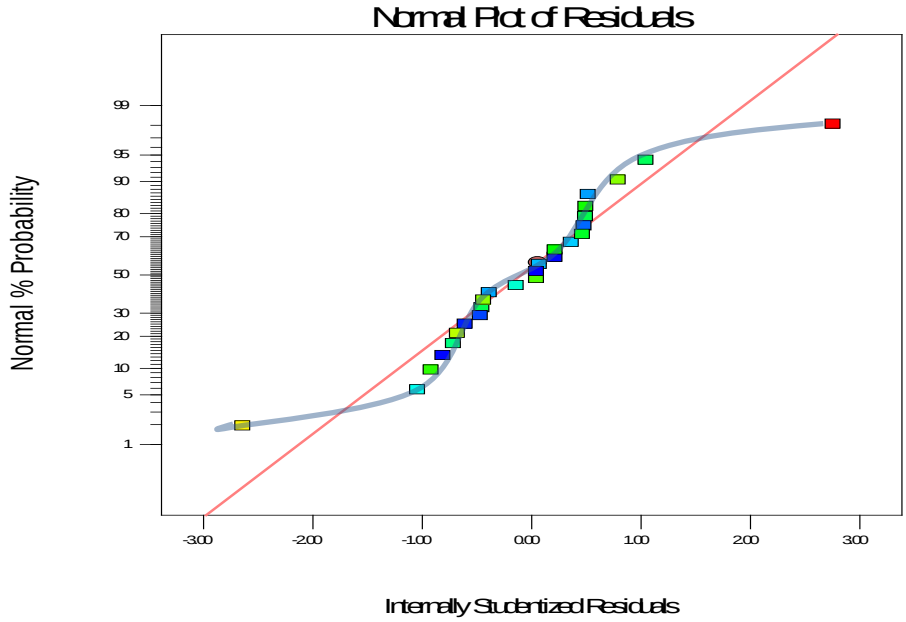

Figure 5.08 *The normal probability plot of the quartic model.*

Residuals vs. Predicted plot

The residuals vs. predicted plots of the cubic model and the quartic model are shown in figures 5.09 and 5.10. The quartic plot shows a tendency of increasing residuals with increasing predicted values. This means that the variance is not constant for the quartic model, which indicates that the quartic model may need a transformation. The cubic plot has a more random scatter of the data points, but there may be some tendency of increasing residuals with increasing predicted values. The cubic model seems to fit better, the data points are scattered so a transformation is probably not needed.

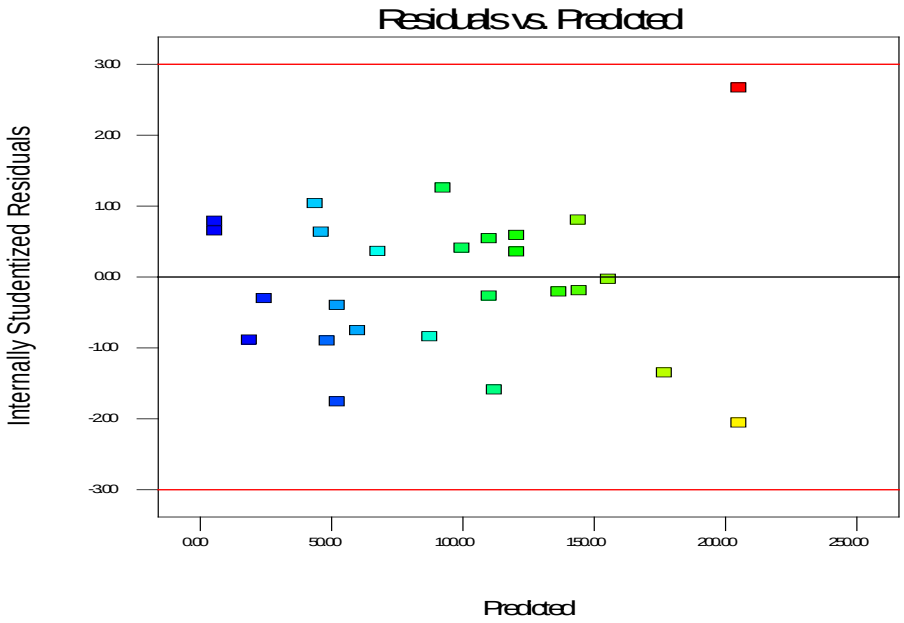

Figure 5.09 *The Residuals vs. Predicted plot of the cubic model.*

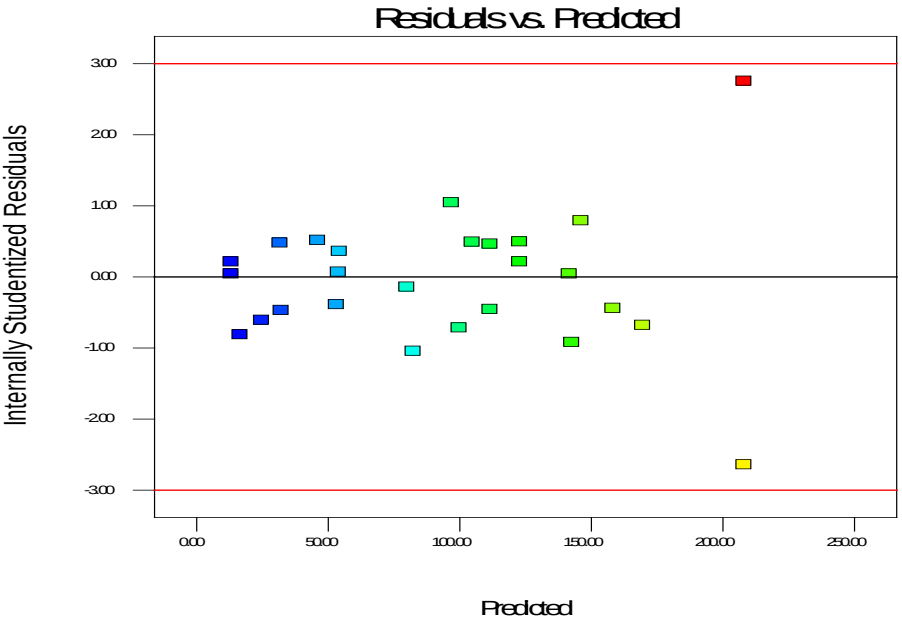

Figure 5.10 *The Residuals vs. Predicted plot of the quartic model.*

Residuals vs. Run plot

The data points are randomly scattered in both these plots (figure 5.11 and 5.12), indicating that there is no systematic errors such as the day to day conditions. The cubic plot shows that run number 3 and run number 12 deviates from the rest of the data points, however they are still within the boundaries. Run number 3 is very close to the upper boundary in the cubic and the quartic plot. Both run number 3 and 12 are 300ppm Flowsolve 113.Nothing abnormal has been noted with these experiments.

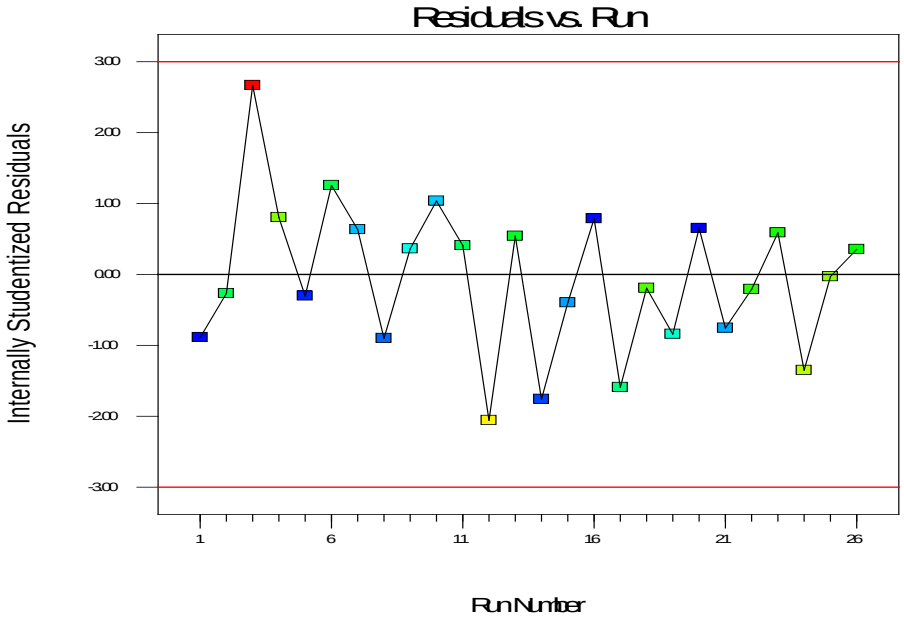

Figure 5.12 *The Residuals vs. Run plot of the cubic model.*

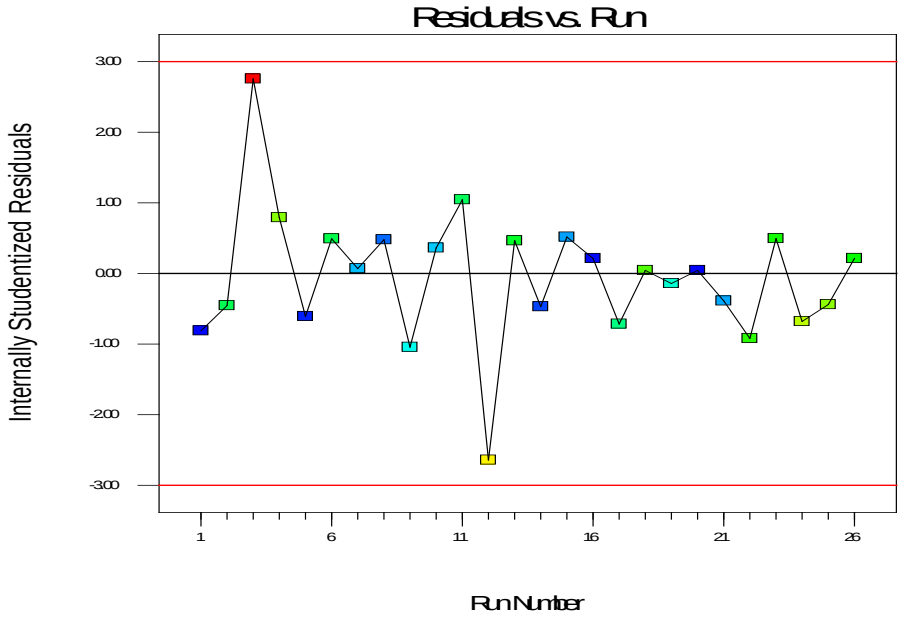

Figure 5.11 *The Residuals vs. Run plot of the quartic model.*

Predicted vs. Actual plot

The highest measured values (235 NTU and 182 NTU) are the ones that deviate from the rest of the values, this means that the model has some difficulties with predicting these values. The quartic plot (figure 5.14) where the data points follow the 45° straight line nicely seems to have a better fit than the cubic plot (figure 5.13) which has more scattered data points. However both these models fit quite nicely as the data points are close to the 45° straight line.

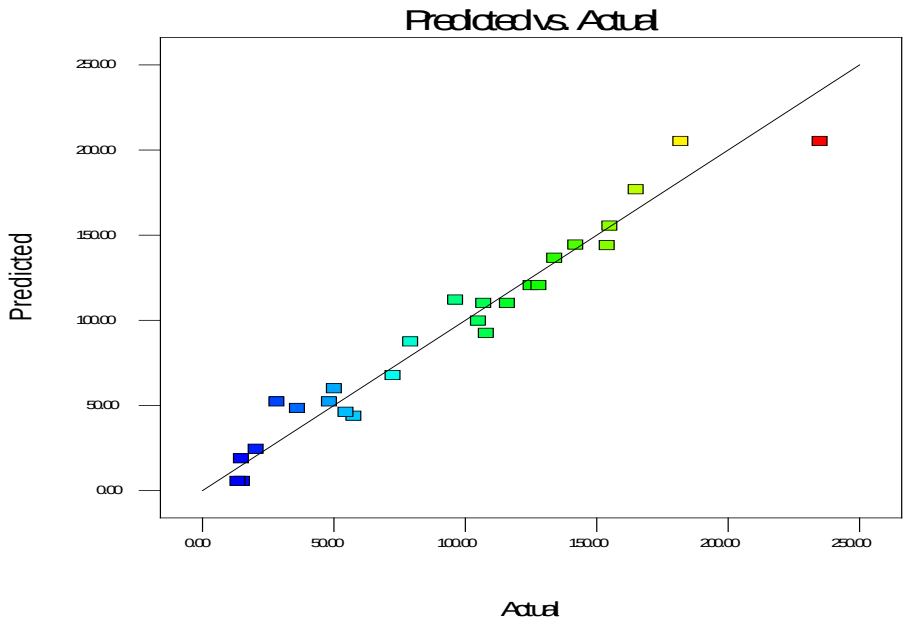

Figure 5.13 *The Predicted vs. Actual plot of the cubic model.*

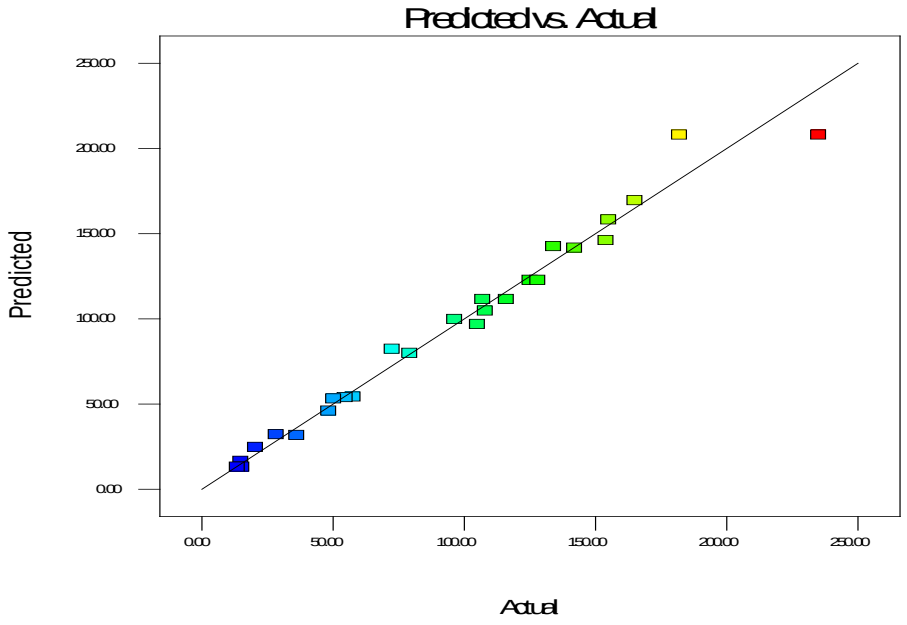

Figure 5.14 *The Predicted vs. Actual plot of the quartic model***.**

Comparison of the cubic and quartic models – Influence from Design Expert

The different influence plots for the cubic and quartic models are shown on the next pages. They will only be briefly commented since there is much deeper statistics involved.

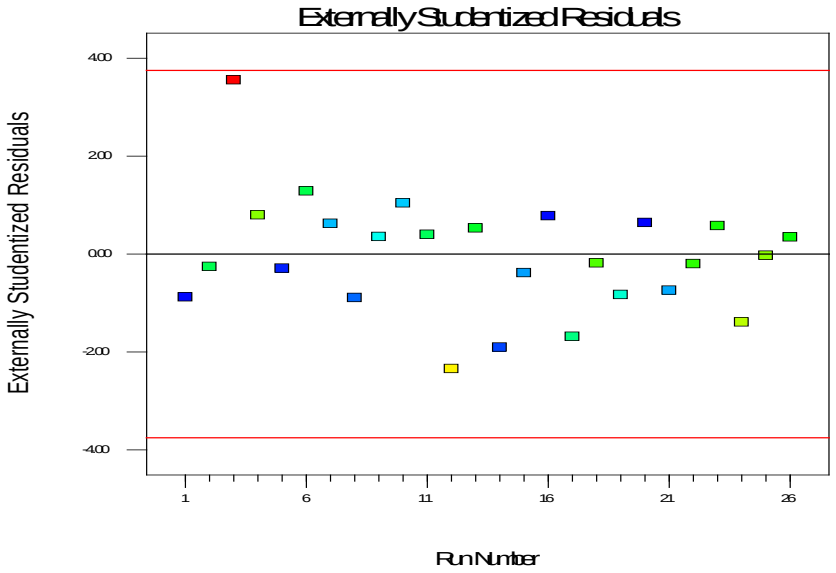

Figure 5.15 *Externally Studentized Residuals vs. Run for the cubic model.*

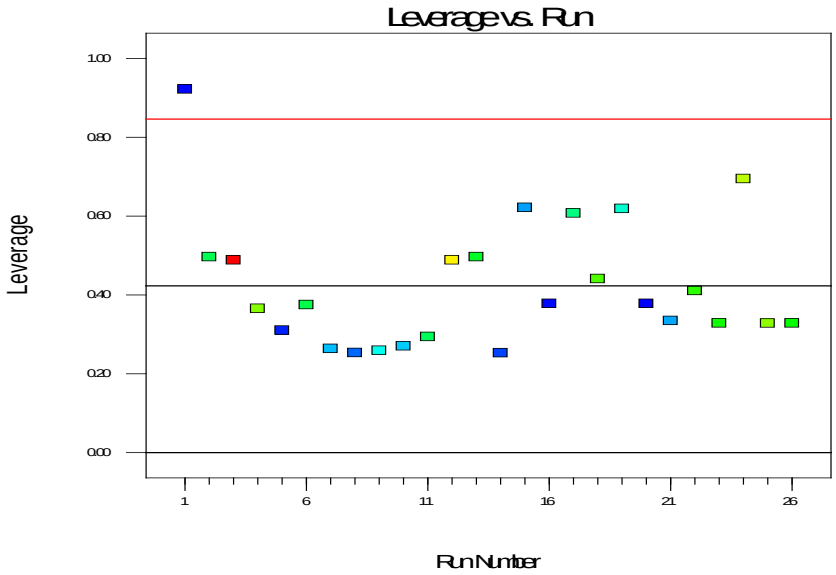

Figure 5.16 *Leverage vs. Run plot for the cubic model.*

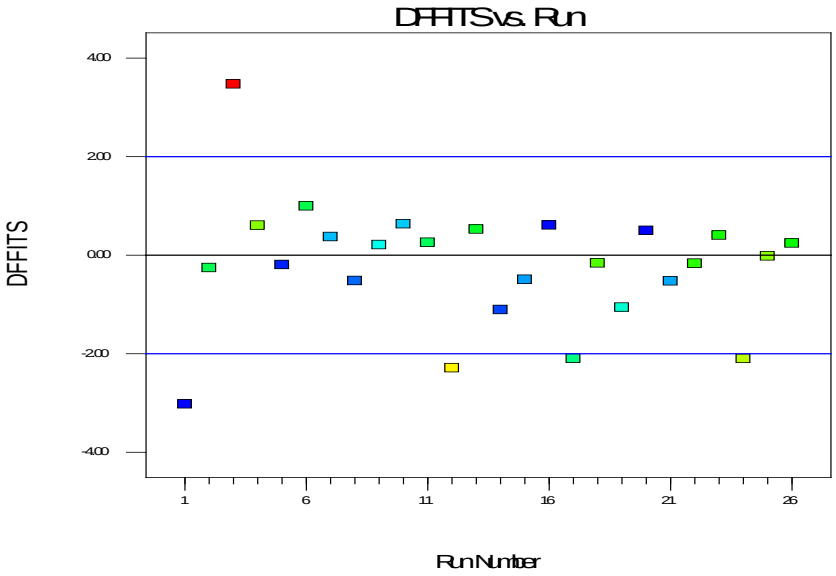

Figure 5.17 *Difference in fits (DFFITS) plot for the cubic model.*

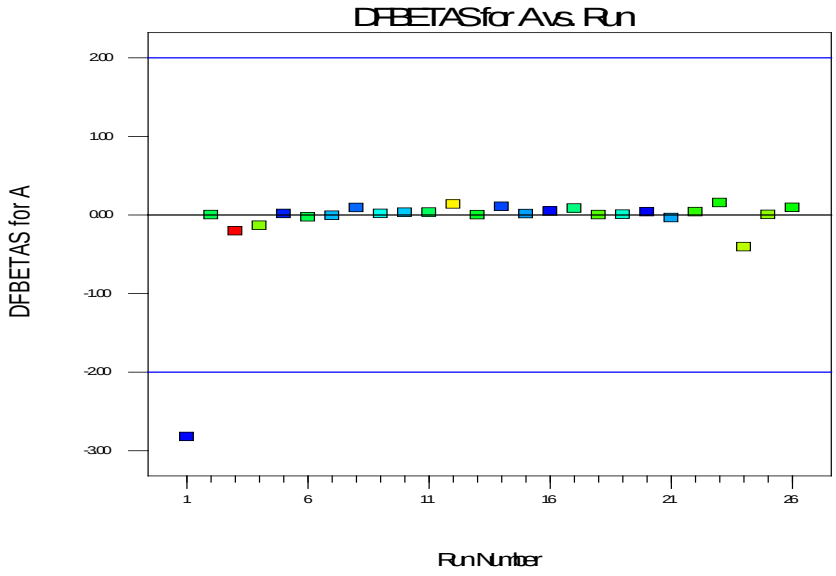

Figure 5.18 *Difference in BETAS plot for factor A (DDBSA).*

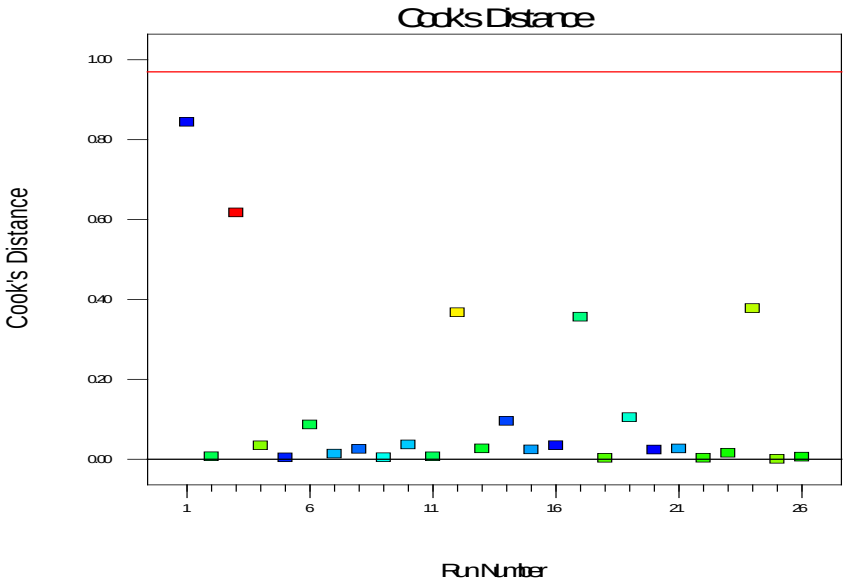

Figure 5.19 *Cook's distance plot for the cubic model.*

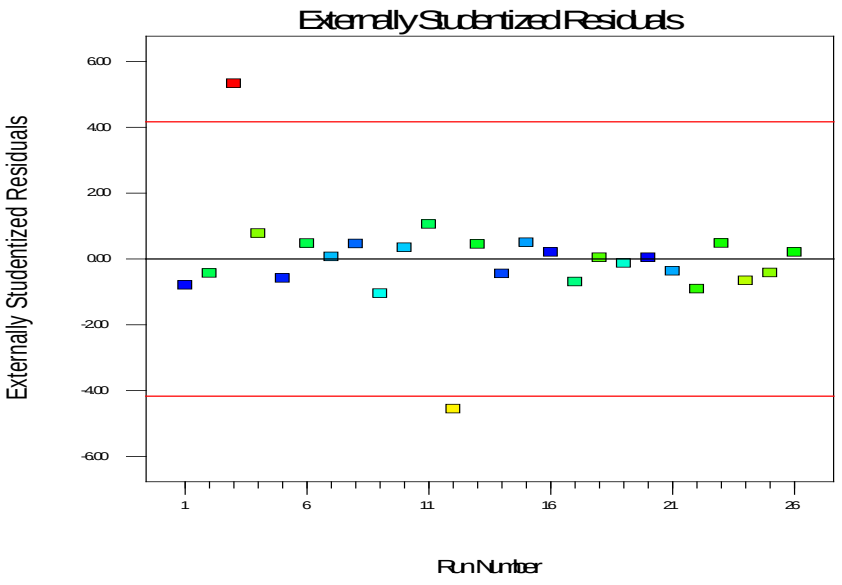

Figure 5.20 *Externally Studentized Residuals vs. Run plot for the quartic model.*

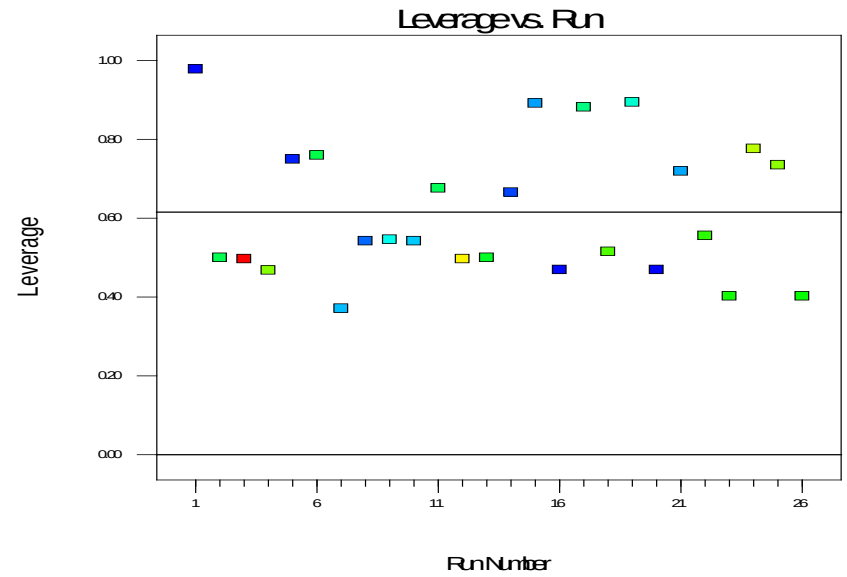

Figure 5.21 *Leverage vs. Run plot for the quartic model.*

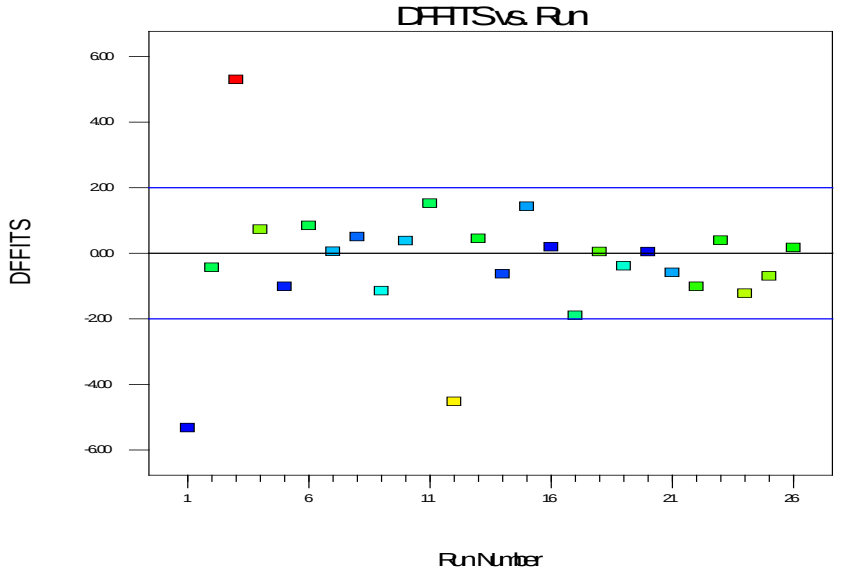

Figure 5.22 *Difference in fits vs. Run plot for the quartic model.*

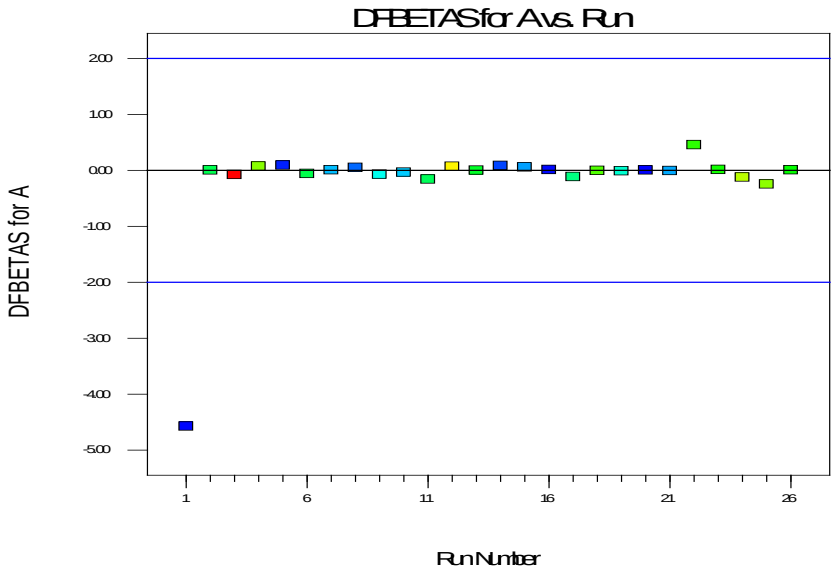

Figure 5.23 *Difference in BETAS plot for the quartic plot.*

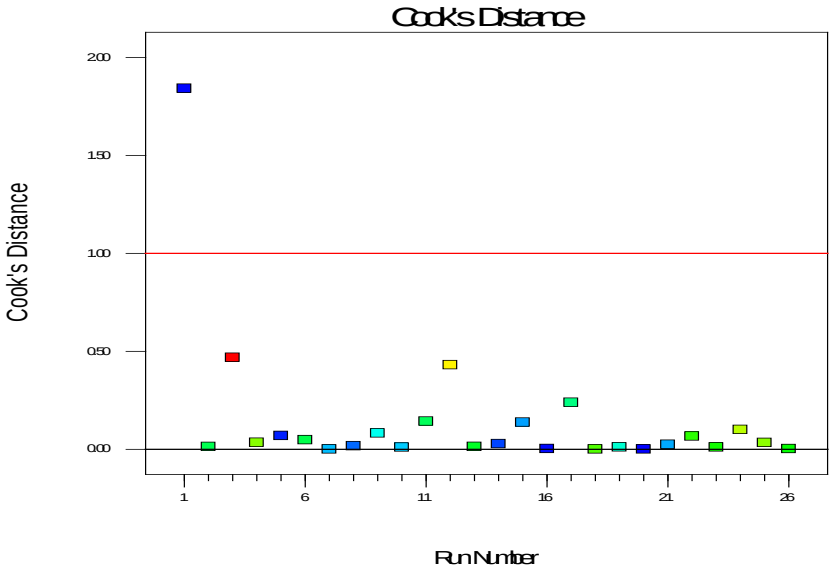

Figure 5.24 *Cook's distance plot for the quartic model.*

Data points outside the boundaries set by Design Expert may influence the model greatly. The data points in question does not necessarily have to be wrong, it just means that the point should be checked in case of errors, uncertainty of the method, uncertainty of the measured turbidity or uncertainty of the interactions in the solution.

The purpose of these plots is to reveal certain tendencies and to try to pinpoint what the cause is and then try to fix the values if it is possible at all (re-tests, more tests, evaluate the method etc.).

In most of these plots (figure 5.15 – 5.24), many of the first tests which were performed are the outliers which reappears. This may be so because for example experience will often diminish errors and increase the accuracy of the experiments.

In general, these plots are satisfactory, the outlying data points have been checked and replicated. However, the replicate turned out to be an outlier, so there is not much more to do in this current model, than to take these points into consideration. As mentioned earlier, there is a much deeper statistical meaning behind these plots, even so they can give an indication of the deviating parameters in which can further be examined for what it is worth.

Comparison of the cubic and quartic models – Optimization from Design Expert

The models were optimized using numerical optimization where the maximum response was set as a goal.

The lower and upper limits were set to 205 NTU and 255 NTU respectively, which are +/- 20NTU from the best measurement (235NTU, 300ppm Flowsolve 113). Figure 5.25 shows the optimised contour plot of the cubic model.

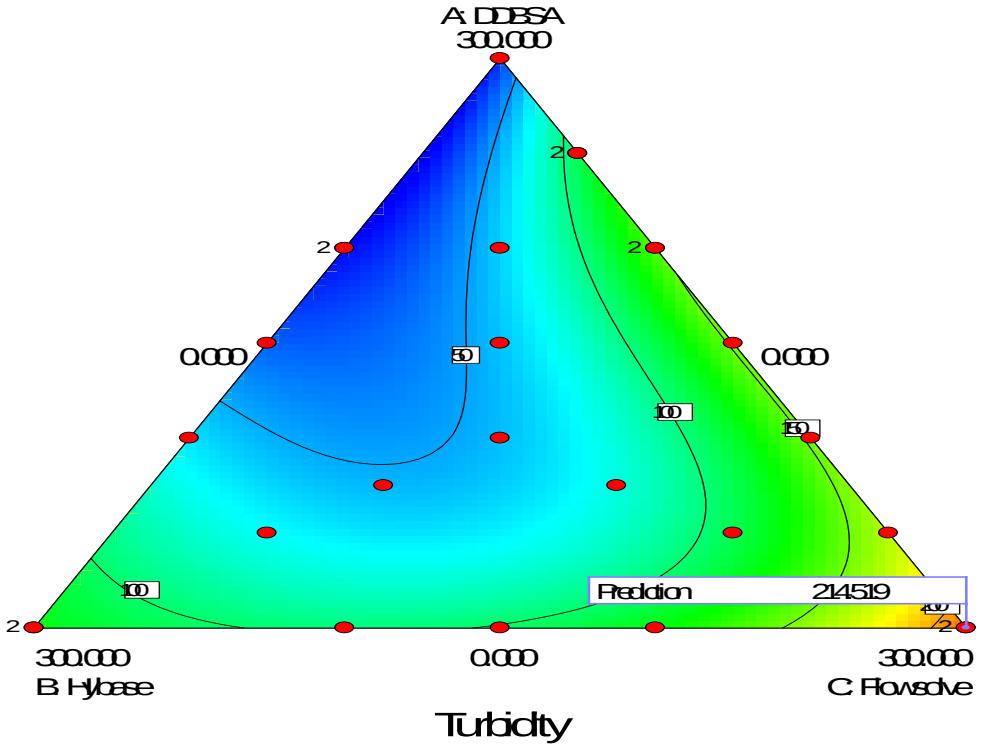

Figure 5.25 *The optimized 2D contour of the cubic model.*

Table 4 show that within the predicted optimization limits, there is one predicted optimal solution. Pure Flowsolve 113 (300 ppm) gives the best predicted value of 214,519 NTU in the cubic model.

Table 4 *Optimization of the cubic model.*

Name	Goal	Lower Limit	Upper Limit	Lower Weight	Upper Weight	Importance
A:DDBSA	is in range	0	300	1	1	3
B:Hybase	is in range	0	300	1	1	3
C:Flowsolve	is in range	0	300	1	1	3
Turbidity	maximize	205	255	1	1	3
Solutions Number	DDBSA	Hybase	Flowsolve	Turbidity	Desirability	
1	0.000	0.000	300.000	214.519	0,19038475	Selected

The quartic model is quite similar to the cubic model in the prediction. Figure 5.26 shows that the only optimal solution was found to be Flowsolve 113 by itself. Design Experts calculations in table 5 show the predicted optimal response to be 215,765 NTU for 300ppm Flowsolve 113.

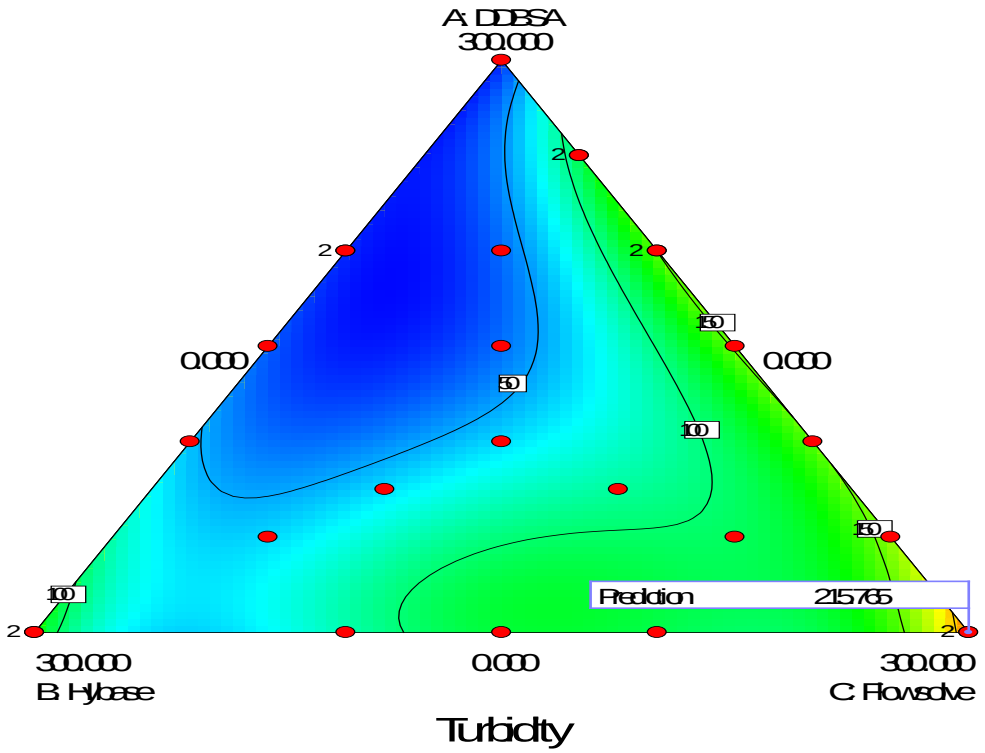

Figure 5.26 *The optimized 2D contour of the quartic model.*

Table 5 *Optimization of the quartic model.*

Name	Goal	Lower Limit	Upper Limit	Lower Weight	Upper Weight	Importance
A:DDBSA	is in range	0	300	1	1	3
B:Hybase	is in range	0	300	1	1	3
C:Flowsolve	is in range	0	300	1	1	3
Turbidity	maximize	205	255	1	1	3
Solutions Number	DDBSA	Hybase	Flowsolve	Turbidity	Desirability	
1	0.000	0.000	300.000	215.765	0,21529578	Selected

5.3.2 The Crudo Metapetroleum design conclusion

Turbidity measurements did not require a lot of time and the equipment was easy to use. Both the models (cubic and quartic models) showed that the dispersant mixture did not give quite the results which were desired. Flowsolve 113 was the best dispersant, and the effect diminished once Flowsolve 113 was mixed with DDBSA, Hybase M-401 or a mixture of the two. The cubic model seems to fit the response values better than the quartic model. Normally the model of the lowest degree should be chosen, if possible, because of the complexity of a higher order model. A transformation (log) was recommended for both these models, however it was decided not to use the recommended transformation because it would be more difficult to interpret the results [1]. The cubic model did not show obvious trends which indicated the need for transformation. The quartic model showed more trends that indicated that a transformation was needed, so the best model in this case would be the cubic model.

Design Expert was somewhat difficult to use at first, with all the statistical background attached to the results. More experience will most likely be an advantage when performing analysis in order to know what to look for in the different plots, but the main objective was to reveal certain tendencies and to get to know the design of experiments method. Design expert was an extremely useful tool in order to easily give an overview of the results, useful statistical and mathematical values in the form of graphical plots. Unfortunately there was a limited amount of time to learn to use Design Expert to its fullest potential. Quick evaluation of the mixture interactions, evaluation of deviations from the model and the ability to reveal tendencies in the experimental performance where some of the important parameters in which Design Expert could present, even though the detailed statistics and mathematics behind the design model were not studied.

5.4 The Hier D02A two component model

The three component mixture model with Crudo-Metapetroleum did not reveal any revolutionary dispersant mixture interactions, hence it would be interesting to test the dispersant mixtures on another crude oil. Hier D02A was chosen, and there seemed to be sufficient asphaltene content in this crude oil (see chapter 4).
A two component model was decided for this crude oil with Hybase M-401 and Flowsolve 113 since the interaction between these dispersants was not thoroughly investigated in the previous model.
The dispersants were mixed to a total concentration of 300ppm of active material.
The same procedure as used before (chapter 5.2.1) for the experiments were followed and completed as similarly as possible.

5.4.1 The Hier D02A design results and discussion

As table 6 show, the highest turbidity measurement was from an experiment with only Flowsolve 113 as the active dispersant (Run#5, 104 NTU). The numbers are in general lower than for the Crudo Metapetroleum turbidity measurements, which may indicate differences in the asphaltene content of the crude oils and different interactions between the dispersants and the crude oils.

Table 6 *shows the experimental plan including the responses of the Hier D02A model.*

Standard Order	Run	Component 1 Hybase M-401	Component 2 Flowsolve 113	Response 1 Turbidity	Comments
4	1	200	100	17,4	
1	2	0	300	98,7	
7	3	100	200	52,3	
3	4	225	75	17,5	
6	5	0	300	104	May have been some acetone in the bottles from when they were washed. It was noticed in the bottle for Run#8, but not in the other bottles.
2	6	75	225	91,1	
8	7	300	0	66,3	
5	8	300	0	37,2	
9	9	0	300	98,4	
10	10	150	150	30,1	
11	11	225	75	25,7	
12	12	75	225	58,7	
13	13	300	0	40	
14	14	150	150	24,4	

Design Expert gave one suggested models as the best fit, a cubic model. A transformation was not suggested in this model.

Model graphs from Design Expert

The model graph for the Hier D02A crude oil shows an obvious antagonistic effect between Flowsolve 113 and Hybase M-401 where Flowsolve 113 is the best dispersant.

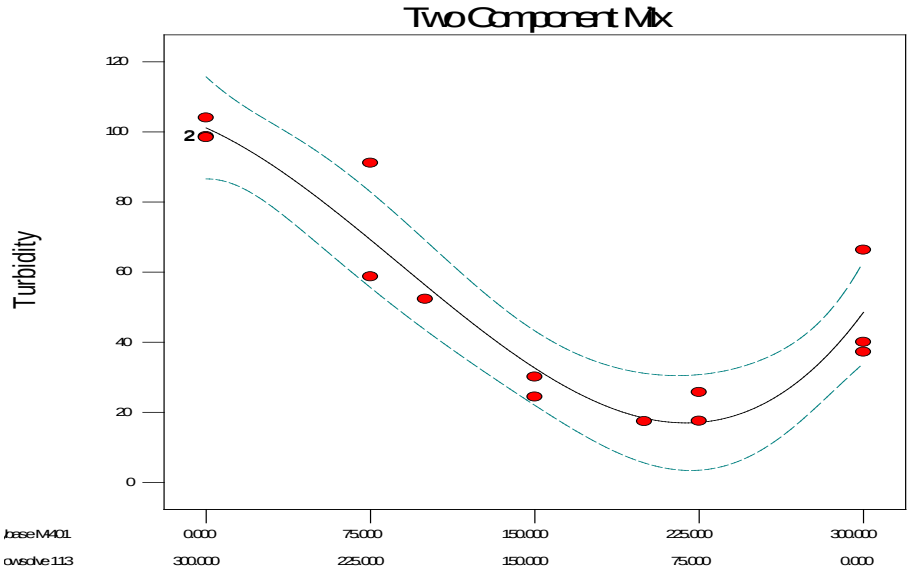

Figure 5.27 *The 2D model graph of the Hier D02A cubic model.*

This plot shows certain ranges of dispersant mixtures which should not be used unless a low turbidity is desired.

Diagnostics results from Design Expert

The different diagnostic plots will be evaluated, and commented. The colours of the different data points in the diagnostics plots represent the value of the measured turbidity. Colours from low values to high values are: dark blue < light blue < green < yellow < orange < red.

Normal plot

This normal probability plot shows some scattering of the residuals, however Design Expert does not recommend a transformation. There is not an obvious s-shaped curve, so the plot is acceptable.

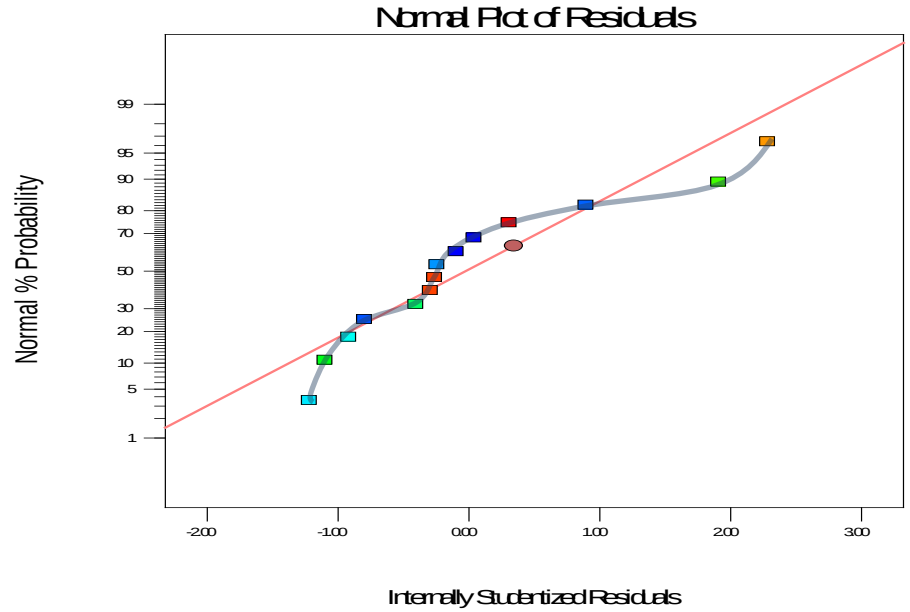

Figure 5.28 *Normal plot for the Hier D02A cubic model.*

Residuals vs. Predicted plot

The data points in this plot show a random scatter, indicating that the variance is constant. The plot show no obvious increasing or decreasing “megaphone” patterns, which indicates that no transformation is needed.

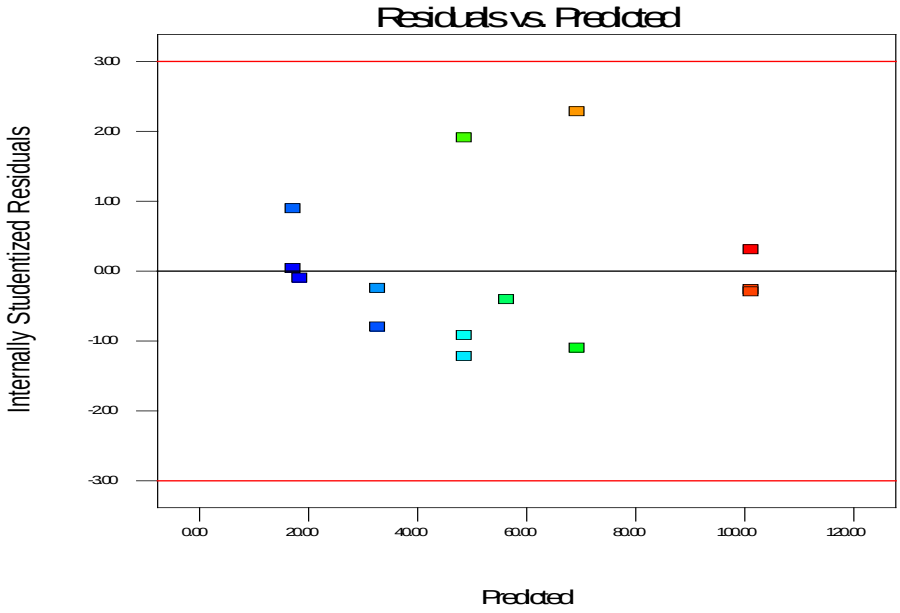

Figure 5.29 *Residuals vs. Predicted plot of the Hier D02A cubic model.*

Residuals vs. Run plot

The data points are randomly scattered except for run number 6 and 7 which have somewhat high residuals, however they are still within the boundaries set by Design Expert. The cause for these deviations could have been because of residues of acetone was discovered in some of the bottles after they were washed. If the following experiments were started too fast, before the acetone could dry, then this might have affected the samples. A replicate was made of run number 6 (run number 12) which does not deviate very much from the plot. The values are still within the boundaries.

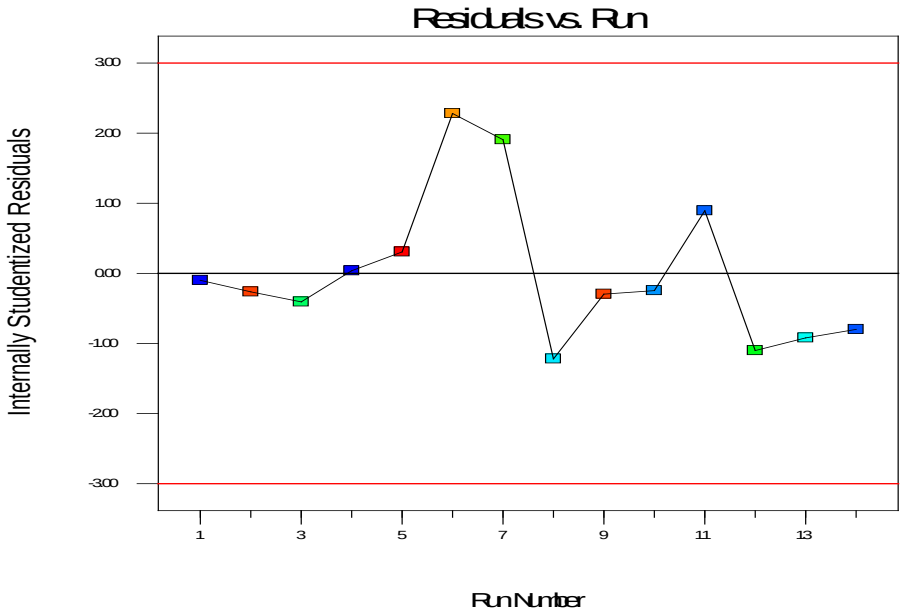

Figure 5.30 *Residuals vs. Run plot of the Hier D02A cubic model.*

Predicted vs. Actual plot

The points are randomly scattered across the 45° line, more points are on the upper side of the line than under the 45° line. The data points do not show any obvious distinct data points that would indicate input errors or that a transformation is needed.

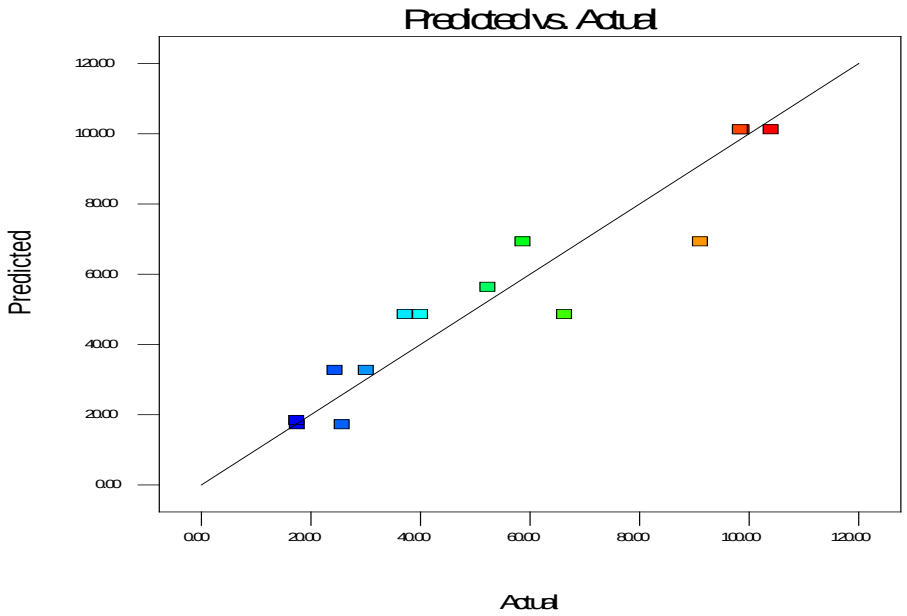

Figure 5.31 *Predicted vs. Actual plot of the Hier D02A cubic model.*

Infuence results from Design Expert

The different influence plots for the Hier D02A cubic model is shown on the next page. They will only be briefly commented since there are much statistics involved.

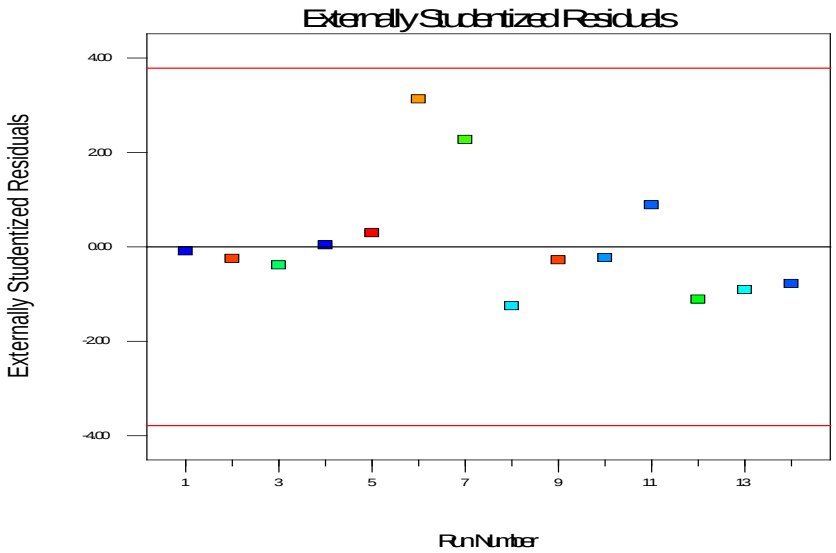

Figure 5.32 *Externally Studentized Residuals plot of the Hier D02A cubic model.*

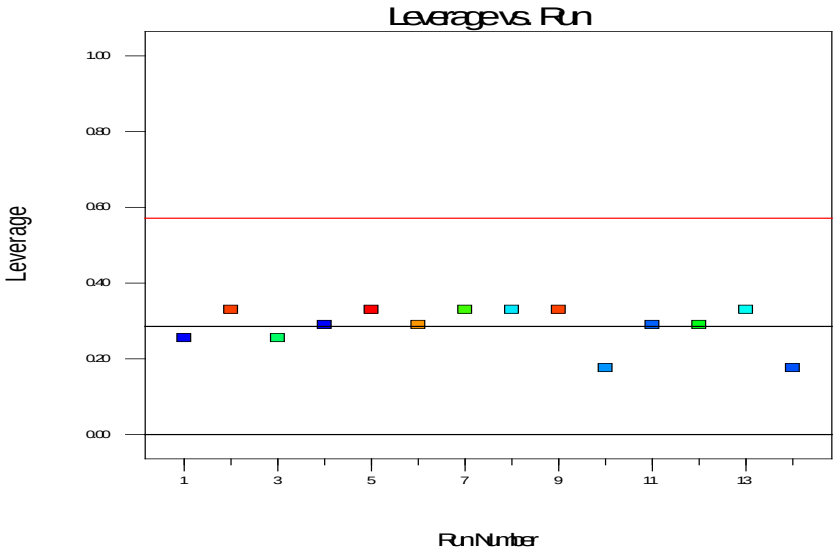

Figure 5.33 *Leverage plot of the Hier D02A cubic model.*

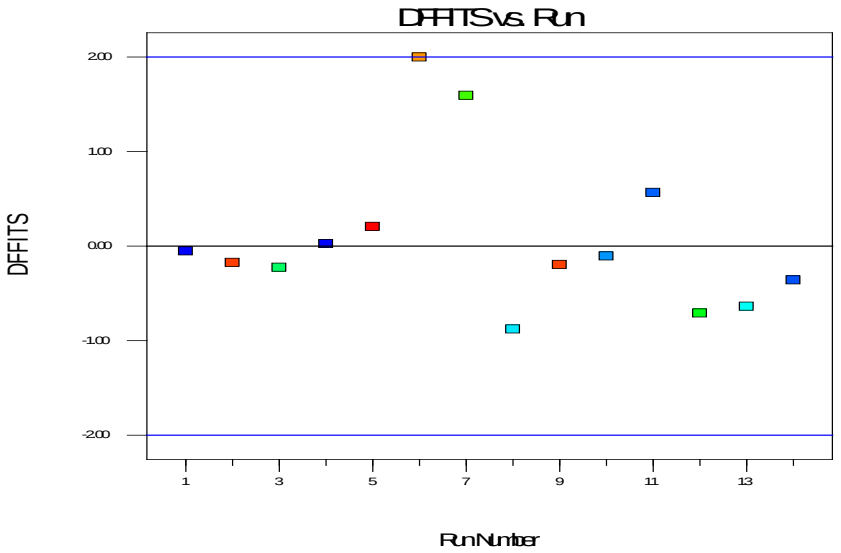

Figure 5.34 *Difference in fits (DFFITS) plot of the Hier D02A cubic model.*

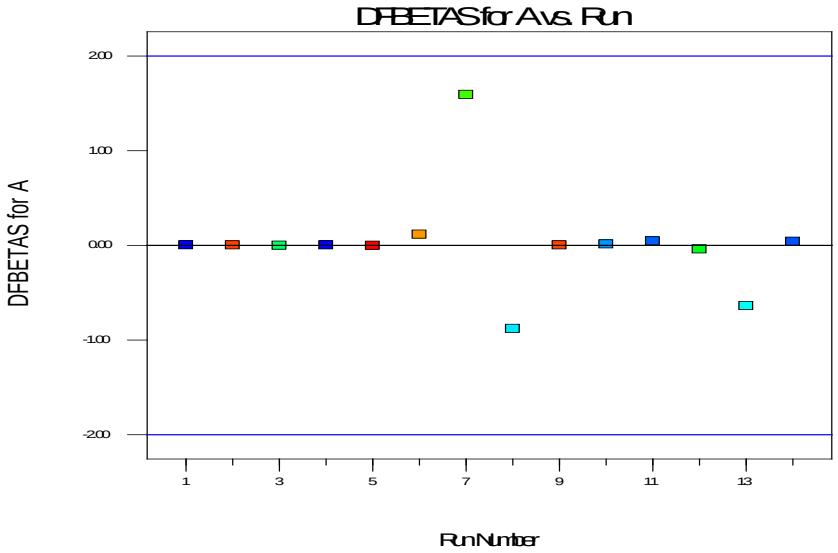

Figure 5.35 *Difference in BETAS (DFBETAS) plot of the Hier D02A cubic model.*

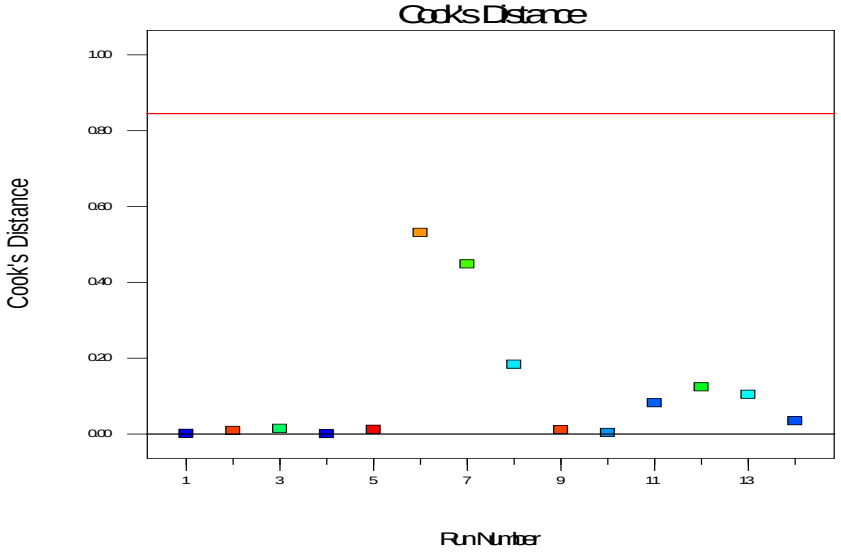

Figure 5.36 *Cook's distance plot of the Hier D02A cubic model.*

The influence plots show that all the data points are within the boundaries, which is desired. The Difference in fits (DFFITS) plot has one data point (run number 6) right on the upper boundary, however that is acceptable. The cause of the deviation of that point is known and a replicate has been performed.
These plots indicate that the model is a good fit.

Optimization results from Design Expert

An optimisation was performed on the model. The chosen limits were set to +/- 20NTU of the best measured turbidity value (104, run number 6, 300ppm Flowsolve 113). Figure 5.34 shows the prediction of the optimised value which is 101,149 NTU and 300 ppm Flowsolve 113 as the predicted dispersant "mixture". The values of the optimisation are also shown in table 7.

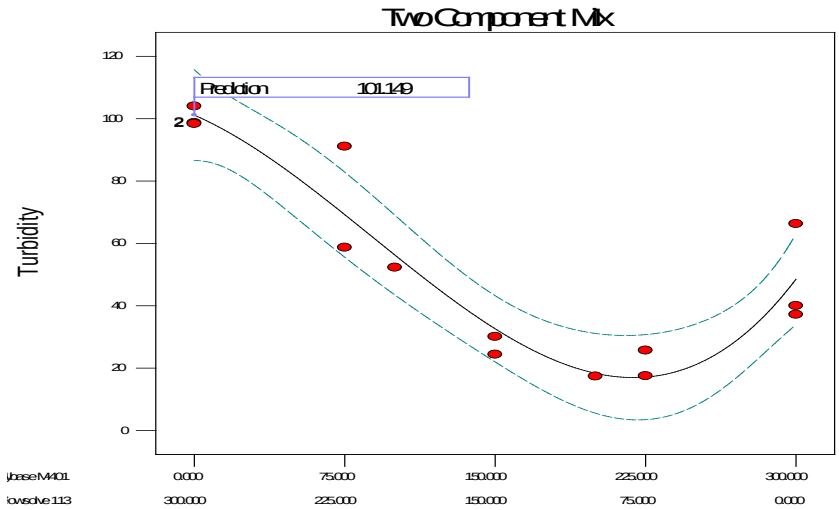

Figure 5.37 *Optimisation plot of the Hier D02A cubic model.*

Table 7 *Optimisation of the Hier D02A cubic model.*

Name	Goal	Lower Limit	Upper Limit	Lower Weight	Upper Weight	Importance
A:Hybase	is in range	0	300	1	1	3
B:Flowsolve	is in range	0	300	1	1	3
Turbidity	maximize	84	124	1	1	3
Solutions Number	Hybase	Flowsolve	Turbidity	Desirability		
1	0.000	300.000	101.149	0,42873122	Selected	

5.3.2 The Hier D02A design conclusion

This model did not show any positive interactions between the chosen dispersants. Compared to the Crudo-Metapetroleum design (cubic model graph), the dispersants showed similar effects. At least the results showed which mixtures should absolutely be avoided.

A three component model with this crude oil would probably not give other results that have not already been observed, so further experimenting on this model will not be carried out.

5.5 The Jordbær two component design

Another crude oil, the Jordbær crude oil contained some asphaltenes and was used to make a two component dispersant mixture design. In this design, Flowsolve 113 and Hybase-M-401 was used as dispersants.

5.5.1 The Jordbær design results and discussion

Table 8 shows the experimental plan and the turbidity measurements made for the Jordbær model. The responses in this model are lower than that of the other two models, which may indicate that the asphaltene content is lower in this crude oil than in the other two crude oils. Flowsolve 113 is the best dispersant (run number 2, 60 NTU) as shown in the table.

Table 8 *shows the experimental plan including the responses of the Jordbær model.*

Run number	Component A Hybase M-401	Component B Flowsolve 113	Response 1 Turbidity	Comments
1	200	100	49,9	
2	0	300	60	
3	100	200	34,2	
4	225	75	50,6	
5	0	300	55,1	
6	75	225	33,1	
7	300	0	53,1	
8	300	0	54,1	
9	0	300	53,8	
10	150	150	38,1	
11	225	75	45,4	
12	75	225	30	
13	300	0	48,2	
14	150	150	33,3	

One model was suggested to fit best for this design, the cubic model. A transformation was not suggested.

The two component model graph (figure 5.38) was examined and 300 ppm Flowsolve 113 gave the best readings again. However there was a small area that seemed to give an interesting positive interaction between the two dispersants (figure 5.38, the red arrow). The analysis was checked and the plots showed no particular abnormalities, hence four new data points were found manually in the model graph in Design Expert and were tested in the lab (Run number 15 – 18) to examine this possible positive interaction.

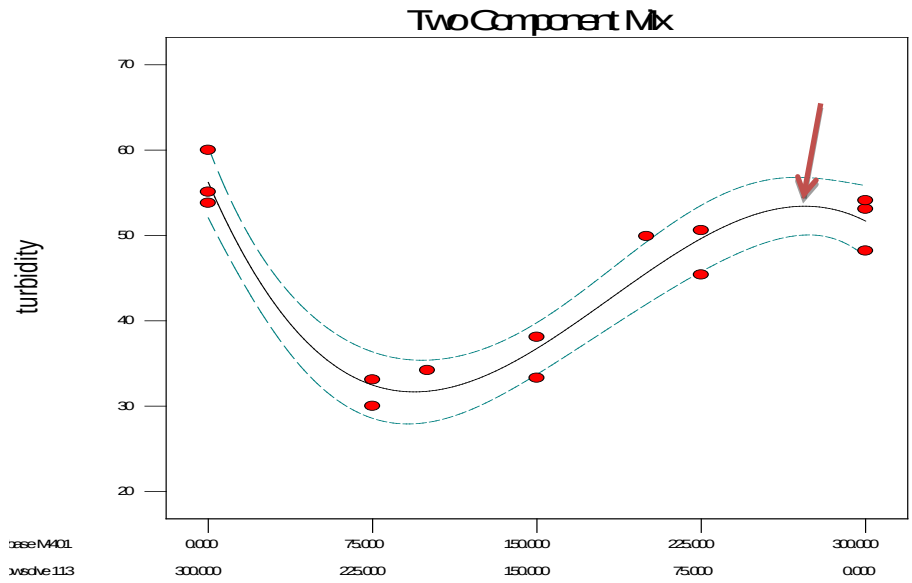

Figure 5.38 *The 2D model graph of the Jordbær crude oil. The red arrow points to a possible positive interaction in the model.*

Table 9 shows all the results done on the Jordbær crude oil. The best suggested model is now the quartic model.

Table 9 *shows the experimental plan including the responses of the Jordbær model.*

Run nunber	Component A Hybase M-401	Component B Flowsolve 113	Response 1 Turbidity	Comments
15	273	27	44,7	
16	273	27	44,2	
17	253	47	40,8	
18	285	15	45,9	

The extra data points which were examined did not give any more desirable results. The new model graph 5.39 seems to show antagonistic effects between the two dispersants. Flowsolve 113 is still the dispersant giving the highest turbidity measurements.

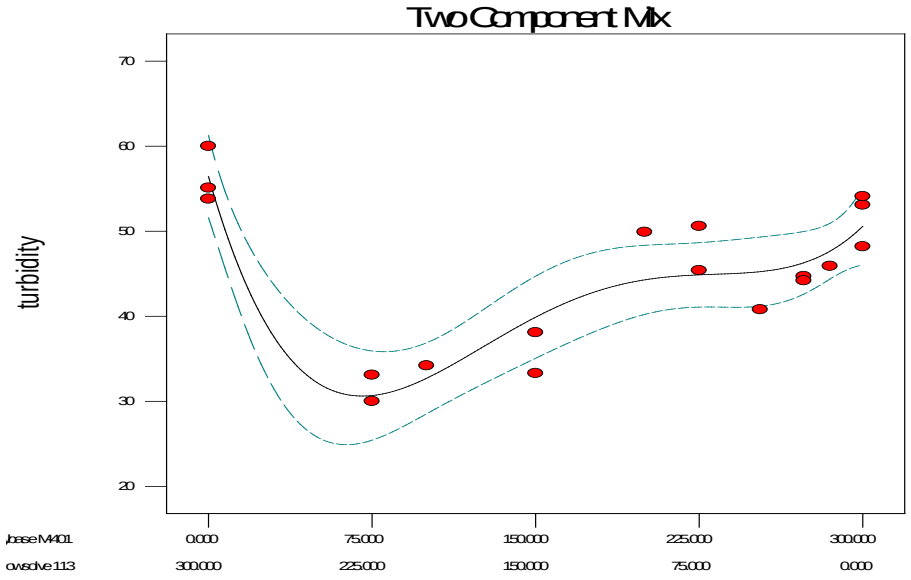

Figure 5.39 *The 2D model graph of the Jordbær crude oil.*

Diagnostics results from Design Expert

The different diagnostic plots will be evaluated, and commented. The colours of the different data points in the diagnostics plots represent the value of the measured turbidity. Colours from low values to high values are: dark blue < light blue < green < yellow < orange < red.

Normal plot

The normal plot (figure 5.40) of the Jordbær quartic model does not show an obvious S-shaped form, there is some scattering of the data points which is acceptable. This indicates that no transformation is needed.

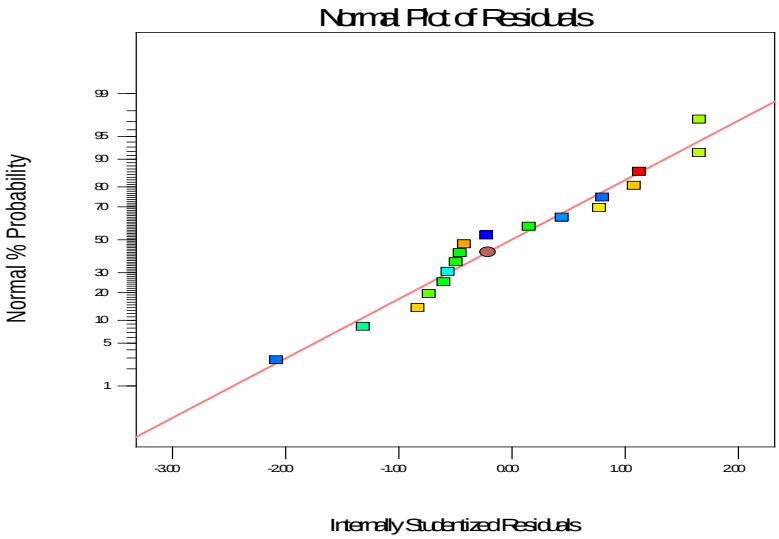

Figure 5.40 *Normal probability plot of the Jordbær quartic model.*

Residuals vs. Predicted plot

The residuals vs. predicted plot (figure 5.41) does not show any increasing or decreasing "megaphone" patterns, which indicates that the variance is constant. The data points show a random scatter meaning that there is no need for a transformation.

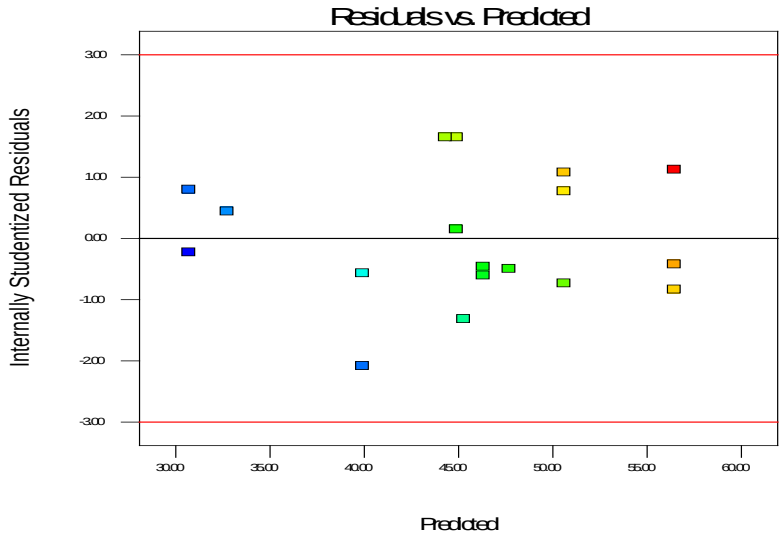

Figure 5.41 *The Residual vs. Predicted plot of the Jordbær quartic model.*

Residuals vs. Run plot

The residuals vs. run plot shows a decreasing trend (see the blue line in figure 5.42). This can be explained by the sampling of the crude oil over time. The crude oil was given in a small bottle, diluted 50:50 in water. Sand was discovered when the tests was poured out so the equipment could be washed. The bottle of crude oil was always shaken before taking out a crude oil sample. However, it seems that the sand sunk quickly to the bottom, so as the crude oil volume decreased, more and more sand was added to the tests. This may explain the systematic tendency seen in figure 5.39. Apart from the decreasing pattern, the data points are all within the boundaries set by Design Expert.

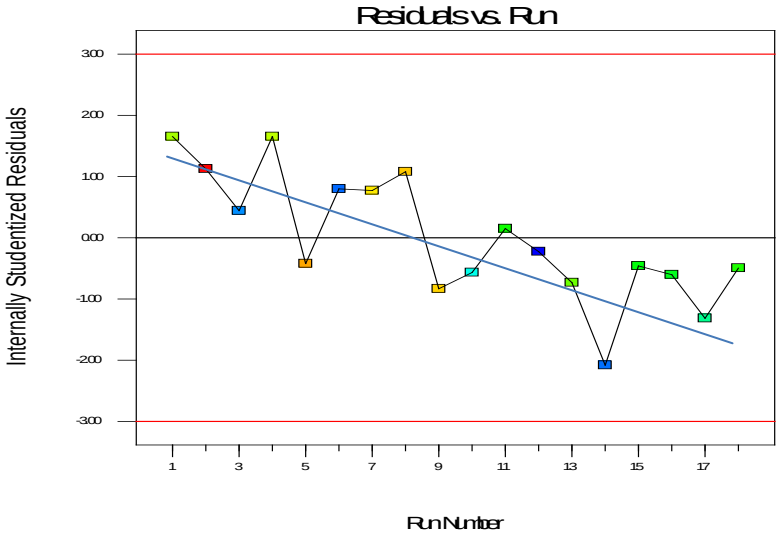

Figure 5.42 *Residuals vs. Run plot of the Jordbær quartic model.*

Predicted vs. Actual plot

This plot (figure 5.43) shows a random scatter of the data points on both sides of the 45° line. There are no data points which deviate from the rest of the points, so the model seems to fit well and there is no sign that a transformation is needed.

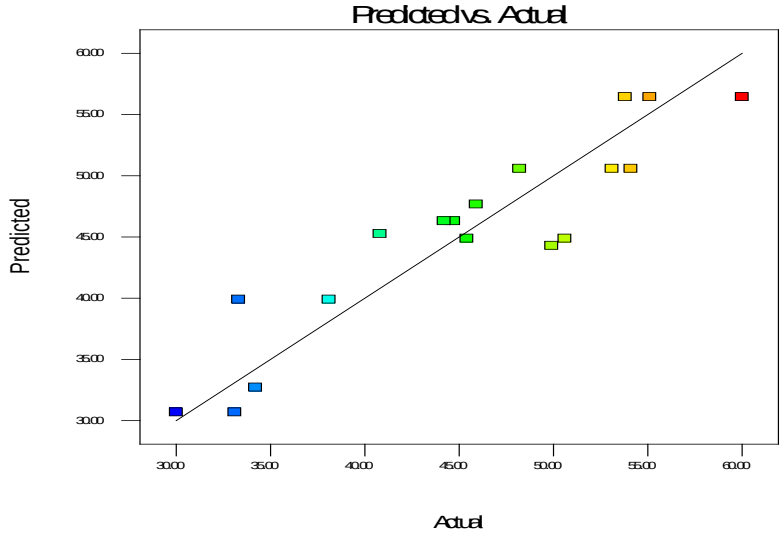

Figure 5.43 *Predicted vs. Actual plot of the Jordbær quartic model.*

Infuence results from Design Expert

The different influence plots for the Hier D02A cubic model is shown on the next page. They will only be briefly commented since there are much statistics involved.

Certain trends are similar to the residuals vs. run plot as seen in the externally studentized residuals plot and the difference in fits (DFFITS) plot. The reason is explained with the sand in the oil sample. All the data points are well within the boundaries, so there is nothing more to add.

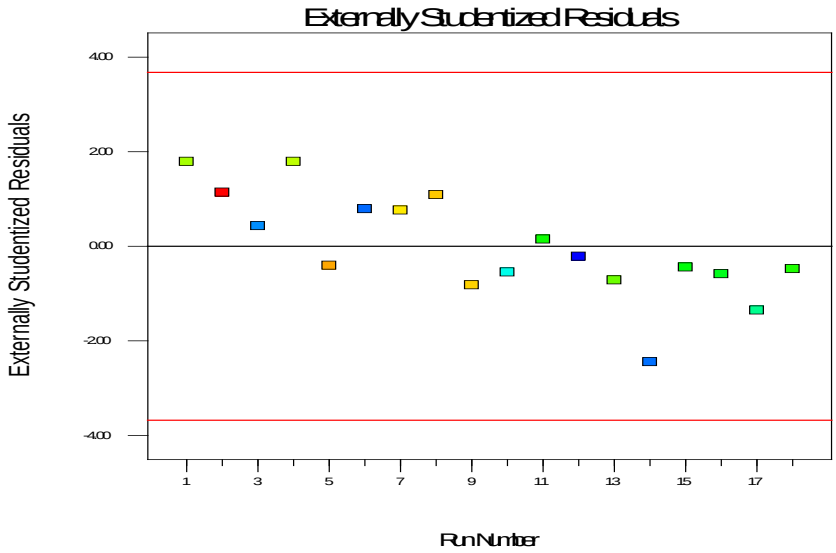

Figure 5.44 *Externally Studentized Residuals plot of the Jordbær quartic model.*

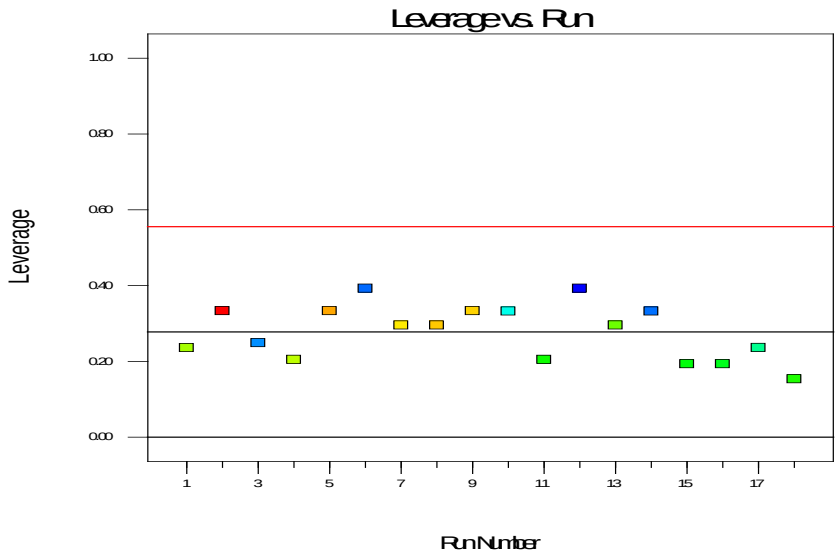

Figure 5.45 *Leverage plot plot of the Jordbær quartic model.*

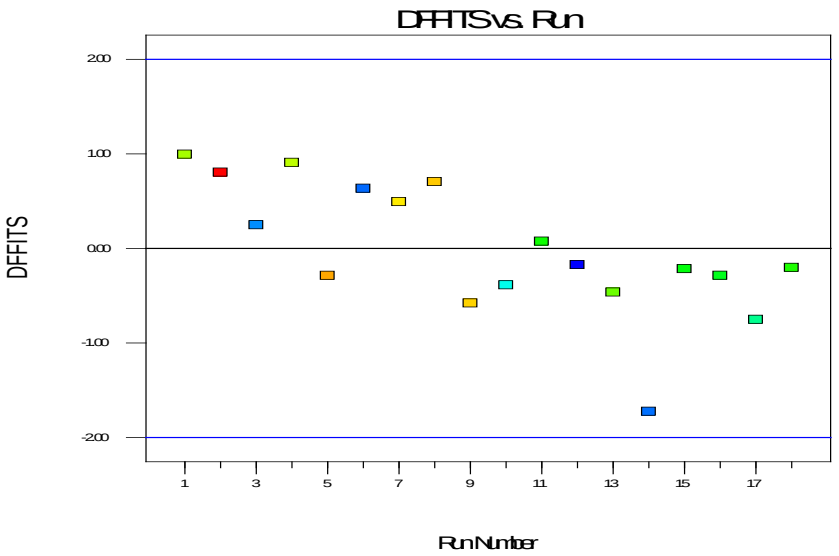

Figure 5.46 *Difference in fits (DFFITS) plot of the Jordbær quartic model.*

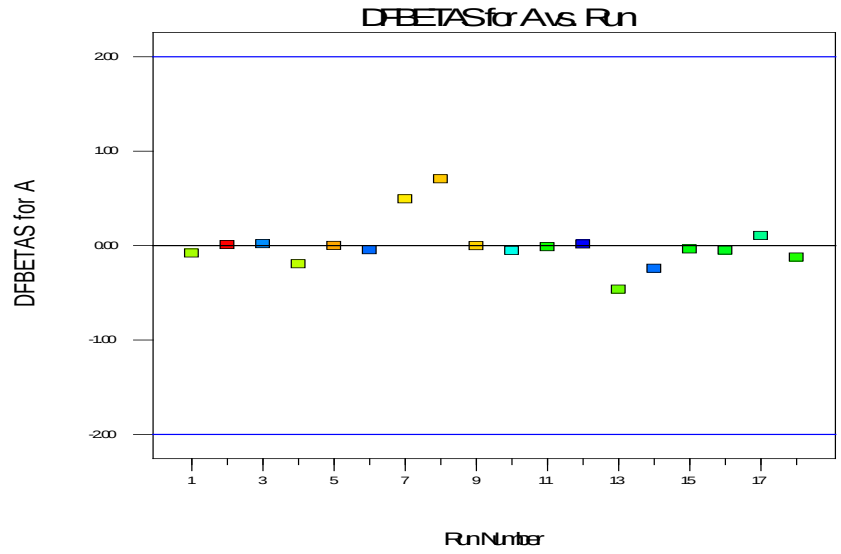

Figure 5.47 *Difference in BETAS (DFBETAS) plot of the Jordbær quartic model.*

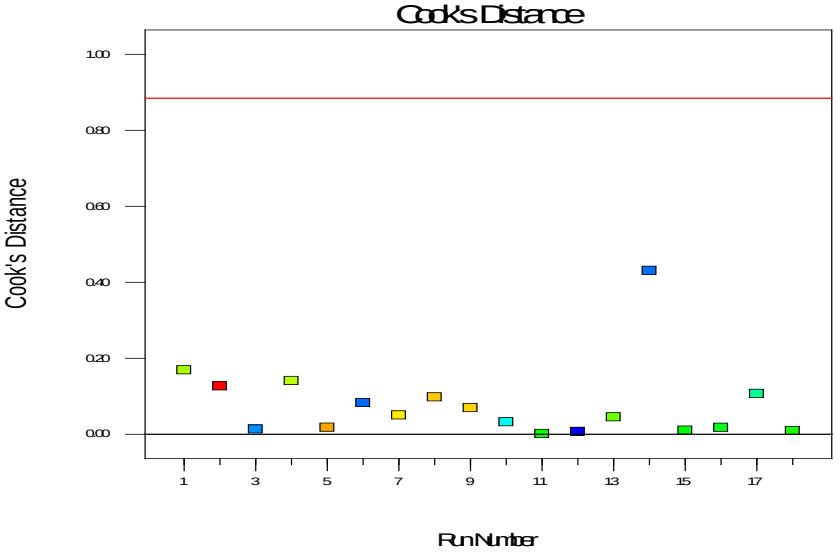

Figure 5.48 *Cook's Distance plot of the Jordbær quartic model.*

Optimisation results from Design Expert

A numerical optimisation was performed on the Jordbær model, the limits were set to +/- 5NTU of the highest measured turbidity (60NTU). Figure 5.46 shows the optimisation plot of the Jordbær quartic model. The predicted optimisation shows that Flowsolve 113 will give the highest turbidity measurements. The optimisation values are shown in table 5.10.

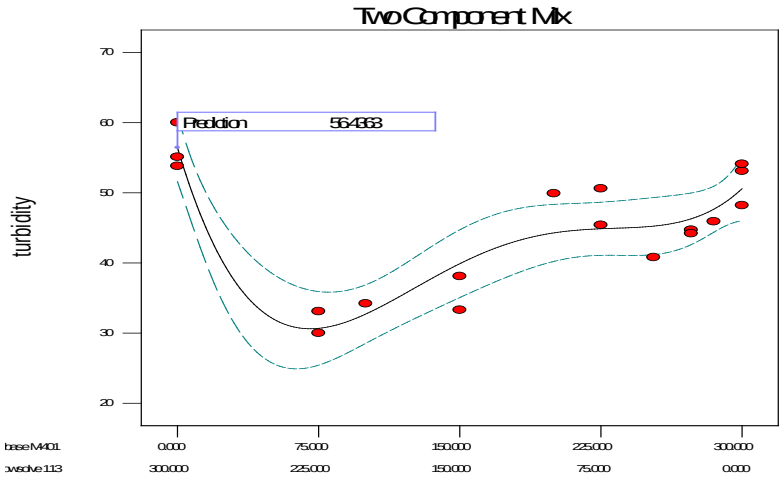

Figure 5.49 *Optimisation plot of the Jordbær quartic model.*

Table 5.10 *Optimisation of the Jordbær quartic model.*

Name	Goal	Lower Limit	Upper Limit	Lower Weight	Upper Weight	Importance
A:Hybase	is in range	0	300	1	1	3
B:Flowsolve	is in range	0	300	1	1	3
turbidity	maximize	55	65	1	1	3
Solutions Number	Hybase M-401	Flowsolve 113	turbidity	Desirability		
1	0.000	300.000	56.4363	0,144	Selected	

5.5.2 Conclusion

The obvious differences between the model graphs, shows the importance of having enough data points in the model. The overall view given by the first turbidity results will give an idea of how the actual system behaves and how it looks like in a model. Any areas interesting points should be further examined and tested further, in order to be certain of the result. The diagnostics and influence will help to find deviations from the model which can help to improve the model.

The Jordbær crude oil did not give any positive interactions between the dispersants, Flowsolve 113 was the best dispersant at the tested concentration and in the tested mixture. A three component model of this crude oil will not be made.

5.6 References

[1] W. F. Smith, *Experimental Design For Formulation*: Society for Industrial and Applied Mathematics, 2005.

Chapter 6 spot test

The third method to be examined was the spot test. The spot test is an easy method for determining the stability of asphaltenes in a certain amount of crude oil. The test results will show either a positive or negative test [1-3]. However, it will be determined in this chapter if it is possible to use this test to rank the different dispersants.
Different versions of the spot test have been described in the literature [1, 3, 4]. A simplified method was devised based on these references. The main differences were:

- Instead if using toluene and naphtha to dissolve the asphaltenes, xylene was used.
- Pentane was used to destabilize the asphaltenes rather than heptane or cetane.
- Whatman no.1 and no.4 filter papers were used instead of Whatman no.2 filter paper.
- Heat was not applied to the system during the experiment (during stirring, when drying the filter paper before and after placing the spots).

6.1 Spot test procedure

Four different Crudo-Metapetroleum solutions with 300 ppm Flowsolve 113, 300 ppm Hybase M-401, 300 ppm DDBSA and a blank test (with no dispersant) were prepared by the procedures described in chapter 4, but the spots were made directly after shaking the tubes for 2 minutes.

Method 1

- The filter paper was attached to a thick piece of cardboard.
- The sample which was spotted was taken with a pipette from the top layer of the solution.
- One drop is placed on the filter papers from each solution.
- When the spots are completely dry, they can be compared.

Another slightly different approach was also tested with the same four solutions, but after shaking the tubes for 2 minutes, they were left for 30 minutes and then a spot was performed:

Method 2

- The filter paper was attached to a thick piece of cardboard.
- The tubes were turned upside down before a sample was taken with a pipette from the top layer of the solution.
- One drop is placed on the filter papers from each solution.
- When the spots are completely dry, they can be compared.

6.2 Titration spot test procedure

Three samples were prepared where one sample at a time was tested. Crudo-Metapetroleum oil (5g) was dissolved in xylene (10ml, 15ml and 20ml), the equipment was set up as shown in figure 6.01.

Figure 6.01 *Titration layout, bottles with the samples (from left to right) 10ml xylene, 15ml xylene and 20 ml xylene samples placed on the magnet stirrer.*

1. The sample was mixed thoroughly with a magnet stirrer.
2. A spot from the sample was made on the filter papers.
3. Pentane (1ml) was added to the sample.
4. After 30 seconds of stirring, a spot was made on the filter paper.

Step 3 and 4 was repeated until a positive spot was visible. The amount of pentane used in the process was noted for each of the samples. The results of the titrations were plotted in a graph as shown in figure 6.02.

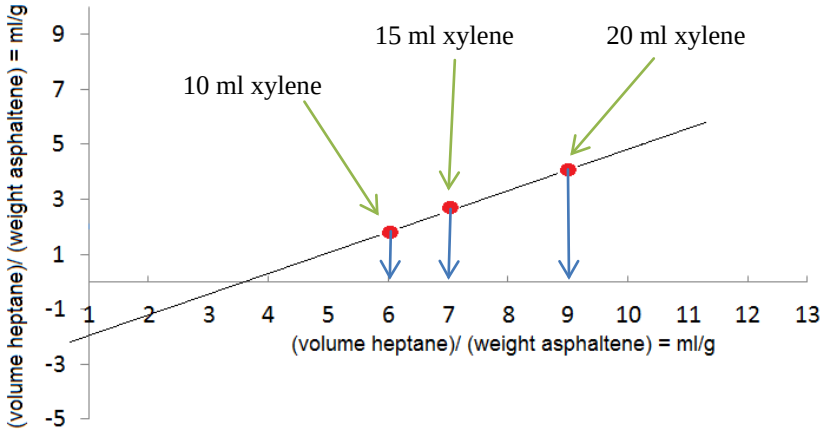

Figure 6.02 *Typical plot to determine asphaltene dispersability, p_a [3].*

The slope, s, can be found from the plot when all the sample results have been inserted and from the following equation (6.01), the value of the dispersibility of the least soluble asphaltenes, p_a, is found.

$$p_a = 1/1 + s \qquad (6.01)$$

6.3 Results and discussion

The results of the spot tests and titration spot tests were compared and evaluated separately. The order in which the samples were placed on the filter papers was:

1. 300 ppm Hybase M-401 sample.
2. 300 ppm Flowsolve 113 sample.
3. 300 ppm DDBSA sample.
4. Blank test with 500 µl Crudo-Metapetroleum solution in pentane.

6.3.1 Spot test results and discussion

Method 1 gave the results shown in figure 6.03. The pipette which was used, was not able to hold in the sample very well, so the spots dripped a bit uncontrollably on the filter papers.

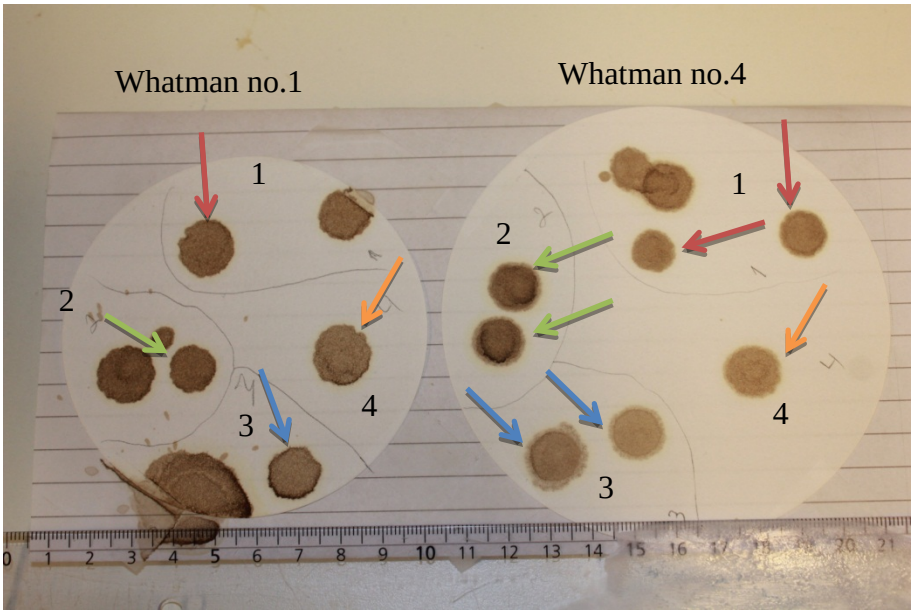

Figure 6.03 *1) Red arrow - 300ppm Hybase M-401. 2) Green arrow - 300ppm Flowsolve 113. 3) Blue arrow - 300ppm DDBSA. 4) Orange arrow – 500µl Crudo-Metapetroleum solution (blank test).*

Evaluation of the single spots was still possible. The arrows point to the spots which could be evaluated. The blank test (4, orange arrows) should be the lightest spots because the asphaltenes are supposed to flocculate and deposit. However, the DDBSA spots (3, blue arrows) seemed lighter at least on the Whatman no.4 filter paper. On Whatman no.1, the blank test seemed to be the lightest spot, the DDBSA spot had a fairly similar colour, but the spot border was darker in the DDBSA spot.
The Flowsolve 113 spots (2, green arrows) were obviously the darkest ones, which indicates that more asphaltenes were in the solution.
The Hybase M-401 spots were uniform in the colour, it seemed that these spots were darker than the DDBSA spots and the blank test spots.
Very small details were difficult to observe with the naked eye.

Method 2 gave the results shown in figure 6.04. These spots were placed on the filter papers with another pipette type, so the spilling was avoided. However it seemed like the spots in this second method were much smaller, that a smaller volume was spotted on the filter papers.

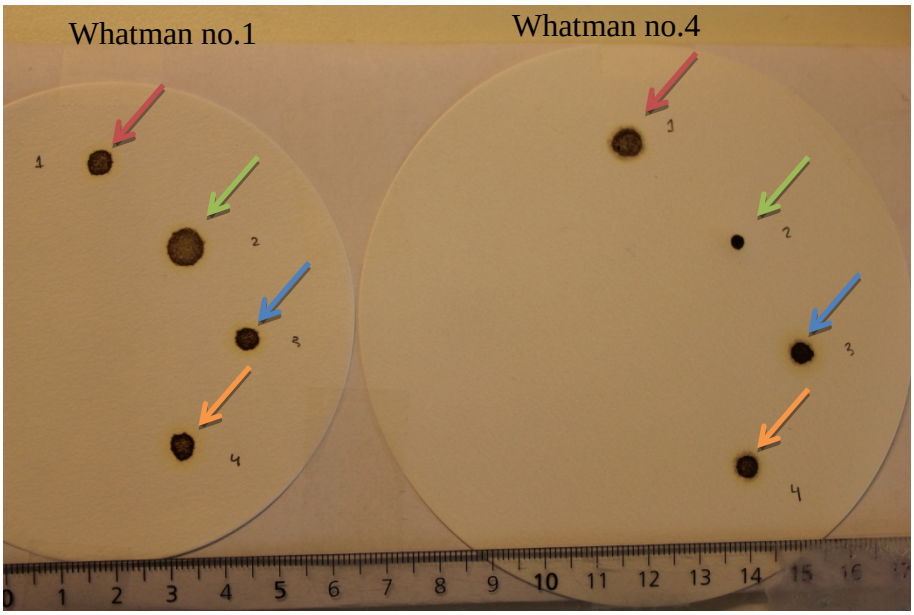

Figure 6.04 *1) Red arrow - 300ppm Hybase M-401. 2) Green arrow - 300ppm Flowsolve 113. 3) Blue arrow - 300ppm DDBSA. 4) Orange arrow – 500µl Crudo-Metapetroleum solution (blank test).*

Even so, all the spots were too dark to be ranked, because the differences were too small and difficult to see.

6.3.2 Titration spot test results and discussion

All these samples (figure 6.05, 6.06 and 6.07) gave a positive spot before pentane was even added to the samples. Thus, more xylene had to be used to dissolve the 5g of Crudo-Metapetroleum. 4 ml of pentane was added in total and 5 spots were placed on the filter papers. The spots were too dark and so it was very difficult to see any differences if there were any at all. The sixth spot was from a 5g Crudo-Metapetroleum sample which was diluted in xylene (10ml, 15ml and 20ml) with 300ppm Flowsolve 113. The spot gave a positive result before pentane was added, similar to the other tests. There were no observed differences in either the inner circle or the outer circle of these spots compared to the spots without dispersants.

Figure 6.05 *5g Crudo-Meta petroleum, 10ml xylene, Whatman no.1&no.4 filter paper.*

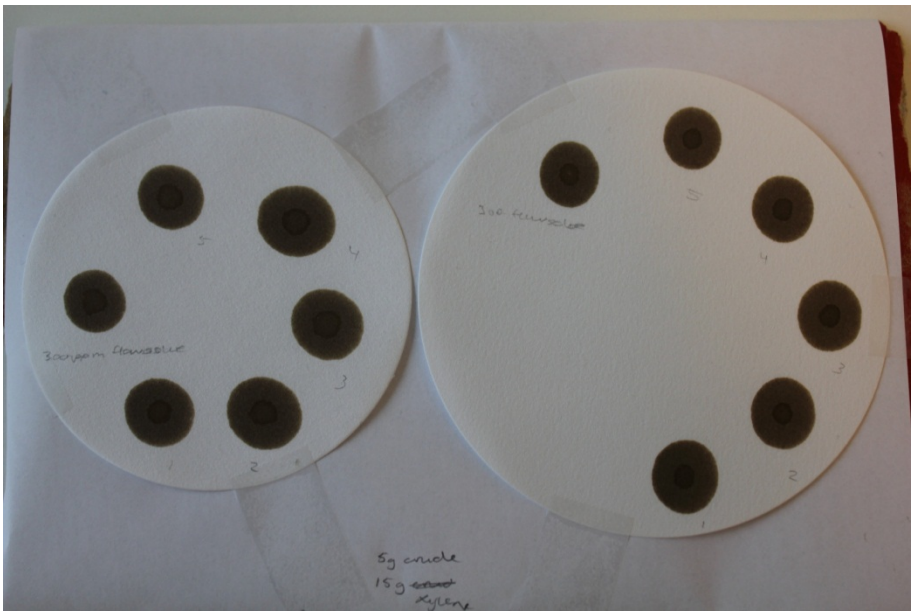

Figure 6.06 *5g Crudo-Meta petroleum, 15ml xylene, Whatman no.1&no.4 filter paper.*

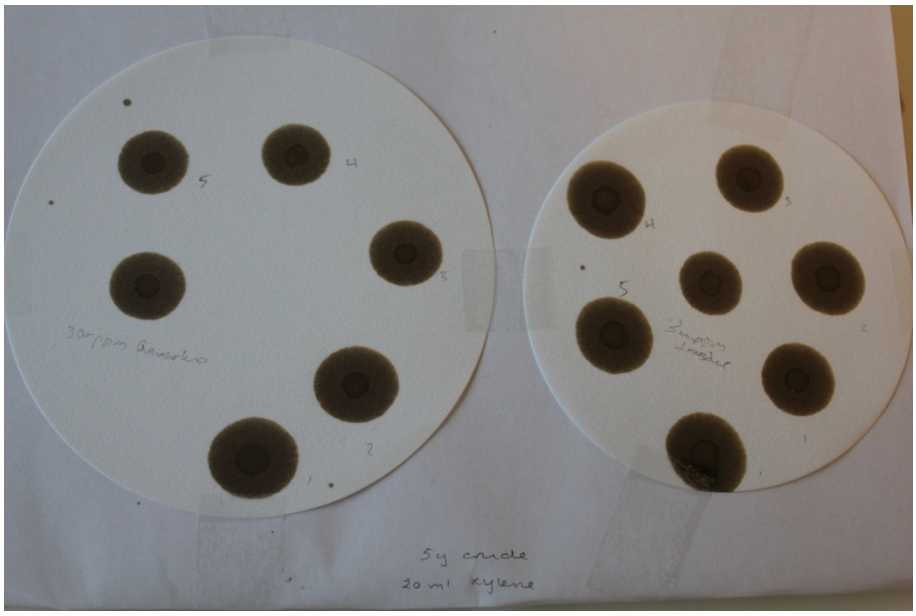

Figure 6.07 *5g Crudo-Meta petroleum, 20ml xylene, Whatman no.1&no.4 filter paper.*

6.4 Conclusion

All of the results showed little or no differences in the spots. The results were subjectively evaluated which should be avoided and proper ranking of the different dispersants would not be possible with the spot test and the titration spot test. These methods will not be used for any more tests.

6.5 References

[1] A. T. Pauli, "Asphalt compatibility testing using the automated Heithaus titration test," *Journal Name: Preprints of Papers, American Chemical Society, Division of Fuel Chemistry; Journal Volume: 41; Journal Issue: 4; Conference: 212. national meeting of the American Chemical Society (ACS), Orlando, FL (United States), 25-30 Aug 1996; Other Information: PBD: 1996*, pp. Medium: X; Size: pp. 1276-1281, 1996.

[2] E. M. Fauber, "ASPHALT OXIDATION," ed: Google Patents, 1971.

[3] "Recent research on bituminous materials: a symposium presented at the Sixty-sixth Annual Meeting, American Society for Testing and Materials, Atlantic City, N.J., June 26, 1963," Philadelphia.

[4] A. International, "Standard test method for cleanliness and compatibility of residual fuels by spot test," in *D4740*, ed, 2002.

Chapter 7 UV/Vis spectrometry tests

The fourth method to be tested was the absorbance measurement of the supernatant from different tests. Preliminary work had to be done in order to know how the equipment worked and which settings were to be used. Different solutions were measured on the UV-Vis spectrometer in order to examine the effects of the different substances.
A high absorbance measurement indicates an effective dispersant, where the asphaltenes in solution absorb the incoming light [1].
The different supernatants were scanned within a certain wavelength range and they were also measured at a fixed wavelength.
The different solutions containing crude oil, pentane and dispersants are made by the same procedures as in chapter 4. The supernatant of each sample was taken out to be measured.

7.1 Preliminary procedure

The following mixtures or pure substances were measured to examine the absorption spectra, absorption peaks and absorbance at fixed wavelengths.

- Pentane
- Xylene-O
- Acetone
- Pentane and 300ppm Hybase M-401
- Blank test (500µl Crudo-Metapetroleum solution, see chapter 4.1, but the sample was centrifuged at 2500rpm for 10 minutes).
- Blank test (500µl Crudo-Metapetroleum solution, see chapter 4.1, but the sample was centrifuged at 2500rpm for 10 minutes) diluted to 0,78% with xylene.
- Dispersant test (500µl Crudo-Metapetroleum solution and 300ppm Hybase M-401, see chapter 4.2, but the sample was centrifuged at 2500rpm for 10 minutes).
- Dispersant test (500µl Crudo-Metapetroleum solution and 300ppm Hybase M-401, see chapter 4.2, but the sample was centrifuged at 2500rpm for 10 minutes) diluted 1:4 with xylene.
- Dispersant test (500µl Crudo-Metapetroleum solution and EPT 2451, see chapter 4.2). Diluted to 0,78% with xylene.
- Dispersant test (500µl Crudo-Metapetroleum solution and EPT 2449, see chapter 4.2). Diluted to 0,78% with xylene.

The supernatants were diluted step by step until a proper spectrum was observed.

A sample (approximately 4ml) was transferred to the cuvette with a cap covering the sample. The sample was placed into the spectrophotometer (Varian, Cary 50 Bio UV-Vis spectrophotometer).
Different parameters were set in the computer software (Cary Win UV):

- Scan – The sample was scanned within a wavelength interval to create a spectrum.
  - 200nm – 800nm.
  - 200nm – 500nm
- Fixed wavelength measurement – the absorbance was measured at a fixed wavelength.
  - 280nm
  - 300nm
  - 400nm
  - 500nm
- Zero and baseline – adjustments for different losses of radiation (see chapter 3.4). After using zero or baseline the sample was scanned or measured at a fixed wavelength.

7.2 Results and discussion

The results were displayed in the program and could be saved to the hard disc.
The fixed wavelengths were chosen based on the appearance of the different spectrums.

7.2.1 Absorbance spectra

Acetone and xylene were scanned and compared to the EPT 2449 supernatant (0,78%) spectrum and the blank test supernatant spectrum. Xylene should absorb at approximately 290nm and acetone should absorb at approximately 330nm (values was found on a poster in the lab), which was also what the scan in figure 7.01 showed. The black curve is the spectrum for acetone, the blue curve is the spectrum for xylene and the red curve is the spectrum for a 50:50 mixture of acetone and xylene. The spectrum of the mixture was almost overlapping the acetone spectrum which had the highest absorbance.

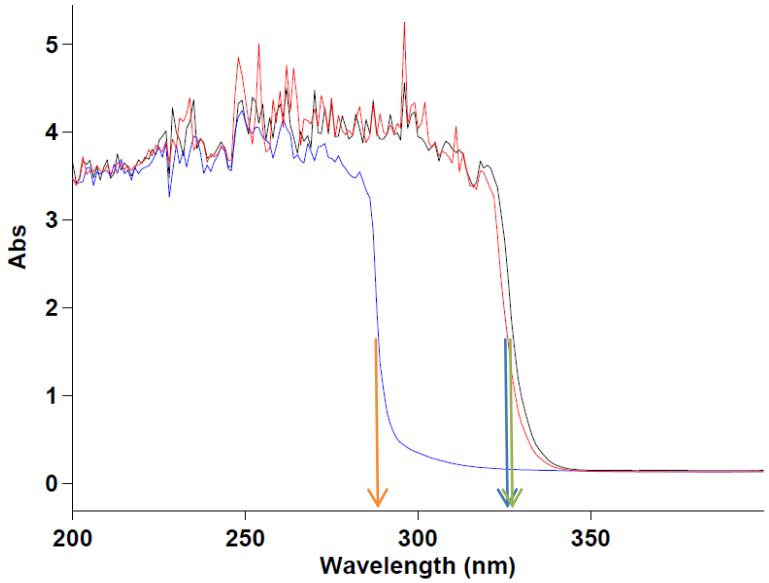

Figure 7.01 *The blue curve represents the xylene spectrum, the black curve represents the acetone spectrum and the red curve represents the 50:50 mixture of acetone and xylene*

The different supernatants containing crude oil had to be significantly diluted in order to get a proper absorbance spectrum. The supernatant containing EPT 2449 gave the spectrum shown in figure 7.02. This supernatant was diluted to 0,78% and the sample was scanned after “zero” adjusting the spectrophotometer.
The absorbance starts at approximately 300nm.

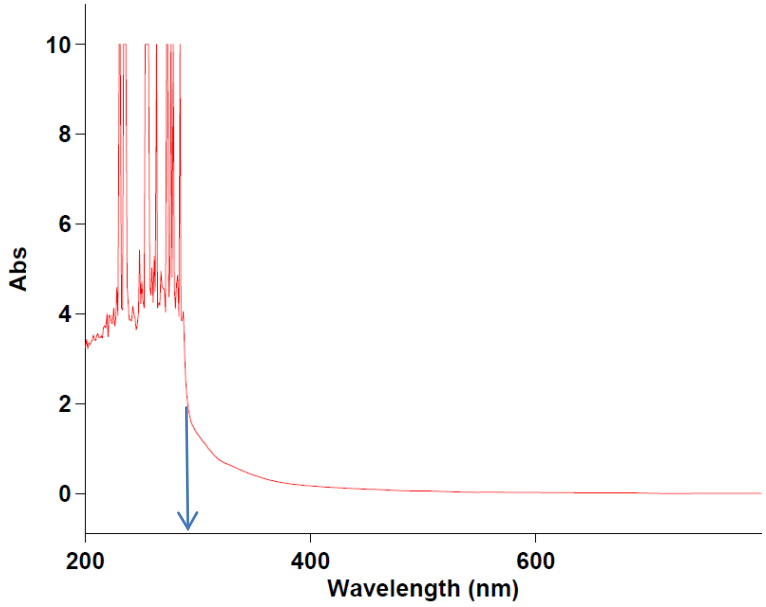

Figure 7.02 *EPT 2449 supernatant diluted to 0,78% with xylene - after zero.*

Figure 7.03 shows the spectrum of the same supernatant (EPT 2449), but this sample was scanned after adjusting the baseline (xylene was scanned as the baseline). This spectrum did not show anything that could be used, so the base line was not set in any of the other spectra.

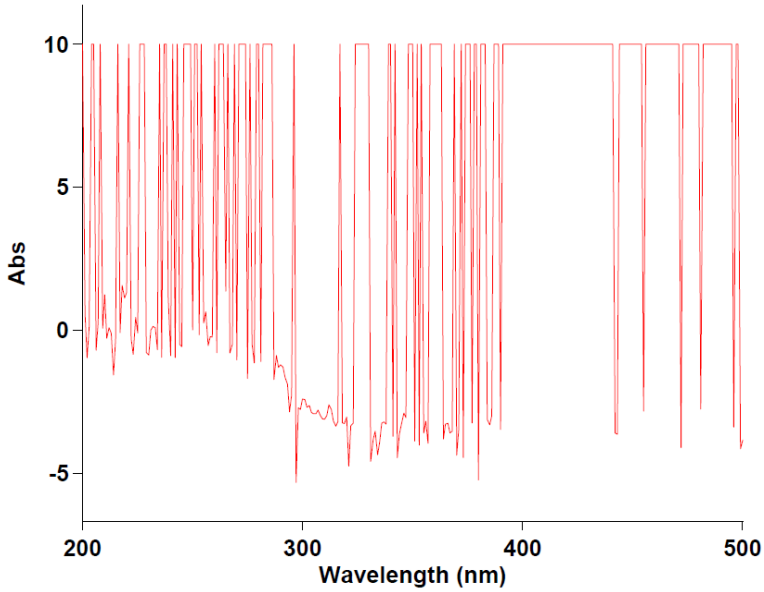

Figure 7.03 *EPT 2449 supernatant diluted to 0,78% with xylene - after baseline.*

The blank test supernatant was also diluted to 0,78% with xylene. The spectrum (figure 7.04) shows that the absorbance started slowly at approximately 430nm - 440nm. Compared to the EPT 2449 supernatant, the blank test measured a higher “start value. It does not seem to be quite correct, since the blank test should have less dispersed asphaltenes than a solution containing a dispersant.

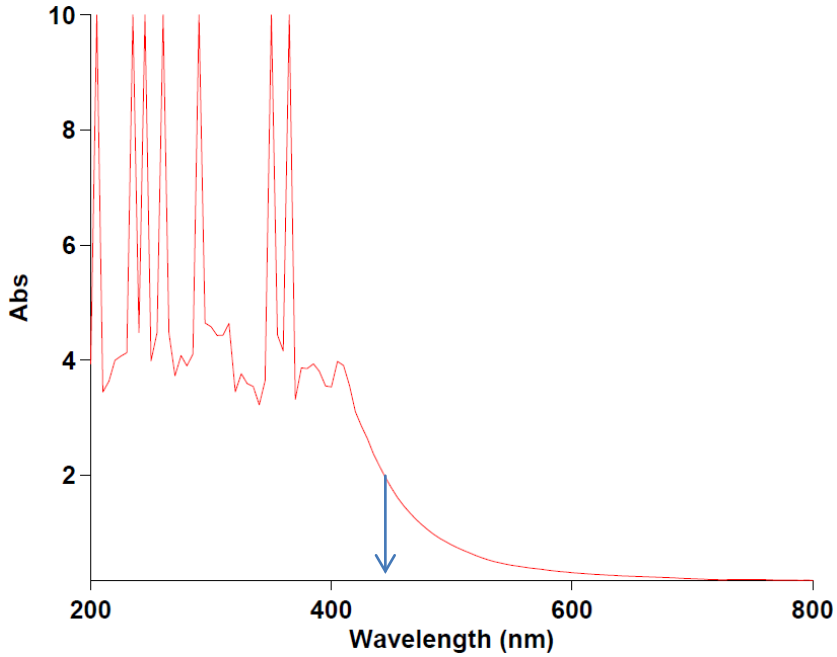

Figure 7.04 *Blank test with 500µl Crudo-Metapetroleum supernatant diluted to 0,78% with xylene.*

7.2.2 Absorbance at fixed wavelengths

From the scans shown on the previous pages (figure 7.01, 7.02 and 7.04), measurements of the absorbance at fixed wavelengths were further examined. Somewhat random wavelengths were chosen, not too high wavelengths because most of the absorbance was observer under 400nm in the examined scans. 280nm was the minimum wavelength which could be chosen, 300nm, 400nm and 500nm was chosen to begin with. The blank test (500µl Crudo-Metapetroleum solution) supernatant and the two dispersant tests (EPT 2451 and EPT 2449) were chosen to be measured (table 7.01).

Table 7.01 *Results of the absorbance measured at 280nm, 300nm, 400nm and 500nm.*

Sample	Absorbance [Abs] at wavelength [nm]			
	280nm	300nm	400nm	500nm
Blank	4,5561	1,4904	0,2274	0,1436
EPT 2451	3,9434	1,4126	0,2880	0,1761
EPT 2449	3,9725	1,4310	0,3203	0,2044

The blank test showed the highest absorbance measurements at 280nm and 300nm, however at 400nm and 500 nm the rank fits the colour of the solutions. The blank supernatant was slightly lighter than the EPT 2451 supernatant and the EPT 2449 supernatant was slightly darker than EPT 2451.
The Blank test was centrifuged at 2500 rpm for 10 minutes, but EPT 2451 and EPT 2449 tests were centrifuged at 1500rpm for 5 minutes, the blank test should have showed lower values because of this. A new blank test was not prepared because the measurements which were done were sufficient to evaluate the method.

7.3 Conclusion

The spectra which were made were a bit too difficult to understand and evaluate. This part of the method will require some experience. However, the different spectra were interesting to compare and they gave some understanding of how a system may react when for example two components were mixed.

The measurements of the absorbance at fixed wavelengths gave some interesting results. The absorbance showed some differences which can be further examined and compared to for example the turbidity measurements of the different dispersants (chapter 5).

This method required very much preliminary work and required too much treatment of the samples before they could be measured. The extreme dilutions can be a significant source for error. The method may be able to rank dispersant tests, however it is probably an advantage to have experience within UV-Vis spectroscopy if the method is to be further examined.
This method will not be used further in this thesis.

7.4 References

[1] A. Yen, Y. R. Yin, and S. Asomaning, "Evaluating Asphaltene Inhibitors: Laboratory Tests and Field Studies," presented at the SPE International Symposium on Oilfield Chemistry, Houston, Texas, 2001.

Chapter 8 Determination of asphaltene content

The determination of the high viscosity of heavy oils is often connected to the asphaltene content of the crude oil. The existing oil recovery techniques for more common light and medium crude oils will not be effective for recovery of the heavy crude oils with extremely high viscosities. Not only does the high viscosity affect the recovery, but also the down-stream surface transporting and refining processes [1].

Most crude oils contain between 1 gram and 10 grams of n-heptane asphaltenes per 100ml oil. The procedure which is followed for the determination of the crude oil contents in this chapter is the "Standard Procedure for Separating Asphaltenes from Crude Oils" [2] which is based on the ASTM D2007-80 (which was not found).
Some differences were made for the dermination of the Crudo-Metapetroleum, Hier D02A and Jordbær crude oils.

- Pentane was used as the asphaltene precipitant, instead of heptane.
- Rather than a MF-millipore mixed cellulose ester membrane filter 0,22µm filter, a Whatman GF/B 1µm filter was used.

8.1 Experimental procedure

As mentioned the "Standard Procedure for Separating Asphaltenes from Crude Oils" was followed step-by step. The instructions were very detailed and easy to follow.

Sample size

As much crude oil as possible, should be used to ensure accurate determination of the asphaltene content. 20 ml crude oil should be adequate in most cases.

Mix crude oil with the precipitant

1. 20 ml crude oil was measured and transferred to a glass flask.
2. 800ml (40 times 20 ml) pentane was added to the flask.
   The flask was sealed with a cap and shaken for 2 minutes.
3. The mixtures were equilibrated for two days at room temperature. During this time the flasks were shaken at least two times for 2 minutes.

Separate solid asphaltenes from oil/precipitant mixture by filtration

After two days of aging, a funnel filter assembly shown on figure 8.01 was used (Kontes Glass Cat.#953805).

4. A weighing vessel and a filter paper (Whatman GF/Bn 1µm) was pre-weighed.
5. The filter was installed into the filter assembly a spring klamp was used to hold the assembly together.
6. Approximately 100 ml of the oil/precipitant mixture was poured into the funnel cup.

7. A vacuum pump was connected to the side arm on the filtration flask so the filtration could begin. The mixture was added little by little as long as the mixture passed through. If the mixture passed very slowly, the the mixture was divided and filtered onto two or more filterpapers, however it is best if the asphaltenes can be collected on a single filter.
8. The asphaltenes was rinsed with pentane just as the last of the mixture passed through the filter, before the deposit layer started to dry and crack.
   After rinsing the vacuum was removed when the asphaltene deposit started to dry and crack.
9. The filter with the asphaltene deposit was carefully peeled off and placed onto the weighing vessel.
10. The asphaltenes were dried in the fume cupboard for several days.

Determination of the asphaltene amount in the crude oil

11. The weight of the asphaltenes were determined by subtracting the weight of the weighing vessel and (all) the filter papers from the total weight. The asphaltene content is calculated by equation (8.01):

$$\text{Asphaltene content } \frac{g}{100\ ml} = \frac{Weight\ of\ asphaltenes\ (g)}{Crude\ oil\ volume\ (ml)} \times 100 \qquad (8.01)$$

Figure 8.01 *The filter assembly and the three flasks of crude oil mixture. From left to right: Crudo-Metapetroleum mixture, Jordbær mixture and Hier D02A mixture.*

8.2 Results and discussion

The three crude oils were prepared by following the same procedure. The Jordbær crude oil mixture was filtered first, Hier D02A second and last the Crudo-Metapetroleum mixture. The Hier D02A mixture aged for three days instead of two days because the filtration time of the Jordbær crude was four hours. The Hier D02A filtration time was approximately six hours, so the half of the Crudo-Metapetroleum mixture aged for four days and the second half aged for five days. This will probably not affect the results very much, it should be better for the mixture to age a long time so most of the asphaltenes will deposit.

Table 8.01 *shows the results of the asphaltene content in the different crude oils.*

	Jordbær	Hier D02A	Crudo-Metapetroleum
Weighing vessel	Not necessary	21,4013 g	1) 21,3986 g 2) 38,9909 g
Filter paper	0,2551 g	0,2580 g	1) 0,2602 g 2) 0,2549 g
Total	0,2993 g	22,1069 g	1) 22,5555 g 2) 40,7798 g
Asphaltene content	0,2210 $\frac{g}{100ml}$	2,2380 $\frac{g}{100ml}$	12,1535 $\frac{g}{100ml}$

Figure 8.02 shows the dried asphaltene deposit of the Jordbær crude oil on the filter paper. This crude oil had the least asphaltene contents.

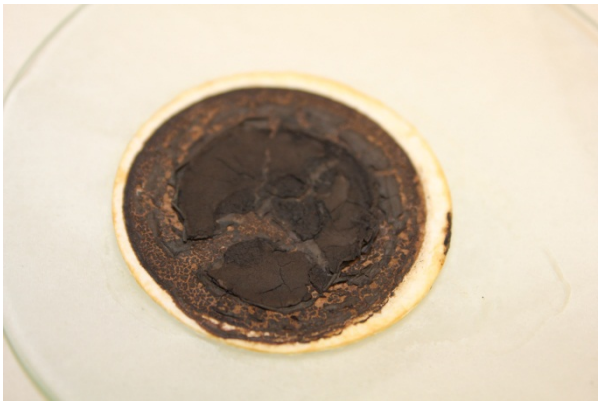

Figure 8.02 *Dried asphaltene deposit from the Jordbær crude oil.*

Hier D02A had somewhat more asphaltene, 2,2380 g/100ml which makes this a common crude oil, figure 8.03 shows the dried asphaltene deposit of the Hier D02A crude oil. When this deposit was transferred to the weighing vessel, it cracked and the smallest particles was difficult to get onto the filter because of electrostatic forces.

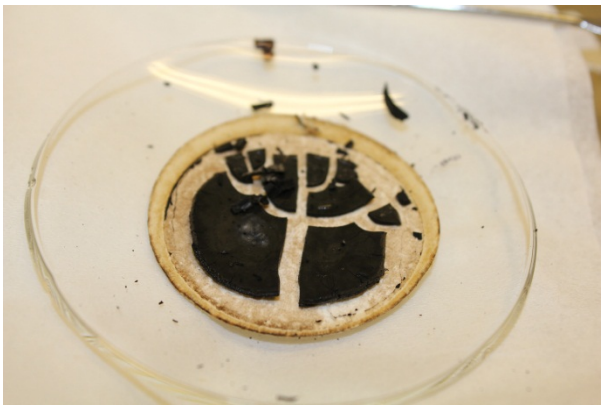

Figure 8.03 *Dried asphaltene deposit from the Hier D02A crude oil.*

The Crudo-Metapetroleum is very viscous, so when 20ml of this crude oil was measured, it was very difficult to transfer it to the flask. Also when this crude oil was filtered, there was some asphaltene still on the funnel cup. Some of it was scraped on to the filter, but it was very difficult to get all of it. The Crudo-Metapetroleum crude oil contained 12.1535 g/100ml. The filtration of this crude oil had to be done on two filters, because the mixture would barely pass through after a while. As figure 8.04 and 8.05 shows, the asphaltene deposit “cakes” were larger than the deposit “cakes” in the other crude oils.

Figure 8.04 *The first half of the Crudo-Metapetroleum asphaltene deposit.*

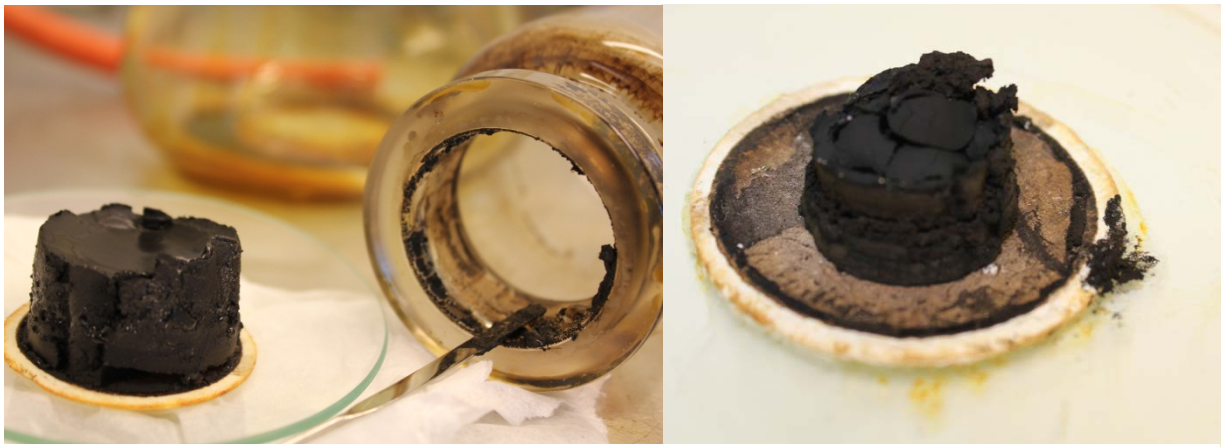

Figure 8.05 *(Left) Crudo-Metapetroleum deposit "cake" right after the filtration ended. (Right) The second half of the dried Crudo-Metapetroleum asphaltene deposit.*

8.3 Conclusion

The “Standard Procedure for Separating Asphaltenes from Crude Oils” procedure [2] states that most crude oils contain from 1 – 10 grams of n-heptane asphaltenes per 100ml crude oil. In this procedure pentane was used, which is of little importance as the ASTM D2007-80 uses pentane as the precipitant.

The results of the asphaltene content fits with the turbidity results of chapter 5. For example Crudo-Metapetroleum gave the highest turbidity measurements and it is also the crude oil with the highest asphaltene content. Crudo-Metapetroleum contains 12,1535g asphaltenes/100ml crude oil, Hier D02A contains 2,2380g asphaltenes/100ml crude oil and Jordbær contains 0,2210g asphaltenes/100ml crude oil.

8.4 References

[1] P. Luo and Y. Gu, "Effects of asphaltene content on the heavy oil viscosity at different temperatures," *Fuel*, vol. 86, pp. 1069-1078, 2007.

[2] P. R. r. center, "Standard Procedure for Separating Asphaltenes from Crude Oils," ed: Jianxin Wang and Jill Buckley, 2002.